FACULTÉ DES ÉTUDES SUPÉRIEURES ET POSTOCTORALES

uOttawa

L'Université canadienne
Canada's university

FACULTY OF GRADUATE AND POSDOCTORAL STUDIES

Koralee Mary Chaisson

AUTEUR DE LA THÈSE / AUTHOR OF THESIS

M.Sc. (Microbiology and Immunology)

GRADE / DEGREE

Department of Biochemistry, Microbiology and Immunology

FACULTÉ, ÉCOLE, DÉPARTEMENT / FACULTY, SCHOOL, DEPARTMENT

Interferon Regulatory Factor-3 Activation in Adenovirus Infection

TITRE DE LA THÈSE / TITLE OF THESIS

Dr. Robin Parks

DIRECTEUR (DIRECTRICE) DE LA THÈSE / THESIS SUPERVISOR

CO-DIRECTEUR (CO-DIRECTRICE) DE LA THÈSE / THESIS CO-SUPERVISOR

EXAMINATEURS (EXAMINATRICES) DE LA THÈSE / THESIS EXAMINERS

Dr. C. Addison

Dr. A. Kumar

Gary W. Slater

Le Doyen de la Faculté des études supérieures et postdoctorales / Dean of the Faculty of Graduate and Postdoctoral Studies

Interferon Regulatory Factor-3 Activation in Adenovirus Infection

by

Koralee Chaisson

Department of Biochemistry, Microbiology, and Immunology

Submitted in partial fulfillment

of the requirements for the degree of

Master of Science

Faculty of Graduate Studies

The University of Ottawa

Ottawa, ON

March 2007

THE UNIVERSITY OF OTTAWA

Your file Votre référence
ISBN: 978-0-494-32445-5
Our file Notre référence
ISBN: 978-0-494-32445-5

ABSTRACT

Adenovirus (Ad) infection is accompanied by an early inflammatory response that is stimulated by the binding and/or entry of the Ad capsid to the cell. Several studies have linked NF-κB to the activation of pro-inflammatory cytokines and chemokines early in Ad infection, however, for many other viruses, another key transcription factor, Interferon Regulatory Factor 3 (IRF-3), also acts early in viral infection. We sought to determine if IRF-3 is activated upon Ad infection, and to examine its importance in establishing an anti-viral state in Ad-infected cells. Our data suggests that wtAd5 infection results in phosphorylation of IRF-3 on a novel amino acid residue, and this event is dependent on virus replication. Moreover, IRF-3 is an important transcription factor for induction of RANTES expression in wtAd5-infected cells. Taken together, these data suggest that IRF-3 activation in response to Ad DNA replication is important in establishing an anti-viral state within the infected cell.

Acknowledgements:

The following thesis, while an individual work, benefited from the insights and directions of several people. First, my supervisor Dr. Robin Parks, provided instructive comments and evaluation and continued to challenge, inspire, and encourage me at every stage in the thesis process. My thesis committee, Dr. Jonathan Angel and Dr. John Bell each provided individual insights that guided my thinking, greatly improving the finished product. In addition, Joel Ross, Bobby Lanthier, Kathy Poulin, Rob Meulenbroek, and Karen Powell – fellow members of the Parks lab – were always available for assistance and support and were a pleasure to work with. I am very thankful for the friendships created with these genuinely wonderful people.

In addition to technical and instrumental assistance above, I received equally important assistance from family and friends. My soon-to-be husband Michael Berghout provided constant support and encouragement throughout the thesis process. My parents Dave and Klara Chaisson instilled in me, from an early age, the desire to dream big and reach high, and continue to be my biggest fans. Finally I wish to thank my friends Jodi Van't Foort and Lyndsey Benvie as well as my sisters Laura, Sarah, Susie, and Carolyn for keeping me in their prayers and showing me the most important things in life.

Table of Contents:

List of Abbreviations:

Ad	Adenovirus (Ad5 refers to serotype 5)
Ad5ts36	Temperature Sensitive Ad5
ARD	Acute Respiratory Disease
ATF-2	Activating Transcription Factor 2
BMDC	Bone Marrow Derived Dendritic Cell
BMMO	Bone Marrow Derived Macrophage
BZIP	Basic Leucine Zipper
CAR	Coxsackie Adenovirus Receptor
CBP	CREB-Binding Protein
CCR5	Chemokine (C-C motif) Receptor 5
CD28RE	CD28 Response Element
ChIP	Chromatin Immunoprecipitation
CIP	Calf Intestinal Phosphatase
CMV	Cytomegalovirus
CREB	cAMP Response Element Binding
CTL	Cytotoxic T Lymphocyte
DC	Dendritic Cell
DMEM	Dulbecco Modified Eagle Medium
DNA-PK	DNA Protein Kinase
DsRNA	Double Stranded RNA
E1	Early gene region 1
E3	Early gene region 3
ΔE1Ad , $E1^{(-)}$Ad	E1-deleted Ad
ΔE3Ad	E3-deleted Ad
ERK	Extracellular Signal-Related Kinase
FgAd	First-Generation Ad
GM-CSF	Granulocyte Macrophage Colony Stimulating Factor
HdAd	Helper-Dependent Ad
HMG-I/Y	High Mobility Group –I/Y
HSV	Herpes Simplex Virus
ICAM-1	Intracellular Adhesion Molecule 1
ICSBP	Interferon Consensus Sequence-Binding Protein
IFN	Interferon
IKKε	Inhibitor of κB Kinase ε
IL	Interleukin
IP-10	Interferon Induced Protein 10
IRF	Interferon Regulatory Factor
ISG	Interferon-Stimulated Gene
ISGF3γ	Interferon-Stimulated Gene Factor 3γ
ISRE	Interferon-Stimulated Response Element
ITR	Inverted Terminal Repeats
JAK/STAT	Janus-Activated Kinase/ Signal Transducer and Activator of Transcription
JNK	c-Jun NH_2-Terminal Kinase

LPS	Lipopolysaccharide
LRR	Leucine Rich Repeat
MAPK	Mitogen-Activated Protein Kinase
MCP-1	Monocyte Chemoattractant Protein 1
MEM	Modified Eagle Medium
MEF	Mouse Embryonic Fibroblast
MeV	Measles Virus
MIP-2	Macrophage Inflammatory Protein 2
MOI	Multiplicity of Infection
MyD88	Myeloid Differentiation Marker 88
Mx	Mxyovirus Resistance (protein)
NDV	Newcastle Disease Virus
NF-AT	Nuclear Factor of Activated T cells
NF-IL-6	Nuclear Factor of Interleukin-6
NF-κB	Nuclear Factor -κB
NK	Natural Killer (cells)
OAS	2', 5'-Oligoadenylate Synthetase
$p125^{FAK}$	Focal Adhesion Kinase
$p130^{CAK}$	Crk-Associated Kinase
PAMP	Pathogen-Associated Molecular Pattern
PBMC	Peripheral Blood Mononuclear Cells
PBS	Phosphate Buffered Saline
PCR	Polymerase Chain Reaction
PFU	Plaque Forming Units
PI_3K	Phosphoinositide-3-OH Kinase
PKA	Protein Kinase A
PKR	Protein Kinase R
PRD	Positive Regulatory Domain
PRR	Pattern Recognition Receptor
RANTES	Regulated on Activation, Normal T-cell Expressed and Secreted
RFLAT-1	RANTES Factor of Late Activation of T-Lymphocytes-1
RGD motif	Arginine-Glycine-Aspartic Acid
RID	Receptor Internalization and Degradation (complex)
RIG-I	Retinoic Acid Inducible Gene-I
RIPA	RadioImmunoPrecipitation Assay (buffer)
RSV	Respiratory Syncytial Virus
RT-PCR	Reverse Transcription Polymerase Chain Reaction
RV	Rabies Virus
SARM	SAM and ARM-Containing Protein
SDS-PAGE	Sodium Dodecyl Sulfate Polyacrylamide Gel Electrophoresis
SeV	Sendai Virus
SR	Serine/Arginine Rich (family of splicing proteins)
TANK	TRAF-Associated NF-κB Activator
TBK-1	TANK Binding Kinase 1
TBS-T	Tris Buffered Saline (with Tween)
Th-1	Helper T cell Type 1
TIR	Toll/IL-1R

TIRAP	TIR-Containing Adaptor Protein
TLR	Toll-Like Receptor
TNF-α	Tumor Necrosis Factor α
TRAF	TNF Receptor Associated Receptor
TRAIL	TNF-Related Apoptosis-Inducing Ligand
TRAM	TRIF-Related Adaptor Molecule
TRIF	TIR-Domain-Containing Adaptor Protein Inducing IFNβ
VAK	Viral Activating Kinase
VSV	Vesicular Stomatitis Virus
wtAd5	Wild-type Ad5

List of Figures:

Chapter 1: INTRODUCTION

Adenovirus infection, both naturally and upon delivery of gene therapy vectors, is accompanied by a strong inflammatory response known as the innate immune response. To date, the innate immune response to Ad is not completely understood. Recent reemergence of Ad-induced acute respiratory disease (ARD) in confined populations, as well as the prevalence of other Ad-related diseases in children, the elderly, and immuno-compromised individuals, demonstrate the need for an Ad vaccine and an effective antiviral compound or form of immunotherapy against Ad. Conversely, in recent years, Ad vectors have become popular gene transfer vehicles in multiple gene therapy studies, yet the delivery of high doses of these vectors results in significant acute inflammation that reduces the effectiveness of the vector. Thus, a current emphasis in Ad gene therapy research is to determine the mechanisms by which Ad induces the early inflammatory response, and to modify Ad vectors accordingly in order to eliminate this very dangerous and even lethal problem. In order to elucidate novel methods to combat severe Ad diseases and innovative strategies for the development of nontoxic therapeutic Ad vectors, an improved understanding of the molecular mechanisms and signaling pathways that shape the immune response to Ad is of great importance.

1.1 Literature Review

I. Adenovirus

i. Adenovirus structure and genetics

Adenovirus (Ad) was first isolated from human adenoid cells by Rowe *et al.* in 1953 (1). Since that time, at least 50 other distinct human Ad serotypes have been identified (2). These serotypes are classified into 6 subgroups (A-F), based on DNA homology, genomic organization, hemagglutination properties, and oncogenicity in rodents (3). The Ad virion is non-enveloped and formed of an icosahedral-shaped protein shell called the capsid. The capsid is composed of 3 major structural proteins, hexon, penton, and fiber, and several other more minor proteins. The surface of the capsid is made up of 240 hexon protein trimers, which together form the 20 triangular faces of the icosahedron. Located at each of the 12 vertices is a penton base protein, from which a fiber protein extends (Fig. 1) (4-8). The fiber protein is used for binding to the host receptor CAR (coxsackie adenovirus receptor). With the exception of subgroup B, CAR is used for attachment and entry of all human Ad groups (9-12). Within the capsid lies a DNA-protein core complex containing a 30- to 40-kb genome of linear double-stranded (ds) DNA (6, 13). The Ad genome is separated into early (E) genes and late (L) genes. The early genes are the first to be transcribed, and they encode proteins that are involved in the control of viral DNA synthesis (E2A and B), transcription (E1A), transport of mRNAs to the cytoplasm (E1B, E4Orf6), and immunoregulation (E3, E1B, E4). The late genes are primarily structural genes and encode the proteins that form the Ad capsid (14).

The "early" and "late" phases of the Ad replication cycle are separated by the onset of viral replication. However, the functional distinction between "early" and "late" events is

Figure 1. Schematic representation Ad virion cross-section.
(Rux and Burnett, 2004 (6). Used with permission)

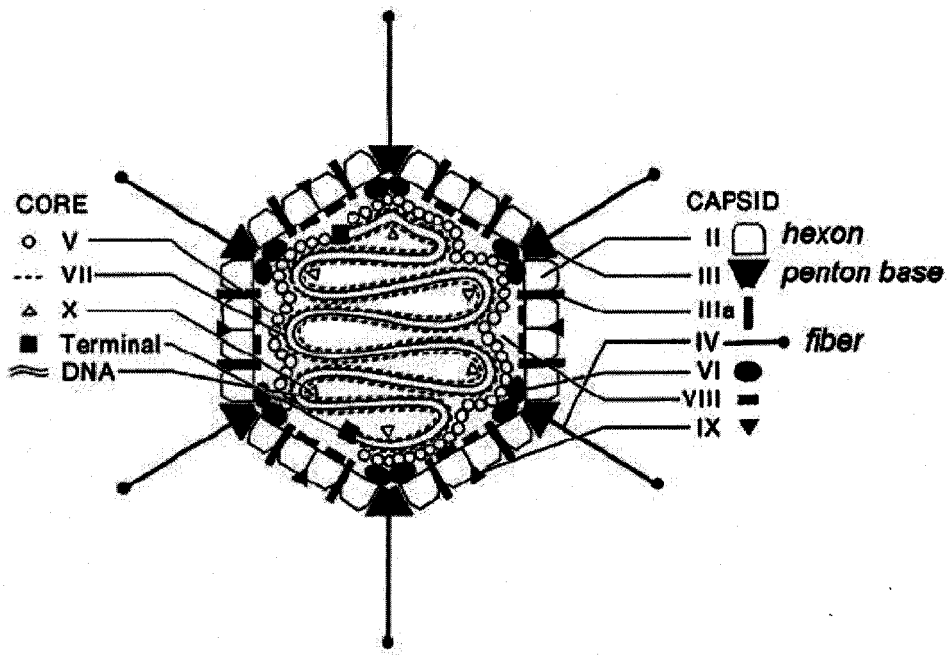

often blurred, as early genes continue to be expressed at late times after infection, and the promoter which controls the expression of the major late transcription unit directs a low level of transcription early after infection (14). In HeLa cells - most often used for Ad studies since Ads grow in them rapidly and to high yield - the "early" phase lasts for about 5-6 hr after which viral DNA is first detected. The "late" phase of Ad replication comes with the onset of DNA replication, and after 20-24 hr, approximately 10^4 progeny virus particles/cell have been produced and the infectious cycle is completed (14, 15).

ii. Ad pathogenicity and disease

Human Ad is a common pathogen, and the diseases caused by Ad are varied. The degree of Ad-induced disease differs between serotypes (2), and each Ad group appears to preferentially infect different tissue groups (5). For example, group B Ads are primarily responsible for lower respiratory tract and urinary tract infections, group A and D Ads often cause diseases in the intestine, Ads 40 and 41 from group F are enteric and cause diarrhea in small children, and Ads 8, 19, and 37 of group D cause keratoconjunctivitis in the eye (5). The most common Ad diseases, however, are infections of the upper respiratory tract. These are caused primarily by group C Ads 2 and 5, which are the most extensively studied serotypes of all human Ad (2, 5, 6, 13). Ads replicate best in epithelial cells and very poorly in lymphocytes, but have also been known to target heart tissue (5, 16, 17). In fact, Ads cause 17% of pediatric and 4% of adult cases of viral myocarditis (18), and Ad-induced myocarditis has, in turn, been linked to sudden infant death syndrome (SIDS) (19).

In most patients, Ad causes relatively minor, self-limiting diseases. However, among pediatric and geriatric populations, as well as in immunocompromised individuals (such as bone marrow and organ transplant recipients and patients affected with acquired immune

deficiency syndrome (AIDS)), Ad infections can be severe and life threatening, most especially in the lung and liver (5). Ads can be very virulent in children, as they are known to cause 8% of all respiratory tract infections and are responsible for 5% of the overall number of infections observed in pediatric populations (20). Ad infection among children often leads to bronchitis, bronchiolitis, or pnemonia, and latent Ad infection can contribute to asthma chronicity (20, 21). In confined populations including day-care centers, nursing homes, and most especially military training venues, acute respiratory disease (ARD) (caused by Ads 4, 7 and to a lesser extent Ad21), is a growing problem (5, 22). Until recently, mandatory vaccination of new military recruits with an oral enteric-coated live Ad vaccine reduced the rate of ARD. Unfortunately, this vaccine is no longer available and there has been a reemergence of Ad-induced ARD back to pre-vaccination levels (5, 23-25). In addition, therapy for serious and severe Ad infection remains unsatisfactory, as no studies show statistical proof of efficacy for any kind of immunotherapy or antiviral compound. Hence, there exists an obvious need for an increase in study directed toward the biology of wild-type Ad infection, with a specific focus on achieving a greater understanding of the immune response to Ad. An improved understanding of Ad-host interactions may elucidate novel methods to combat severe Ad disease and eliminate the increasingly widespread problem of Ad-induced ARD.

iii. Ad vectors

In recent years, a major emphasis in Ad research has been directed towards the use of Ad5-based vectors as vehicles for gene delivery in gene therapy studies (see (26) for review). There are several reasons why Ad is an excellent vector choice, making it a widely popular vehicle for gene transfer. Ad is well characterized both biochemically and

genetically, it is easy to manipulate, and can be grown to high titers (27). More importantly, Ad is able to transduce a wide array of cell types in a cell cycle independent manner, and the deletion of non-essential protein coding regions from its genome increases cloning capacity by allowing for the insertion of foreign DNA (28). For example, first-generation Ad vectors (fgAd), are deleted of the E1 and E3 genes and can accommodate up to 8 kb of therapeutic DNA (29). Second-generation Ad vectors are also deleted of E1 and E3 genes, but contain other deletions or inactivated E2 or E4 genes (27). A more recent vector strategy further increases cloning capacity as it involves the creation of vectors deleted of all viral sequences with the exception of those required for viral DNA replication and packaging (*i.e.* the viral ITRs (inverted terminal repeats) and packaging elements). These vectors, known as helper-dependent Ads (hdAd), are created through dual infection with a complementing helper virus that provides the necessary proteins *in trans* for replication and packaging of all other viral proteins. Cre-mediated removal of the packaging element from the helper virus prevents its encapsulation into virions and this ensures the recovery of high titer, relatively pure hdAd (27, 30, 31).

iv. Ad vectors: efficacy and safety

First-generation Ad vectors are frequently used as all-purpose expression vectors and as viral vaccines. They have also been used in gene therapy applications, but have performed relatively poorly during pre-clinical and clinical studies due to fgAd-induced innate (early) and adaptive (late) immune responses that work to eliminate the vectors, thereby making stable (long term) transgene expression unachievable (32-37). Early inflammation (innate immune response) following Ad infection is caused by the detection of the infecting virion proteins injected at the time of treatment, while later inflammation

(adaptive immune response) is associated with the expression of viral proteins from the Ad vector backbone (30, 34, 38). Unfortunately, the intensity of these *in vivo* responses not only limits the efficacy of the vectors, but also the safety of those receiving the treatment (13, 28). Significant morbidity and major damage to healthy tissue are possible additional hazards faced by each recipient of gene therapy (39, 40). In extreme cases, death can occur (41).

Second-generation Ad vectors with deleted or inactivated E2 genes persist longer in transduced cells and are associated with a reduced early inflammatory response (42-44). Vectors with deleted or inactivated E4 genes also cause decreased early inflammatory response, but unfortunately have a significantly reduced time frame of transgene expression (30, 45-48). Relative to first- and second-generation Ad vectors, however, hdAd vectors have excellent expression characteristics, and can provide high levels of transgene expression for considerably longer periods of time. This is achievable since hdAd do not elicit the later (adaptive) inflammatory response because they are deleted of all viral coding sequences (30). However, although the problem of late inflammation appears to be eliminated with the use of hdAd, the delivery of high doses of hdAd required in most gene therapy studies can lead to a very dangerous and even lethal early inflammatory response, as observed in non-human primates (49). Therefore, the current emphasis in Ad gene therapy research is to determine the mechanisms by which Ad induces the early inflammatory response, and to modify Ad vectors accordingly in order to eliminate this problem.

II. Innate Immune Response to Viral Infection

i. Pathogen recognition: the Toll-like Receptors

The innate immune response is a host's first line of defense against invading pathogens. Working via immune effector cell recruitment and complicated signaling

cascades, it allows for the rapid detection, attenuation, and eradication of infection (50). In order to trigger the cascade of events necessary for the elimination of infection, the target cell (or resident macrophage) must first be able to detect the invading pathogen. Therefore, the innate immune response begins with one of its principle functions: pathogen recognition which occurs through a number of different pattern recognition receptors (PRRs) located in both intracellular and extracellular compartments (51). Toll-like receptors (TLRs), the best-studied family of PRRs, are type I transmembrane receptors that recognize invariant molecular structures shared by pathogens of various origin. These structures are also known as pathogen associated molecular patterns (PAMPs) (52, 53). There are 11 known TLRs in humans (TLR1-11) however the functionality of human TLR11 has yet to be determined (54). Although TLRs were originally thought to be strictly extracellular transmembrane receptors, certain TLRs (TLR3, 7/8, 9) are localized to intracellular compartments, particularly in the endoplasmic reticulum, and within endosomes of certain subsets of cells (55-57).

Each TLR has three distinct domains: an extracellular domain characterized by leucine-rich repeats (LRRs), a single transmembrane domain, and an intracellular signaling domain known as the Toll/IL-1R (TIR) domain. All TLRs share similar extracellular LRRs, however, each recognizes a different microbial signature (58). In fact, each TLR has many ligands, both exogenous and endogenous, indicating a potential for each TLR to contain multiple binding sites, and perhaps also to act as an integrator of signaling with other receptors. In this way, it may not be necessary for the TLRs to bind directly to each ligand, explaining why in most cases, direct binding between a TLR and a putative microbial ligand has not been demonstrated (58, 59). The intracellular TIR domain is responsible for the recruitment of signaling molecules to activate downstream signaling pathways that lead to

the activation of transcription factor NF-κB (nuclear factor-κB) and the IRFs (interferon regulatory factors) that activate the immune response through the induction of cytokines and interferons (IFNs) (58). With the exception of TLR3, all TLRs transduce signals through the adaptor protein MyD88 (myeloid differentiation marker 88). Four other adaptor proteins – TIRAP (TIR-containing adaptor protein), TRIF (TIR-domain-containing adaptor protein inducing IFNβ), TRAM (TRIF-related adaptor molecule), SARM (SAM and ARM-containing protein) – are also used differentially by the TLRs (59).

Although studies centering on innate immunity and TLRs were initially focused on bacterial models, it is becoming more evident that viral recognition also occurs through TLRs (13). Specifically, TLR2, 3, 4, 7/8, and 9 are involved in the antiviral innate immune response (Fig. 2) (60). These TLRs interact with various viral components: envelope glycoproteins (TLR2 and 4), viral double-stranded RNA (dsRNA) (TLR3), single-stranded RNA (ssRNA) (TLR7 and 8), and CpG motifs contained in viral DNA (TLR9). TLR3 and TLR9, which are localized intracellularly, are also in the ideal position for mediating the intracellular recognition of viral particles (13, 59, 60).

ii. Signaling cascades and the effector cells of the innate response

Following viral particle recognition by innate receptors, a cascade of events is triggered in an effort to limit and eradicate infection. One of the first events to take place is the activation of transcription factor NF-κB via signal transduction through the mitogen-associated protein kinases (MAPKs) including extracellular signal-related kinases (ERK), p38 kinases (p38), and the c-Jun NH_2-terminal kinases (JNK), which ultimately results in the transcription of host cytokine and chemokine genes (51, 61). These genes confer local

Figure 2. TLR-virus interactions.
(Finberg and Kurt-Jones, 2004 (60). Used with permission)

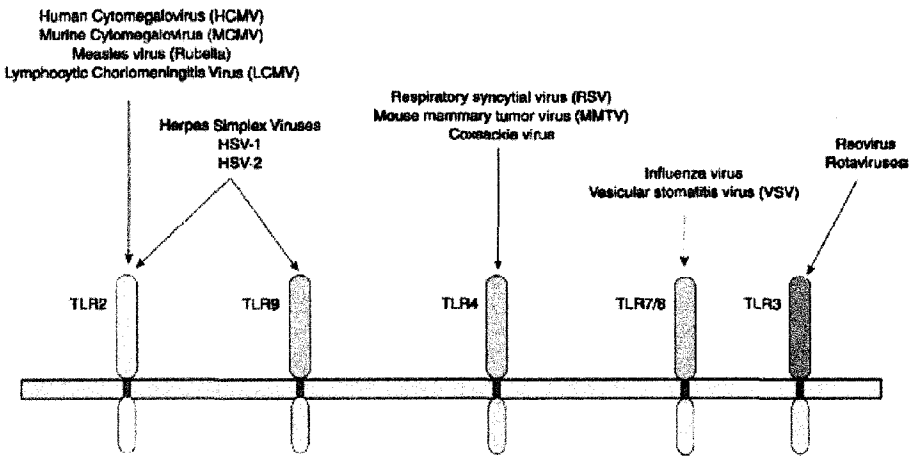

control of infection and recruit different types of effector leukocytes (granulocytes, monocytes/macrophages), natural killer (NK) cells, and NK T-cells to the site of infection. As phagocytes, monocytes/macrophages act to ingest and destroy viral particles, but also secrete antiviral cytokines and participate in antigen presentation required to prime the adaptive immune response (62, 63). Granulocytes (neutrophils) recruited to the site of infection are also an important source of cytokines that have antiviral activity and amplify the immune response (13). NK cells, large granular lymphocytes, perform seven cytolytic functions that restrain viral infections, and along with NK T cells, secrete IFN (interferon)-γ which is essential for the development of helper T cell type 1 (Th-1)-dominant adaptive immune responses (64).

III. Innate Immune Response to Ad

To date, most of the studies examining the immunological responses to Ad are based on *in vivo* and *in vitro* studies with Ad vectors (13, 50). However, several aspects of Ad vector biology differ from wild-type Ad infection. For example, Ad vectors are replication-deficient and some lack all or many viral coding sequences. Some of these viral coding regions, specifically those within the Ad E3 gene region, encode viral immunoregulatory genes that target processes essential for the survival of the virus during acute and latent infection, and this region is deleted from most gene therapy vectors (5). In addition, the titers of Ad vectors required to achieve efficient gene transfer *in vivo* are many folds higher than viral particle numbers observed in early wild-type Ad infection (13). Thus, studies based on characterization of immune responses to Ad vectors cannot always be accurately extrapolated to the immunological events surrounding wild-type Ad infection.

i. Immune cell response

The innate immune response to Ad vectors is dose-dependent, occurs within 24 hr of host transduction and is independent of viral or transgene transcription (Fig. 3) (13, 38). The inflammatory genes induced by Ad vectors *in vivo* are numerous, and include cytokines tumor necrosis factor-α (TNF-α), IL-6 (interleukin-6), IL-1β, IFN-γ, and IL-12 and chemokines IFN-γ-inducible protein-10 (IP-10), RANTES (regulated on activation, normal T-cell expressed and secreted), macrophage inflammatory protein-2 (MIP-2), MIP-1α, MIP-1β, and monocyte chemoattractant protein-1 (MCP-1) (13, 40, 65-67). Ad preferentially infects the liver after systemic and local delivery (68) so it is not surprising that within 60 minutes of Ad vector transduction in mice, the induction of multiple chemokine mRNAs can be observed in liver tissue (34). In addition, Kupffer cells (the resident macrophages of the liver) are quick to take up the vectors and in turn release TNF-α, IP-10, and RANTES (34, 66) which are together associated with leukocyte recruitment (50). Indeed, Ad vector-transduced tissues are also quickly infiltrated with neutrophils and NK cells (34, 69).

Recently, micro-array studies by Hartman *et al.* (70) demonstrated a potent cellular transcriptome response in murine liver samples as early as 6 hr following intravenous administration (via retro-orbital sinus) of high-titer ΔE1/E3 or ΔE1/E2b/E3 Ad vectors. In addition, transcriptome analysis revealed that the complex innate response to the Ad vectors used was very similar to that observed when mice were challenged with LPS (lipopolysaccharide). However, unique aspects of the Ad-dependent transcriptome response included the upregulation of RNA regulatory mechanisms and apoptosis-related pathways

Figure 3. The innate immune response to Ad vectors.
Ad infection of several tissue types results in immediate stimulation of signal transduction pathways that ultimately lead to expression of pro-inflammatory cytokines (Muruve, 2004 (13). Used with permission)

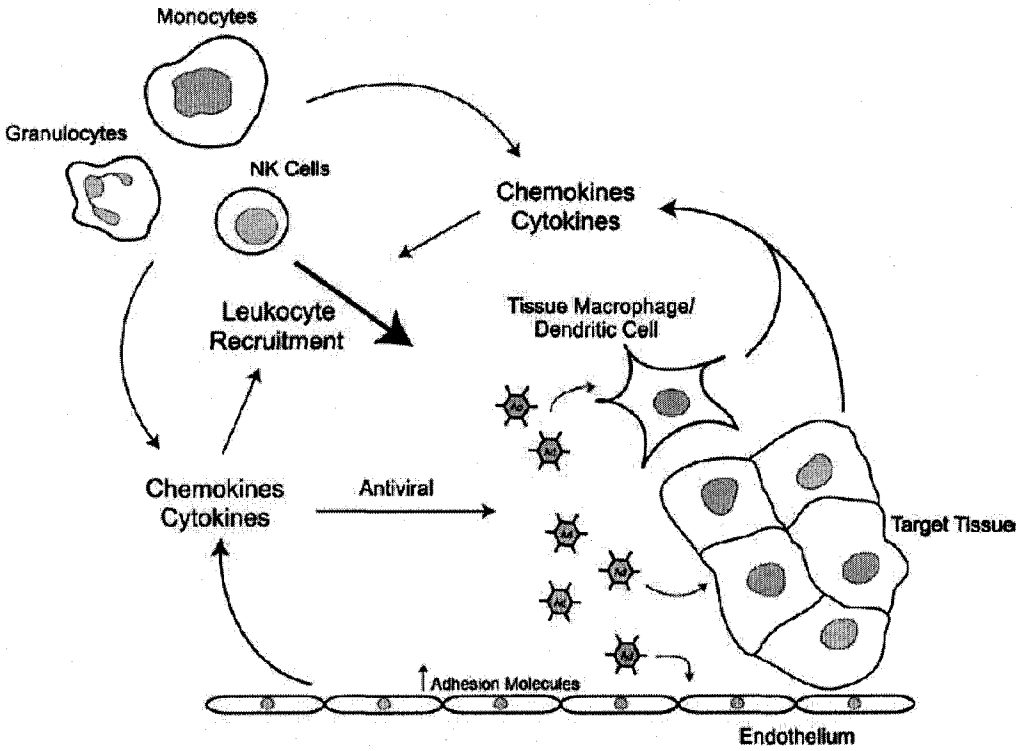

and the suppression of lysosomal and endocytic genes. The TLR system, specifically TLR adaptor MyD88, was also implicated in these responses, demonstrating an important role for MyD88 as an amplifier and regulator of Ad vector immunity *in vivo* (70).

In lung tissue, Zsengeller *et al.* (71) observed that within 10 minutes after Ad vector administration there was a rapid accumulation of vector in alveolar macrophages which was associated with up-regulation of cytokines IL-6 and TNF-α, and chemokines MIP-2 and MIP-1α. Additionally, Otake *et al.* (66) observed the induction of RANTES in lung tissue within hr of Ad vector transduction. *In vitro* studies have also demonstrated that Ad vectors can stimulate the expression of cytokines and chemokines in peripheral blood mononuclear cells (PBMC) (72). Specifically, when Ad vectors were administered at a dose of 1000 PFU (plaque forming units) per cell, a minimal release of TNF-α and IL-1β, a significant increase in IL-6 and RANTES, and a steady increase in GM-CSF (granulocyte/macrophage colony stimulating factor), MIP-1α, Gro-α (an inducible neutrophil chemotactic factor), and IL-8 was observed over 96 hr (72). Furthermore, when the experiment was repeated using UV-psoralen-inactivated vector particles or empty capsids, the aforementioned response did not diminish thereby confirming the importance of the viral particle/capsid and not viral gene expression in this process (72).

ii. Non-immune cell response

Ad vectors also induce the expression of various cytokines and chemokines in non-innate cell types such as epithelial and endothelial cells (50). For example, in primary kidney epithelial cells, RANTES, IP-10, and MIP-2 are induced within 6 hr of Ad vector transduction (38). Furthermore, early induction of various chemokines including RANTES,

IP-10, and IL-8 has been observed following Ad vector transduction in HeLa cells, non-small cell lung adenocarcinoma cell line A549, and mouse insulinoma cell line TGP61 (38, 73-76). Aside from cytokine and chemokine induction, Ad vectors can also induce the expression of other genes involved in the inflammatory response. For instance, in epithelial A549 cells and endothelial cells (human umbilical vein and bone marrow macrovascular cells), Ad vectors induce the expression of leukocyte adhesion molecules ICAM-1 (intracellular adhesion molecule-1) and VCAM-1 (vascular cell adhesion molecule-1) (77, 78) that facilitate leukocyte recruitment to Ad vector-transduced tissues (79). In addition, recent micro-array analysis of ΔE1/E3Ad-transduced mouse embryonic fibroblast cell isolates (MEFs) demonstrated a similar transcriptome response to that observed in murine liver tissue upon intravenous administration of high-titer ΔE1/E3 or ΔE1/E2b/E3 Ad vectors (70, 80). This widespread gene expression program involved significant changes in the expression of genes involved in focal adhesion, tight junction, and RNA regulation in addition to TLR pathway and other innate sensing genes (80).

iii. Cell entry

In vitro and *in vivo* studies have clearly demonstrated that viral capsid binding and/or entry into the cell initiate the earliest events in the innate immune response to Ad infection (13, 50). There is a good basis of understanding of the many different signaling pathways that are used by group C Ads (Ad2 and Ad5) to internalize and infect cells. However, while it is not surprising that Ad vector entry into the cell triggers the innate immune response, the impact of signal activation on host inflammation and the antiviral responses that occur during this process are poorly understood (13, 50).

In epithelial cells, group C Ad cell entry is mediated by interactions with the high affinity receptor CAR and α_v-integrins (9, 81). Ad attaches to the CAR receptor through an interaction with the carboxy terminus of its fiber knob protein (9). Viral internalization occurs by receptor-mediated endocytosis through clathrin-coated vesicles. This process is mediated by a low affinity interaction between α_v-integrins ($\alpha_v\beta_3$, $\alpha_v\beta_5$, $\alpha_v\beta_1$) and an RGD motif (arginine-glycine-aspartic acid) on the Ad penton base capsid protein (81, 82). Within 10 minutes of internalization, Ad penetrates the endosome in a pH-dependent manner believed to involve a conformational change in the Ad penton base protein and an interaction with $\alpha_v\beta_5$ integrins (83-85). In addition, protein VI, once exposed during capsid disassembly, has been shown to exhibit pH-independent membrane lytic activity (86). Traveling through the cytoplasm along microtubules, partially uncoated Ad virions reach the nuclear pore complex 30-40 minutes after endoplasmal escape (83, 87, 88), and entry of viral DNA into the nucleus is facilitated by the binding of hexon protein to histone H1(89). Initial cell binding of group C Ads can also be mediated by heparan sulphate glycosaminoglycans (90). In addition, studies with Ad vector infection in the monocytic cell line THP-1, demonstrate important interactions with other integrins such as $\alpha_M\beta_2$ and $\alpha_L\beta_2$, indicating that in macrophages, group C Ads use different cell surface molecules for binding (91). It is possible that this property of group C Ads might also be observed in other cell types.

iv. Signal transduction

Several independent studies supported the idea that the whole Ad capsid can trigger a series of early signals initiating the inflammatory response, however, not much was known about the role played by Ad surface domains (knob, hexon, penton base). Previous studies

had suggested that CAR does not appear to be specifically necessary for signal activation by Ad vectors (75, 92, 93). In these studies CAR-ablated fiber knob mutant vectors induced similar levels of IP-10 gene expression when compared with wild-type capsid vectors (93, 94). Recently, however, Tamanini *et al.* (8) demonstrated that the binding of the Ad fiber knob protein to CAR on A549 cells is responsible for the induction of MAP kinases (ERK1/2 and JNK) and transcription factor NF-κB and the resulting gene transcription of different chemokines (IL-8, Gro-α, Gro-γ, RANTES, IP-10). Furthermore, when the interaction of Ad fiber to CAR was blocked in A549 cells, they did not observe any residual activation (8). Tamanini *et al.* (8) argue that discrepancies between studies can be explained by considering the different cell types studied (renal epithelial cells versus alveolar type II-derived cells) and the very high concentration of CAR-ablated fiber knob mutant vectors used. However, group B Ad particles that do not use CAR as a high affinity receptor (11) can still equally induce IP-10 and RANTES in epithelial cell lines (75, 93). Taken together, this data suggests that signal transduction in response to CAR binding appears to be cell-type and group specific, and has yet to be completely elucidated.

Although Tamanini *et al.* (8) demonstrated that other major Ad surface domains (hexon, penton base) are not involved in MAPK and NF-κB pro-inflammatory signaling, they also showed that binding of Ad penton base protein to α_v integrins resulted in the activation of $p125^{FAK}$ (focal adhesion kinase), $p130^{CAS}$ (Crk-associated kinase), PI_3K (p85/phosphoinositide-3-OH kinase), and PKA (protein kinase A). Indeed, integrins have been implicated in a wide array of signaling events that regulate protein kinases, growth factor receptors, and the organization of the actin skeleton (13, 50, 92, 95).

Despite an incomplete understanding of signal transduction in response to CAR binding, several *in vitro* studies have described steps in the signaling pathways that occur in response to infection by Ad vectors. In HeLa cells, Bruder and Kovesdi (76) demonstrated Ad vector-induced ERK signaling, and linked this event with IL-8 expression. Within 5 minutes of Ad vector transduction, they observed the activation of Raf-1 (the downstream effector of the Ras GTP (guanosine triphosphate) binding protein) followed by p42/MAPK phosphorylation 10 minutes later (76). Other studies with a mouse kidney-derived epithelial cell line (REC; renal epithelial cells) revealed the activation of p38 and ERK (but not JNK) as early as 10 minutes and persisting up to 3 hr following Ad vector transduction (93). Furthermore, the activation of these kinases was linked directly to chemokine IP-10 gene expression (93). Finally, further studies have demonstrated that within 2 hr of transduction in both REC and HeLa cells, Ad vectors can induce nuclear translocation and subsequent activation of transcription factor NF-κB, an event that is directly involved in the transcription of chemokines such as IP-10 and RANTES (74, 75). Indeed, the activation of NF-κB represents an important first step in the cascade of events controlling both innate and adaptive immunity to Ad (51, 61).

IV. Interferon Regulatory Factor 3 (IRF-3)

For many viruses, another important transcription factor involved in the innate immune response is interferon regulatory factor 3 (IRF-3) (96). Characterized by Au *et al.* (97), IRF-3 is a unique member of the human IRF family of transcription factors. This family is comprised of nine members (IRF-1, IRF-2, IRF-3, IRF-4, IRF-5, IRF-6, IRF-7, interferon consensus sequence-binding protein (ICSBP), and interferon-stimulated gene

factor 3γ (ISGF3γ)), each member with distinct roles in host defense against pathogens, immunomodulation, and growth control (98, 99). IRF-3 is activated in response to infection by a number viruses including Sendai Virus (SeV), Measles Virus (MeV), Newcastle Disease Virus (NDV), Vesicular Stomatitis Virus (VSV), Respiratory Syncytial Virus (RSV), human Cytomegalovirus (CMV), and Herpes Simple Virus (HSV) type I (99-104).

i. IRF-3 signaling pathway

The IRF-3 gene encodes a 427 amino acid phosphoprotein that is constitutively expressed in all cell types and tissues (96, 105). Studies by Karpova *et al.* (106) have demonstrated that IRF-3 mRNA can be alternatively spliced by the SR (serine/arginine rich) family of splicing factors to form a 50 kDa splice variant known as IRF-3a. IRF-3a contains a unique 20 amino acid sequence in place of a portion of the N-terminal DNA binding domain that is lost in the splicing event (106). Like IRF-3, IRF-3a is ubiquitously expressed in all cell types and tissues. It appears as though IRF-3 mRNA splicing may be regulated in a tissue-specific manner; the highest ratio of IRF-3a to IRF-3 is found in brain tissue (107).

In its latent form in uninfected cells, IRF-3 exists in two monomeric isoforms (forms I and II) of about 55 kDa that can be resolved by SDS-PAGE (96, 101). Phosphorylation of IRF-3 can occur in four different regions; the first two regions are located within the N-terminus of the protein (residues Ser^{135} and Thr^{188}), while the second two regions are located within the C-terminus of the protein (residues Ser^{385}/Ser^{386}, and $Ser^{396}/Ser^{398}/Ser^{402}/Thr^{404}/Ser^{405}$) (Fig. 4) (96). Upon viral infection, IRF-3 is phosphorylated within the C-terminus of the protein, resulting in forms III and IV, which are resolved by SDS-PAGE as more slowly migrating isoforms than forms I and II (101, 108).

Figure 4. Schematic representation of human IRF-3.
Four important regions of human IRF-3 are demonstrated: the N-terminal interferon regulatory factor (IRF) binding domain, the nuclear export sequence (NES) containing a proline-rich region (PRO), the IRF association domain, and the C-terminal signal response domain. The region between residues 128-142, 186-198, and 382-414 are expanded below the schematic to demonstrate the amino acids, *in large letters*, that are known to be phosphorylated by DNA-protein kinase (DNA-PK, Thr^{135}), a member of the map kinase family (MAPK, Ser^{188}), and a viral activating kinase (VAK, Ser^{385}/Ser^{386}, and $Ser^{396}/Ser^{398}/Ser^{402}/Thr^{404}/Ser^{405}$). Adapted from Servant *et al.* 2002 (96).

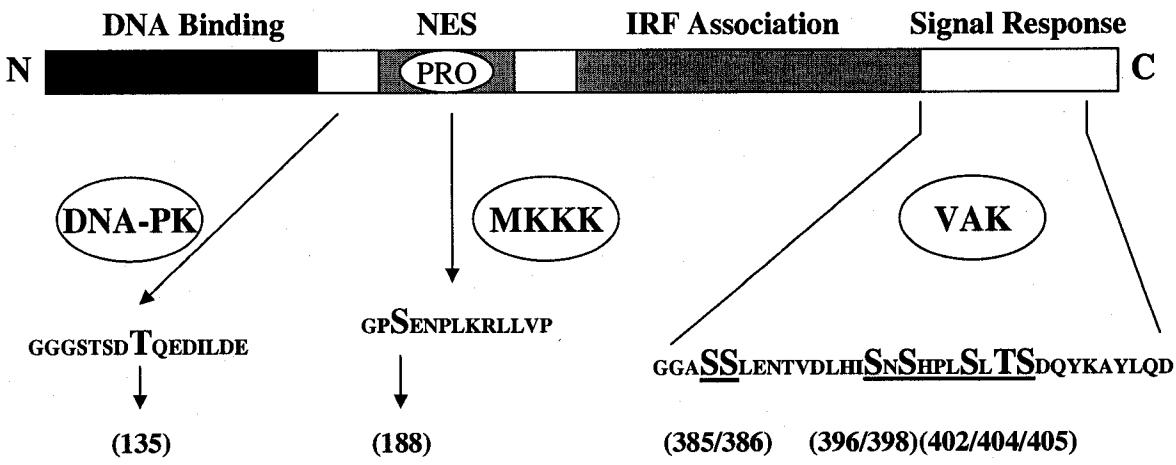

i. a.) C-terminal phosphorylation

It is widely accepted that true activation of IRF-3 occurs only when it is phosphorylated within the 385-405 amino acid C-terminal region of the protein (96, 101, 105, 109, 110), although the exact phosphorylation site within this region remains the subject of great debate (105, 108-112). In addition, the mechanism of IRF-3 activation and the identity of the viral activating kinase (VAK) responsible vary depending on the virus and the stimuli, and it is likely that multiple signaling pathways and kinases lead to activation of IRF-3 (96, 99). Recently, IKK-related kinases IKKε (Inhibitor of κB kinase ε) and TBK1 (Tank binding kinase 1) have been identified as components of the VAK responsible for C-terminal phosphorylation of IRF-3 during Sendai virus infection (113, 114).

Phosphorylation of IRF-3 by the VAK results in a conformational change in IRF-3 that exposes its DNA binding and transcriptional activation domains (96, 105, 115) thereby promoting homodimerization and binding to the IRF-3 consensus DNA binding site (96, 105, 109, 110). At the same time, this phosphorylation event is required for interaction with the histone acetyltransferase nuclear proteins CBP (CREB binding protein) and p300, which stop IRF-3 from shuttling in and out of the nucleus and enable it to remain predominately nuclear (Fig. 5) (96, 105, 109, 110, 116). Once in the nucleus, IRF-3 and CBP/p300 form a larger complex called the IFN-β enhanceosome, also consisting of the NF-κB p50/p65 heterodimer, and the b-ZIP (basic leucine zipper) proteins ATF-2 (activating transcription factor 2) and c-Jun, and all assembled on the HMG-I/Y (high mobility group- I, Y) architectural protein (117). This complex induces transcription by binding to distinct positive regulatory domains (PRD) in the type I IFN promoters (including IFN-β) and select ISRE (interferon-stimulated response element) sites in target genes (96, 105, 109, 110, 115, 118-120). Full induction

Figure 5. Basic schematic representation of IRF-3 activation pathway in response to RNA viruses VSV and SeV. Following infection by an RNA virus such as VSV or SeV, IRF-3 is phosphorylated by a viral activating kinase (VAK). This phosphorylation causes a conformational change in IRF-3, allowing for dimerization, CBP/p300 binding, and migration to the nucleus. Here, activated IRF-3 is retained and the IFN-β enhanceosome is formed from dimerized IRF-3 and CBP/p300 (as well as the NF-κB p50/p65 heterodimer, ATF-2, and c-Jun). The IFN-β enhanceosome complex induces transcription IFN-β, and subsequent IFN stimulated genes (ISGs). Activated IRF-3 can also directly lead to the induction of pro-inflammatory chemokines (RANTES, IP-10) and cytokines (IL-15) as well as ISGs such as ISG56. IRF-3 is rapidly degraded following activation.

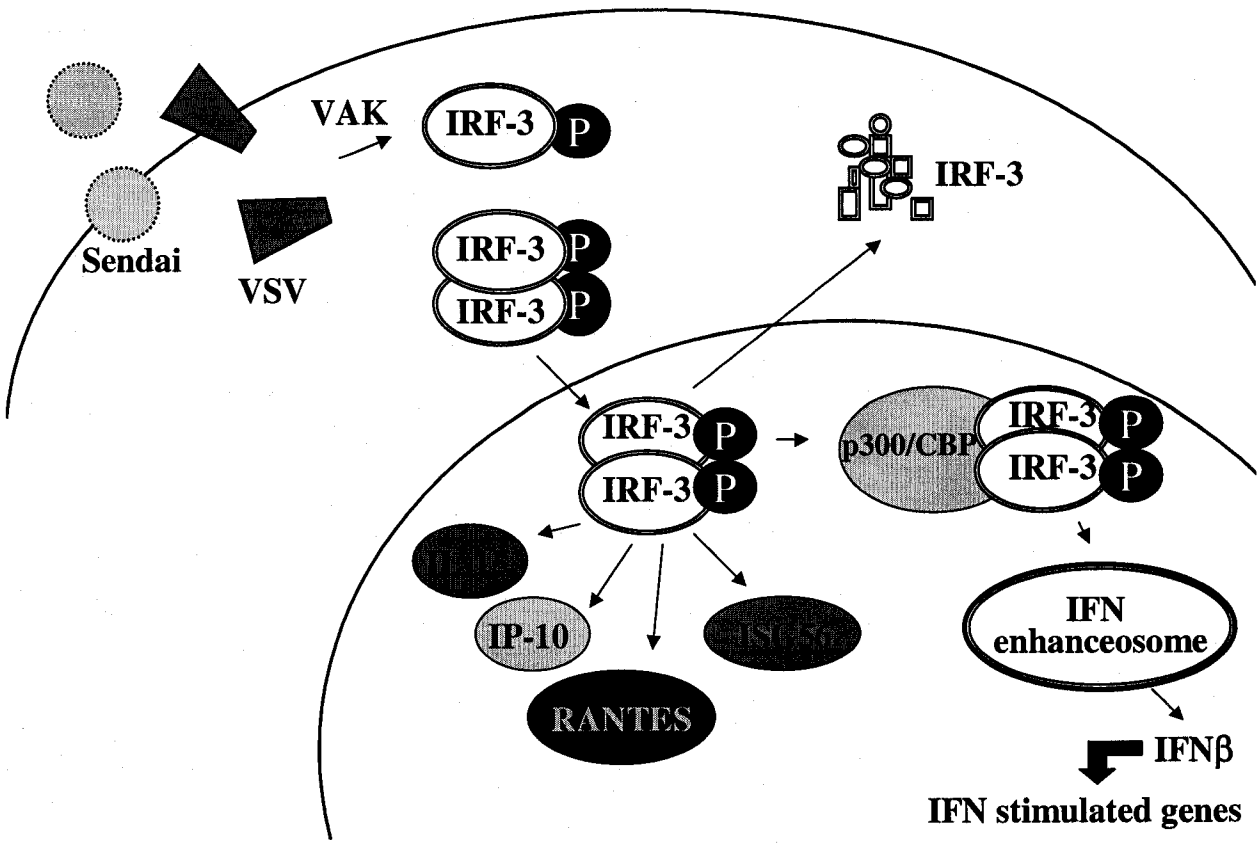

requires binding of all enhanceosome components, however, transcription can be stimulated from the IFN-β promoter following viral infection, through IRF-3 binding alone (121-123). Finally, activated IRF-3 is rapidly degraded through a proteasome-mediated pathway, ensuring that the inflammatory response will rapidly subside once the stimulus is eliminated (96, 105, 124).

i. b.) N-terminal phosphorylation

Phosphorylation in the N-terminal region of IRF-3 has been associated with cellular stimulation by stress inducers and DNA damaging agents, and is accomplished by DNA-protein kinase (DNA-PK) at Thr^{135} and a member of the MAPK family at Ser^{188} (101, 125-127). The functional implication of N-terminal phosphorylation has yet to be elucidated, although several different scenarios have been suggested. N-terminal phosphorylation via the stress-induced pathway may allow for a conformational change in IRF-3 structure, making the C-terminal Ser-Thr residues more accessible for phosphorylation by the VAK (101, 126). N-terminal phosphorylation may also serve to control IRF-3 activity prior to nuclear translocation (101, 109), and could also regulate the stability of the protein (96). Finally, it is possible that N-terminal phosphorylation has no effect on IRF-3 activity as a transcription factor, but could be involved in another distinct function of IRF-3. This latter hypothesis is based on an observation made by Servant *et al.* (101), that IRF-3 interacts with regulatory proteins that are not associated with transcriptional control.

ii. Virally-induced IRF-3 activation

IRF-3 is activated by many RNA viruses including SeV, MeV, NDV, VSV, and RSV, through VAK activation resulting from the detection of viral dsRNA produced within

the cell (99-102). Cellular receptors for dsRNA within the cell include PAMP receptors such as TLR-3, and cytoplasmic pattern recognition receptors such as RIG-I (retinoic acid inducible gene-I), a highly inducible RNA helicase that binds dsRNA (128, 129). Although the role of RIG-I and TLR-3 in dsRNA recognition are cell-type dependent, both are key activators of the IRF-3 activation pathway (130, 131). IRF-3 is also activated upon infection by the DNA viruses human CMV and HSV type I, and occurs in the absence of virally produced dsRNA. Virus internalization is required for HSV-mediated activation of IRF-3, whereas in CMV infection, binding to the cell is sufficient (103, 104).

iii. IFNs and viral resistance

Following early IRF-3-mediated induction of the type I IFN promoter, the resulting IFNα/β protein is secreted from the cell. Acting in an autocrine and paracrine fashion, these IFNs proceed to bind to and stimulate their common receptor on both the infected and neighboring cells (59). The stimulated receptor then activates a JAK/STAT (janus activated kinase/signal transducer and activator of transcription) signaling pathway, resulting in the expression of hundreds of IFN-stimulated genes (ISGs) which act to set up an antiviral, antiproliferative, and immunoregulatory state in host cells (53, 59, 132-139). The best-characterized ISGs are cellular antiviral proteins that act directly to prevent viral replication. These ISGs are induced in non-immune cells and include dsRNA-activated serine/threonine kinase protein kinase (PKR), enzymes 2',5'-oligoadenylate synthetase (OAS) and RNase L, and the myxovirus-resistance (Mx) proteins (53, 140).

Another ISG, IRF-7, is the closest relative of IRF-3 and shares common features (141). During the second phase of induction, heterodimeric IRF-3 and 7 bind PRD elements

to further enhance the expression of IFNα/β (142, 143). Indeed, the synthesis and activation of IRF-7 is required to bring about the induction of the rest of the IFN-α genes (39-40), as IRF-3 alone can only induce the expression of IFN-α4 (144). IRF-7, however, is also very distinct from IRF-3. Unlike IRF-3, inactive IRF-7 expression occurs mainly in lymphoid tissues at very low basal levels and is strongly induced by IFN treatment (141, 145). This represents a highly regulated system, since in the absence of continual IFN stimulus, IRF-7 levels drop significantly and the antiviral state within the cell is quickly reversed.

In addition to their role in ISG induction in non-immune cells, IFNs released from infected cells act as a signal for the recruitment and activation of immune cells such as macrophages, NK cells, and cytotoxic T lymphocytes (CTL) to the site of infection. Once they have relocated to the area, NK cells and CTL release a number of antiviral cytokines including TNF-α and IFN-γ (62, 146). These immunoregulatory cytokines act to control viral infections directly by purging the cell through cytopathic or non-cytopathic means, or indirectly, by modulating the induction, amplification, recruitment, and effector functions of the immune response (62).

Interestingly, IRF-3a functions in a dominant-negative manner and selectively impedes IFN-β production in response to viral infection. In this way, relative levels of IRF-3a in a cell can dictate the extent of IFN-β produced by that cell. *In vitro* experiments, however, have demonstrated that several-fold over-expression of IRF-3a in relation to IRF-3 is required for significant modulation of IRF-3 transcriptional activity (106).

iv. RANTES expression

The pro-inflammatory CC-chemokine RANTES is a well-established chemoattractant for leukocytes (eosinophils, basophils, monocytes), NK cells, and T cells, including memory T lymphocytes, during inflammation and the immune response (147-150). In addition, RANTES is also believed to be an important mediator of T-lymphocyte-dependent immune responses (75). Both RANTES and its receptor CCR (CC chemokine receptor)-5 have been associated with Th1 immune responses and play an important role in T cell activation (75, 151-154).

In many cell types including monocytes/macrophages, fibroblasts, and epithelial cells, RANTES is expressed within hours of pro-inflammatory stimulation (155). However, RANTES gene expression typically varies between tissue type and applied stimulus, since the transcriptional machinery controlling RANTES expression differs between the cell types (148, 155-159). As there exists a large number of potential consensus sites within the immediate upstream region of the RANTES promoter, multiple control points of expression must be present (160). Indeed, different combinations of *cis*-regulatory elements of the promoter are required for optimal levels of transcription in several types of immune cells following cytokine stimulation (148, 155-159). For example, in T lymphocytes, NF-κB, NF-IL-6 (nuclear factor of interleukin-6), NF-AT (nuclear factor of activated T cells), and CD28RE (CD28 response element) binding sites are important regulatory elements of RANTES promoter activity (148, 160). Late RANTES mRNA expression, which occurs 3-5 days after T-cell activation (161), is believed to occur through binding of the late transcription factor RFLAT-1 (RANTES factor of activated T-lymphocytes-1) to the RANTES promoter. RFLAT-1 is induced 3 days after T-cell activation, and is a strong activator of the RANTES promoter in T-cells (162).

Working synergistically with NF-κB, IRF-3 plays an essential role in virus-inducible activation of RANTES gene expression through its activation and binding to the ISRE (IFN stimulated response element) on the RANTES promoter (100, 148, 149, 163). In this way, RANTES expression can be directly induced by activated IRF-3 in the absence of cytokines such as TNF-α, IL-1, and IFN-γ that are produced during acute inflammation (143, 163-165). Therefore, if the virus is able to attenuate IFN function, the production of RANTES from the infected cell will still allow for the recruitment of immune cells to the site of infection.

Both *in vivo* and *in vitro* studies have demonstrated an induction of RANTES expression very soon after Ad vector transduction. For example, Otake *et al.* (66) observed the induction of RANTES in murine lung tissue within hours of Ad vector transduction, and Muruve *et al.* (34) observed the induction RANTES mRNAs in murine liver tissue within 60 minutes of Ad vector delivery. In studies with PBMC, Higginbotham *et al.* (72) observed a significant up-regulation of RANTES expression over a 96-hour window following *in vitro* infection with wtAd5, ΔE1 and/or ΔE3 Ad5 vectors, and empty Ad capsids. Early induction of RANTES has also been observed following Ad vector transduction in HeLa cells, and in mouse insulinoma cell line TGP61 (34, 75). Furthermore, in primary kidney epithelial cells, RANTES expression is induced within 6 hr of Ad vector transduction (38), and in other epithelium-derived cell lines, RANTES induction can occur within hours of Ad vector transduction, and in the absence of TNF-α or type I IFNs (34, 73-76). Thus, in many cell types, RANTES induction can be used as a measure of innate immune activation by Ad.

1.2 Objective

The inflammatory response that accompanies Ad infection can be problematic for gene therapy studies, or beneficial as in wild type Ad infection. In either case, this response occurs early, as it is stimulated by the binding and/or entry of the Ad capsid to the cell and does not require viral gene expression. To date, the signal transduction pathways that direct this inflammatory response to Ad are not completely understood. Several studies have described the important role of transcription factor NF-kB in the activation of pro-inflammatory cytokines and chemokines early in Ad infection. For many other viruses, another key transcription factor, IRF-3, also acts early in viral infection. In addition to its ability to initiate the recruitment of pro-inflammatory cytokines and chemokines, IRF-3 is also responsible for the activation of a number of genes involved in the antiviral interferon response. While most studies have examined the IRF-3 signal transduction pathway in response to RNA viruses, to date, little work has focused on the activation of this pathway and its role in response to infection by DNA viruses such as Ad, which have strikingly different genetics, kinetics, and life cycles than those of RNA viruses. Thus far, no studies have determined if Ad infection initiates the pathways responsible for the phosphorylation and activation of IRF-3. Consequently, in this project, we sought to determine if Ad infection activates IRF-3 and is important in establishing an antiviral state in Ad infected cells by acting as a transcription factor to up-regulate pro-inflammatory genes associated with the interferon response.

1.3 Hypothesis

Since a number of studies using RNA viruses have revealed an important role for IRF-3 in the antiviral interferon response that corresponds with early inflammation, we

believe that IRF-3 also plays an important role in response to infection by DNA viruses, specifically adenovirus. We hypothesize that IRF-3 is phosphorylated and activated following wtAd5 infection. Furthermore, we hypothesize that IRF-3 plays an important role in the establishment of antiviral resistance to wtAd5 infection, specifically as a transcription factor in the up-regulation of pro-inflammatory chemokine RANTES.

1.4 Approach

Phosphorylation status of IRF-3 will be analyzed in infected cells, and an attempt will be made to determine which amino acid residue(s) are phosphorylated in response to Ad infection. In addition, we will determine the importance of IRF-3 in the induction of RANTES in Ad-infected cells through the use of reporter constructs containing various regions and transcription factor binding sites from the RANTES promoter. Taken together, these data will elucidate the importance of IRF-3 in the induction of innate immunity in Ad-infected cells.

1.5 Rationale

To date, the innate immune response to Ad is not completely understood. The recent reemergence of Ad-induced ARD in confined populations, as well as the prevalence of other Ad-related diseases in children, the elderly, and immuno-compromised individuals, demonstrate the need for an Ad vaccine and an effective antiviral compound or form of immunotherapy against Ad. Conversely, a current emphasis in Ad gene therapy research is to determine the mechanisms by which Ad induces the early inflammatory response, and to modify Ad vectors accordingly in order to eliminate this very dangerous and even lethal problem.

In order to elucidate novel methods to combat severe Ad diseases and develop nontoxic Ad vectors for gene therapy, a greater understanding of the immune response to Ad is necessary. With the goal of identifying potential targets for intervention to enhance/ repress the immune response to Ad, this project focuses specifically on the role of IRF-3, an important transcription factor that has not yet been investigated in Ad-induced immunity. *In vitro* characterization of the innate immune response to wtAd5 and Ad5-based vectors, with respect to IRF-3 activation, will map a major signaling pathway used by many viruses to combat infection, thus bringing new insight into the early immune response to Ad.

Chapter 2: MATERIALS AND METHODS

Reagents:

See Appendix A for list of reagents, solutions, and buffers used.

Cell culture and viral infections:

HeLa (human epithelium-derived; American Type Culture Collection [ATCC] CCL 2) and MRC5 (normal human lung fibroblast; ATCC CCL 171) cells were maintained in Dulbecco Modified Eagle Medium (DMEM, Sigma) supplemented with 10% fetal bovine serum (FBS), 1% GlutaMax, and 1% Antibiotic/Antimycotic (Invitrogen) at 37°C in 5% CO_2 atmosphere. 293 (166) and A549 (human lung epithelial adenocarcinoma; ATCC CCL 185) cells were maintained under the same conditions in Modified Eagle Medium (MEM, Sigma) supplemented with 10% FBS, 1% GlutaMax, and 1% Antibiotic/Antimycotic.

Wild type adenovirus serotype 5 was obtained from J. Bell (Ottawa Health Research Institute, Ottawa ON). Ad5 vectors used in the experiments were: AdCA35 (ΔE1Ad) from Addison *et al.* 1997 (167), AdRP2233 ($E1^{+}$ΔE3Ad) from Sargent *et al.* 2004 (168), Δ28lacZ (hdAd) from Palmer and Ng 2003 (169), and Ad5ts36 (DNA polymerase, temperature sensitive mutant of Ad5) from Wilkie *et al.* 1973 (170). All Ad infections were performed in DMEM-PBS (DMEM-phosphate buffered saline, Sigma) at multiplicities of infection (MOI) ranging from 1 to 500 PFU/cell for 1 hour at 37°C. A Vesicular Stomatitis Virus expressing green fluorescent protein (VSV-GFP), provided by J. Bell (Ottawa Health Research Institute) was used as a positive control in all experiments. Infections with VSV were carried out in serum-free MEM at MOI ranging from 1 to 10 PFU/cell for 1 hour at 37°C.

IRF-3 plasmid constructs and mutagenesis:

For a complete list of mutant FLAG-tagged IRF-3 plasmids used, including a detailed description of their construction, see Appendix B. Briefly, FLAG-tagged human IRF-3 was cloned into pcDNA3. Various serine/threonine residues representing possible IRF-3 phosphorylation sites were then mutated to alanine in a series of cloning steps involving the insertion of various mutated oligonucleotides (Sigma) into the pcDNA-FLAG-IRF-3 vector. In order to simplify cloning steps, many of the IRF-3 mutant sequences were also cloned into pBluescriptKS+ (Stratagene) vectors. Plasmid DNA was transformed into RbCl competent cells (prepared as in (171)) by heat shock method. Small scale preparation of DNA was preformed by alkaline lysis following methods described by Birnboim and Dolly (172), while large scale preparation of DNA was preformed by alkaline lysis with purification by CsCl buoyant density centrifugation as described in Sambrook *et al.* (173). All constructs were sequenced by StemCore Labs (Ottawa Health Research Institute, Ottawa, ON) to confirm their identity.

RANTES promoter constructs and mutagenesis:

The RANTES promoter reporter constructs (-296, -181, -90, -296mutNF-κB) used in this project were provided by D.A. Muruve (University of Calgary, Calgary AB). For a summary of each construct, see Appendix B. An additional plamsid -181mutISRE, was constructed for these studies and contains point mutations within the IRES of the RANTES promoter (see Appendix B for details). Briefly, a fragment of pGL2-RANTES(-181) containing the IRES was cloned into a pBluescriptKS+ vector, oligonucleotides (Invitrogen) containing the IRES point mutations were cloned into the -181 fragment, and the mutated

−181 fragment was then cloned back into the pGL2-RANTES(-181) vector. The ISRE mutation was created in the -181 construct and not the -296 construct simply due to the ease at which the smaller fragment could be cloned in and out of the pBluescriptKS+ vector. Transformation of plasmid DNA and preparation of small/large scale DNA were preformed as above. Mutations created in the -181mutISRE construct were confirmed by sequencing.

Transient transfections:

On the day prior to DNA transfection, 293 and HeLa cells were seeded at ~$1.0x10^6$ cells/35mm dish. Transfection of these cell lines were preformed in serum-free MEM and DMEM with Lipofectamine 2000 (Invitrogen) as per manufacturer's instructions. In all experiments, infection of transfected cells occurred 24 hr after transfection.

Immunoblot analysis:

HeLa, A549, MRC5, or 293 cells in 35mm dishes were harvested with 250 μL of 2x denaturing sample buffer containing β-mercaptoethanol, 10-15 μL of these lysates were subjected to electrophoresis on small or large format 7.5% acrylamide gels. Proteins were electrophoretically transferred onto PVDF membranes using semi-dry transfer (BioRad). The membranes were blocked in Tris-buffered saline (TBS) containing 5% nonfat dry milk and 0.1% Tween 20 (TBS-T), for 1 hr at room temperature with shaking, or at 4°C overnight. Primary and secondary antibodies were diluted in the blocking solution and incubated with the membranes at room temperature for 1 hr with shaking. After incubation with each antibody, the membranes were washed (with shaking) twice with TBS-T for 15 min at room temperature. The primary antibodies used in these studies were anti-IRF-3 rabbit polyclonal

(FL-425, Santa Cruz) (1:1700), anti-FLAG M2 mouse monoclonal (F3165-1MG, Sigma) (1:15000), anti-αtubulin mouse monoclonal (Ab-1, Oncogene) (1:5000), and anti-p38 rabbit polyclonal (sc-535, Santa Cruz) (1:200). Secondary antibodies used in these studies were IgG (H+L)-HRP-conjugated goat anti-rabbit (BioRad) (1:5000) and goat anti-mouse (BioRad) (1:5000). Membranes were developed with Pierce ECL Western Blotting Substrate (Pierce) or using the ECL+ plus Western Blotting Detection System (Amersham BioSciences) according to the manufacturer's instructions. To remove bound antibody from membranes for re-probing, membranes were washed (with shaking) twice with TBS-T for 5 min at room temperature and incubated in 15-20 mL Restore Western Blot Stripping Buffer (Pierce) for 20 min at 37°C. Membranes were washed (with shaking) twice with TBS-T for 5 min at room temperature then blocked in blocking solution for 1 hr at room temperature with shaking, or 4°C overnight.

Phosphatase treatment:

After removal of culture medium, infected/mock-infected HeLa cells were washed twice with cold DMEM PBS. Cells were incubated in 30 μL RIPA (RadioImmunoPrecipitation Assay) buffer for 20 min, monolayers removed by scraping into an microcentrifuge tube, and cell debris removed by centifugation for 15 min at 14000 x g, 4°C. The supernatent was divided into 4 separate tubes (70 μL each), and 10 mM $MgCl_2$ (final concentration) was added to each. Phosphatase treatment was started by adding calf intestinal phosphatase (CIP, New England Biolabs) to 3 of the 4 tubes in increasing concentrations (50, 200, 500 units). The first tube was not treated with CIP, but with the following phosphatase inhibitors: (final concentration) 10 mM NaF, 0.4 mM Na_3VO_4. The

reactions were incubated overnight at 37°C, after which 2x denaturing sample buffer was added to each tube. The samples were then resolved by SDS-PAGE, and analyzed by immunoblotting using anti-IRF-3 antibody.

Luciferase Assays:

After removal of culture medium, HeLa cells were harvested with 300 μL (for a 35mm dish) of Reporter Lysis Buffer (Promega) and frozen at -80°C. Cell lysates were thawed and pelleted after centrifugation at 14000 x g at 4°C for 2 min. Cell supernatant (50 μL) was added to 100 μL of Luciferase Assay Substrate (Promega), and luciferase activity was measured in relative luciferase units using a Lumat LB 9507 luminometer (EG&G Berthold).

Chapter 3: RESULTS

IRF-3 is phosphorylated rapidly after VSV infection and late after wtAd5 infection

Through immunoblot analysis, many studies have demonstrated IRF-3 phosphorylation in response to infection by RNA viruses (MeV, SeV, NDV, RSV, VSV) (99-101). This phosphorylation can be visualized as a shifting of band intensity from non-phosphorylated IRF-3 isoform I to a more slowly migrating isoform (form II) and by the presence of phosphorylated forms III and IV (indicative of IRF-3 activation), all of which are about 55kDa and can be detected by SDS-PAGE (96, 101, 108). For simplicity, a change in phosphorylation from that observed in mock-infected cells to a more highly phosphorylated form (*i.e.* a greater proportion of total IRF-3 located within the more highly phosphorylated isoform) will henceforth be referred to simply as "phosphorylation of IRF-3".

In order to examine IRF-3 phosphorylation in response to VSV infection, A549 cells were mock-infected or infected with VSV (MOI 10 PFU/cell) and harvested at 2, 6, and 24 hr post-infection for SDS-PAGE and immunoblot analysis. At 2 hr post-infection, there was no evidence of IRF-3 phosphorylation. However, by 6 hr, IRF-3 phosphorylation was confirmed through the detection of IRF-3 phosphorylated form III (Fig. 6*A*). Finally at 24 hr post-infection, IRF-3 was only detectable as isoform II, thus indicating degradation of activated IRF-3. A similar experiment using HeLa cells also demonstrated phosphorylation of IRF-3 at 6 hr following VSV infection, however the presence of IRF-3 phosphorylated form III could not be detected in this cell line (data not shown). Taken together, this data supports previous studies that IRF-3 is phosphorylated and activated after VSV infection, and also shows that this event coincides with VSV genome replication.

Figure 6. VSV and wtAd5-induced IRF-3 phosphorylation.
(*A*) A549 cells were mock-infected or infected with VSV (MOI 10 PFU/cell). (*B*) A549 cells were mock-infected (-) or infected with wtAd5 (MOI 1, 10, 50, 100, and 500 PFU/cell). In panels *A* and *B*, cell lysates were harvested with 2x denaturing sample buffer at 2, 6, and 24 hr post-infection, resolved by large format 7.5% SDS-PAGE, transferred to a PVDF membrane, and probed using anti-IRF-3 antibody (Santa Cruz). IRF-3 phosphorylation forms I, II, and III are indicated on each panel. Blots were re-probed with an antibody against α-tubulin to ensure equal loading.

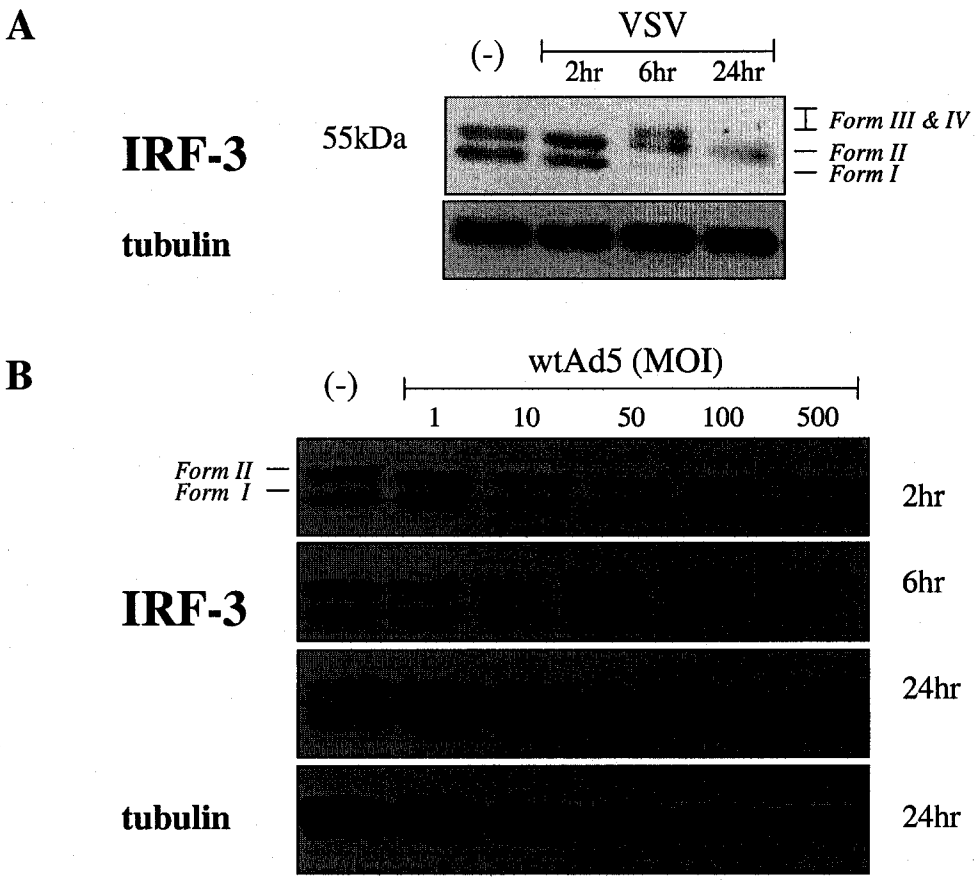

Although IRF-3 phosphorylation has been widely demonstrated to occur in response to infection by RNA viruses (99-101), phosphorylation of IRF-3 following Ad infection has not yet been investigated. To determine if wtAd5 infection leads to IRF-3 phosphorylation, A549 cells were mock-infected or infected with wtAd5 at increasing MOI (1-500 PFU/cell), and harvested at 2, 6, and 24 hr post-infection for SDS-PAGE and immunoblot analysis. At 2 hr post-infection, regardless of the MOI used on the cells, there was no evidence that IRF-3 phosphorylation had occurred (Fig. 6*B*). However, at 6 hr post-infection in cells infected at an MOI of 500 PFU/cell only, IRF-3 phosphorylation was evidenced as a shift in band intensity from non-phosphorylated IRF-3 isoform I to isoform II. At 24 hr after infection, this shift in band intensity was detected in all samples. Furthermore, as the MOI increased, so did the proportion of IRF-3 isoform II, so that at MOIs of 50, 100, and 500 PFU/cell, almost all IRF-3 was present in the upper isoform II band. Regardless of the MOI used, the presence of IRF-3 phosphorylated form III was not detected at 2, 6, or 24 hr post-infection. Comparable experiments with wtAd5-infected HeLa and MRC5 (normal human lung fibroblast) cells demonstrated a similar pattern of late IRF-3 phosphorylation (24 hr) without the detection of IRF-3 phosphorylated form III (data not shown). Although the band pattern in the tubulin loading control is uniform, in some instances it appears as though there may be more total IRF-3 when comparing IRF-3 isoform bands between sample lanes. It should be noted that while further testing is warranted, recent experiments in the Parks Lab have demonstrated that IRF-3 may be transcriptionally upregulated upon wtAd5 infection (~2 to 3-fold, R. Parks, personal communication).

To establish that the shift in IRF-3 band intensity observed in response to wtAd5 infection was due to phosphorylation, lysates of mock and wtAd5 infected HeLa cells were subjected to overnight treatment with increasing concentrations of calf intestinal phosphatase

(CIP) before separation by SDS-PAGE and subsequent immunoblot analysis. Although the presence of the upper IRF-3 band corresponding to phosphorylation form II remained detectable, the intensity of the band was dramatically diminished after CIP treatment, suggesting sensitivity to phosphatase treatment (Fig. 7). Therefore, the shift in IRF-3 band intensity observed in wtAd5-infected cells can be attributed to increased phosphorylation. Taken together, this data indicates that although IRF-3 phosphorylation form III is not detected, wtAd5 does induce phosphorylation of IRF-3. Furthermore, this phosphorylation event occurs late (24 hr) regardless of MOI, yet can occur early (6 hr) when cells are infected at a high MOI.

WtAd5 immunomodulatory genes affect IRF-3 phosphorylation

Much of the Ad E3 gene region codes for viral immunoregulatory genes that target processes essential for the survival of the virus during acute and latent infection (5). To investigate if these immunomodulatory genes affect wtAd5-induced IRF-3 phosphorylation, A549 cells were mock-infected or infected with an $E1^{+}\Delta E3Ad$ at increasing MOI (1-500 PFU/cell), and harvested at 24 hr post-infection for SDS-PAGE and immunoblot analysis. As previously described, at 24 hr post-infection, IRF-3 phosphorylation in wtAd5-infected A549 cells increased with increasing MOI, such that at MOIs of 50, 100, and 500 PFU/cell, almost all IRF-3 was present in the upper isoform II band (Fig. 6*B*). However, at 24 hr after $E1^{+}\Delta E3Ad$ infection, from MOIs of 10 PFU/cell onward, almost all IRF-3 was present in the upper isoform II band (Fig. 8). Additionally, at an MOI of 1 PFU/cell, the proportion of IRF-3 present in the lower isoform I band was comparable to that of wtAd5-infected cells at an MOI of 10 PFU/cell (Fig. 6*B*). From this data, it appears as though the proteins

Figure 7. Phosphatase sensitivity of wtAd5-induced IRF-3 phosphorylation.
HeLa cells were mock-infected (-) or infected with wtAd5 (MOI 10 PFU/cell). At 24 hr post-infection, cell lysates were harvested with RIPA buffer containing protease inhibitors. Lysates were subjected to overnight treatment with increasing concentrations of calf intestinal phosphatase (CIP), or phosphatase inhibitors (PI: NaF, Na_3VO_4) only (*lanes 1* and *5*) at 36°C. An equal volume of 2x denaturing sample buffer was added and the lysates were separated by 7.5% SDS-PAGE, transferred to a PVDF membrane and probed using anti-IRF-3 antibody (Santa Cruz).

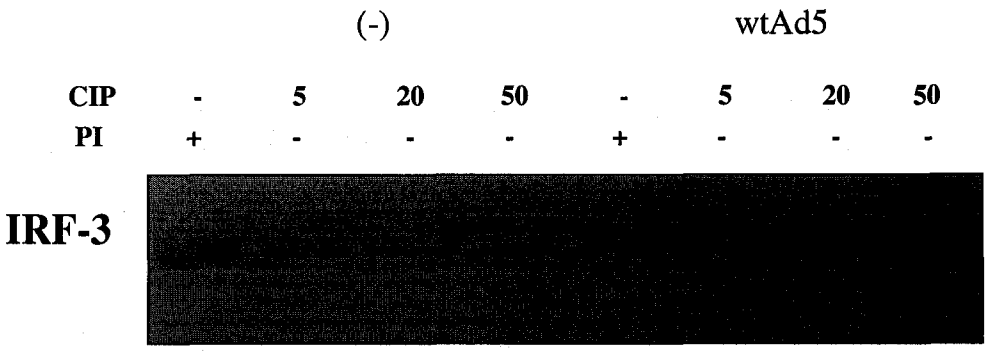

Figure 8. IRF-3 phosphorylation in ΔE3Ad infection at increasing MOI.
A549 cells were mock-infected or infected with $E1^{+}\Delta E3Ad$ (AdRP2233, MOI 1, 10, 50, 100, and 500 PFU/cell). Cell lysates were harvested with 2x denaturing sample buffer at 24 hr post-infection, resolved by large format 7.5% SDS-PAGE, transferred to a PVDF membrane, and probed using anti-IRF-3 antibody (Santa Cruz). IRF-3 phosphorylation forms I and II are indicated on each panel. The blot was re-probed with an antibody against α-tubulin to ensure equal loading (data not shown).

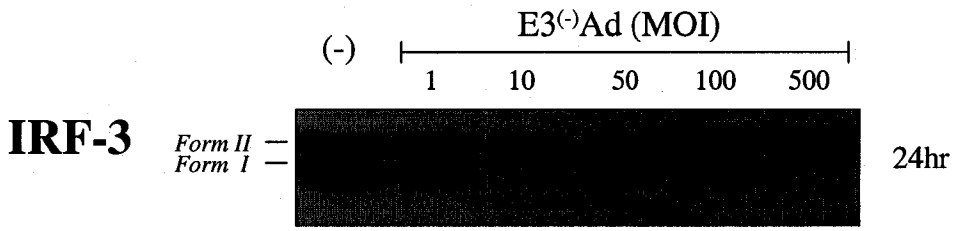

encoded within the E3 region may act to reduce phosphorylation of IRF-3 in the infected cell.

WtAd5-induced IRF-3 phosphorylation is replication-dependent

Interestingly, late wtAd5-induced IRF-3 phosphorylation occurs during the same time frame as the peak of Ad DNA replication. Two experiments were conducted to investigate whether virus replication is important for IRF-3 phosphorylation to occur in wtAd5-infected cells. First, HeLa cells were mock-infected or infected with wtAd5 (MOI 10 PFU/cell) or Ad5ts36 (MOI 10 PFU/cell), a temperature sensitive virus able to replicate at 32.5°C but not 38.5°C (170). The infected cells were incubated at 32.5°C or 38.5°C, and assayed for IRF-3 phosphorylation 24 and 48 hr after infection. Using immunoblot analysis, IRF-3 phosphorylation was detected at either temperature in the wtAd5-infected cells, however, for cells infected with Ad5ts36, phosphorylation of IRF-3 occurred only at the permissive temperature, 32.5°C, suggesting a requirement for DNA replication (Fig. 9). Basal differences in the proportion of IFR-3 phosphorylation forms I and II at 24 hrs in cells infected with wtAd5 incubated at different temperatures is most likely the result of Ad replication occurring more rapidly at the higher temperature.

In the next experiment, HeLa cells were mock-infected or infected with an E1-deleted Ad (ΔE1Ad) at increasing MOI (10-500 PFU/cell) or a hdAd (MOI 500 PFU/cell). At 24 hr post-infection, cells were harvested for separation by SDS-PAGE and subsequent immunoblot analysis. Although ΔE1Ads are replication deficient vectors, at very high MOI ΔE1Ads can circumvent the replication block created by the deletion of the E1 gene region (174). Regardless of MOI, hdAds are incapable of replication and, as such, IRF-3

Figure 9. IRF-3 phosphorylation in temperature sensitive Ad5ts36 infection.
HeLa cells were mock-infected (-) or infected with wtAd5 (MOI 10 PFU/cell) or Ad5ts36 (MOI 10 PFU/cell) and incubated at 32.5°C or 38.5°C. Cell lysates were harvested with 2x denaturing sample buffer at 24 and 48 hr post-infection, resolved by large format 7.5% SDS-PAGE, transferred to a PVDF membrane, and probed using anti-IRF-3 antibody (Santa Cruz).

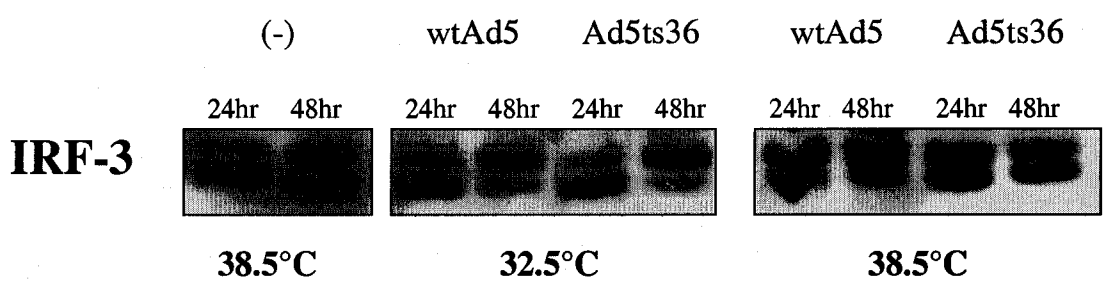

phosphorylation was not detected in the hdAd-infected cells (Fig. 10). In contrast, in the ΔE1Ad-infected cells, slight increases in the proportion of IRF-3 localized to isoform II were observed with increasing MOI, but IRF-3 phosphorylation was most apparent at an MOI of 500 PFU/cell, an MOI at which ΔE1Ad can replicate in HeLa cells. Data obtained from these two experiments clearly demonstrate that wtAd5-induced IRF-3 phosphorylation does not occur in the absence of replication. Thus, wtAd5-induced IRF-3 phosphorylation is replication-dependent.

The primary target for wtAd5-induced IRF-3 phosphorylation is a novel residue(s)

Phosphorylation of the IRF-3 protein can occur in four different regions: two within the N-terminus (residues Thr^{135} and Ser^{188}), and two within the C-terminus (residues Ser^{385}/Ser^{386}, and $Ser^{396}/Ser^{398}/Ser^{402}/Thr^{404}/Ser^{405}$) (96). The functional implication of N-terminal phosphorylation has yet to be fully elucidated, although, it is known that DNA-PK phosphorylation of Thr^{135} leads to nuclear retention of IRF-3, and that Ser^{188} is phosphorylated by a member of the MAPK family in response to stress and DNA damage (96, 101). Alternatively, C-terminal phosphorylation is indicative of IRF-3 activation, and occurs upon viral infection (96, 101, 105, 109, 110). The exact phosphorylation site required for virus-induced IRF-3 activation is still unclear, however experiments by Mori *et al.* and Servant *et al.* using SeV have narrowed down the most probable residues to Ser^{386} (108) or Ser^{396} (99).

To determine which amino acid residues of IRF-3 were phosphorylated in response to wtAd5 infection, a series of mutant FLAG-tagged IRF-3 plasmids containing substitutions of serine/threonine to alanine were generated for all known IRF-3 phosphorylation sites. These

Figure 10. IRF-3 phosphorylation in ΔE1Ad infection at increasing MOI.
HeLa cells were mock-infected (-) or infected with ΔE1Ad (AdCA35, MOI 10, 50, 100, and 500 PFU/cell) or hdAd (Δ28lacZ, MOI 500 PFU/cell). Cell lysates were harvested with 2x denaturing sample buffer at 24 hr post-infection, resolved by 7.5% SDS-PAGE, transferred to a PVDF membrane, and probed using anti-IRF-3 antibody (Santa Cruz). The blot was re-probed with an antibody against α-tubulin to ensure equal loading (data not shown).

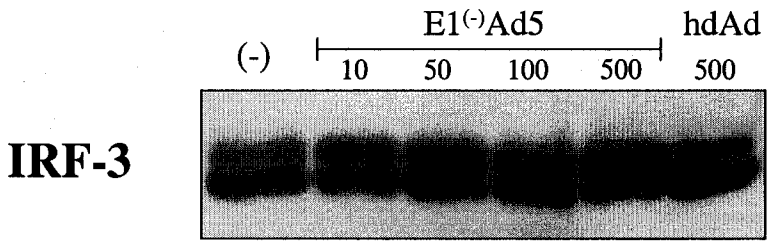

included mutations at Ser^{385}/Ser^{386} (mut2A) and $Ser^{396}/Ser^{398}/Ser^{402}/Thr^{404}/Ser^{405}$ (mut5A) within the C-terminus, as well as residues Thr^{135} (mut135) and Ser^{188} (mut188) within the N-terminus (Fig. 11*A*). A FLAG-tagged wild-type IRF-3 plasmid (wtIRF-3) was also created. All constructs were sequenced to confirm their identity. Equal expression of the constructs was confirmed by transfection into 293 cells, which were harvested for immunoblot analysis after 24 hr (Fig. 11*B*). The mutant FLAG-tagged IRF-3 plasmids were then transfected into HeLa cells, and either mock-infected or infected with wtAd5 (MOI 10 PFU/cell) 24 hr later. Cell lysates were harvested 24 hr post-infection for immunoblot analysis. Following wtAd5-infection, there was no significant effect on IRF-3 band distribution (Fig. 12), as most of the mutant proteins exhibited a similar distribution. Curiously, form II was detected with over-expression of the all-mutant IRF-3 construct (mut135/188/2A/5A). Since this construct is mutated in all known phosphorylation sites, this suggests there is another, as yet unidentified phosphorylation site that is normally partially phosphorylated in HeLa cells and is specifically hyperphosphorylated upon Ad infection.

RANTES induced after wtAd5 infection occurs late and is replication-dependent

The data shown above clearly demonstrates that Ad infection induces the phosphorylation of IRF-3. In the Ad-infected cell, phosphorylation appears to occur on a residue not previously identified in the literature. Importantly, mutation of amino acids previously associated with IRF-3 activation by RNA viruses (Ser^{386} and Ser^{396}) did not significantly alter the pattern of IRF-3 phosphorylation, as determined by immunoblot analysis. However, Collins *et al.* (175) have suggested that only a minor proportion of IRF-3 needs to be activated in a cell in order for a full interferon response to occur, and that this may not be detectable as a visible change in IRF-3 phosphorylation status by SDS-PAGE.

Figure 11. Mutant IRF-3 plasmids used to determine phosphorylation site(s) in wtAd5 infection. (*A*) Schematic representation of human IRF-3. The region between residues 128-142, 186-198, and 382-414 are expanded below the schematic to demonstrate the amino acids, *in large letters*, targeted for alanine substitutions. The point mutations are indicated below the sequence: T135A, S188A, 2A (S385A, S386A), and 5A (S396A, S398A, S402A, T404A, S405A). (*B*) Mutant FLAG-tagged IRF-3 plasmids mut135/188/2A/5A, mut2A/5A, mut135/188, mut2A, mut5A, mut135, and mut188 as well as a wt FLAG-tagged IRF-3 plasmid, were transfected into 293 cells to verify expression. At 24 hr post-transfection, cell lysates were harvested with 2x denaturing sample buffer, resolved by 7.5% SDS-PAGE, transferred to a PVDF membrane, and probed using anti-FLAG M2 antibody (Sigma). Panel *A* is an adaptation of a figure from Servant *et al.* 2002 (96).

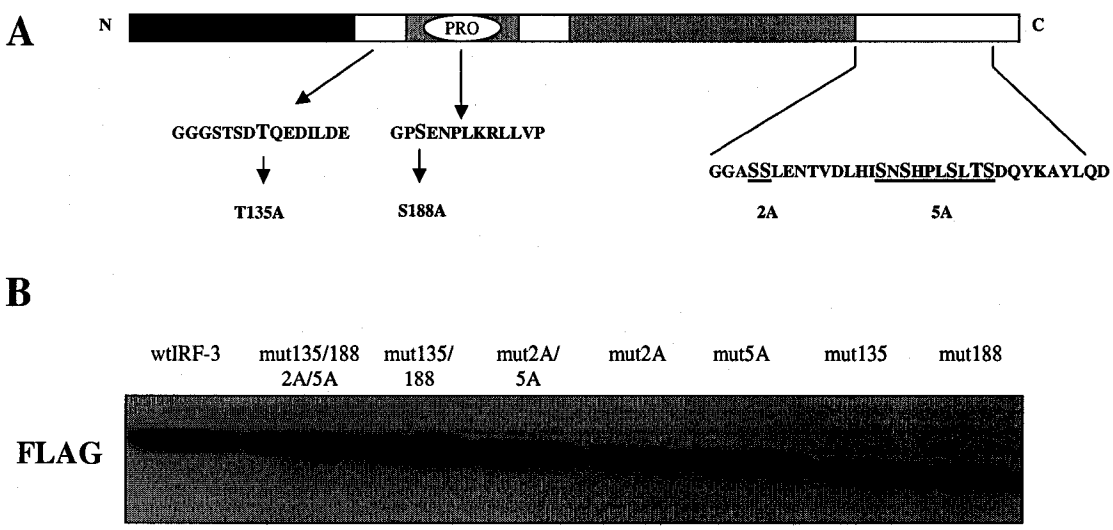

Figure 12. Analysis of wtAd5-induced IRF-3 phosphorylation.
HeLa cells were transfected with the FLAG-tagged IRF-3 plasmids, mut135/188/2A/5A, mut2A/5A, mut135/188, mut2A, mut5A, mut135, and mut188, and wt IRF-3. At 24 hr post-transfection, cells were mock-infected (-) or infected with wtAd5 (MOI 10 PFU/cell). Cell lysates were harvested with 2x denaturing sample buffer at 24 hr post-infection, resolved by large format 7.5% SDS-PAGE, transferred to a PVDF membrane, and probed using anti-FLAG M2 antibody (Sigma). The blot was re-probed with an antibody against p38 to ensure equal loading (data not shown).

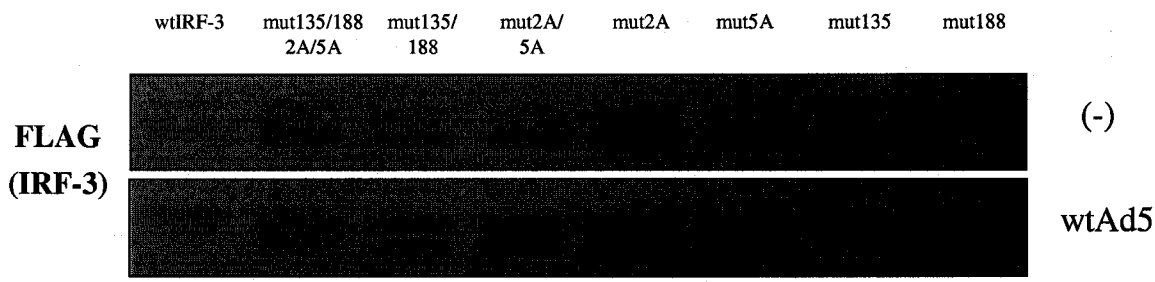

Therefore, an examination of IRF-3 activation was conducted by investigating its role in establishing an anti-viral state in wtAd5-infected cells. This was carried out by specifically examining the importance of IRF-3 as a transcription factor in the upregulation of the pro-inflammatory chemokine RANTES. Working synergistically with NF-κB, IRF-3 is known to play an essential role in virus-induced activation of RANTES gene expression through binding to the ISRE on the RANTES promoter (100, 148, 149, 163).

In this experiment, HeLa cells were transfected with the luciferase reporter construct pGL2-RANTES(-296) containing a fragment of the human RANTES promoter from position -296 (296 nucleotides from the transcription start site) (75). After 24 hr, transfected cells were either mock-infected or infected with wtAd5 (MOI 10 PFU/cell), and at 2 or 24 hr post-infection, crude lysates were prepared and assayed for luciferase activity. At 2 hr post-infection, luciferase activity levels were comparable in the mock and wtAd5-infected cells (Fig. 13). However, by 24 hr, there was a 7-fold increase in luciferase activity in the wtAd5-infected cells as compared to the mock-infected cells. This increase in luciferase activity represented a 3-fold increase in the induction of RANTES expression from 2 to 24 hr in wtAd5-infected cells. In a similar experiment, HeLa cells were transfected with pGL2-RANTES(-296), and 24 hr later were mock-infected or infected with wtAd5 at increasing MOI (1-100 PFU/cell). Cell lysates were harvested and assayed for luciferase activity 24 hr post-infection. Luciferase activity increased with increasing MOI to a maximum at an MOI of 50 PFU/cell (Fig. 14). At an MOI of 100 PFU/cell, luciferase activity levels were comparable to those measured in cells that were infected at an MOI of 10 PFU/cell; however, at an MOI of 100, the cell monolayer showed significant cytopathic effect, suggesting the virus had caused substantial cell death at the higher MOI. These data indicate that RANTES expression is induced by wtAd5, and this occurs late in the Ad life cycle.

Figure 13. WtAd5-induced RANTES expression.
HeLa cells were transfected with the luciferase reporter construct pGL2-RANTES(-296) containing a fragment of the human RANTES promoter (Bowen *et al.* (75)), and either mock-infected or infected with wtAd5 (MOI 10 PFU/cell) 24 hr post-transfection. Cell lysates were harvested with reporter lysis buffer at 2 or 24 hr post-infection and analyzed for luciferase activity (expressed in RLU, relative light units). Each value represents the average of duplicate samples, while error bars represent the range between duplicate samples. The data are representative of two different experiments with similar results. Statistical analysis was preformed by a two-tailed Student's t-Test assuming two-sample equal variance. Statistically significant differences ($p \leq 0.025$) are noted (**).

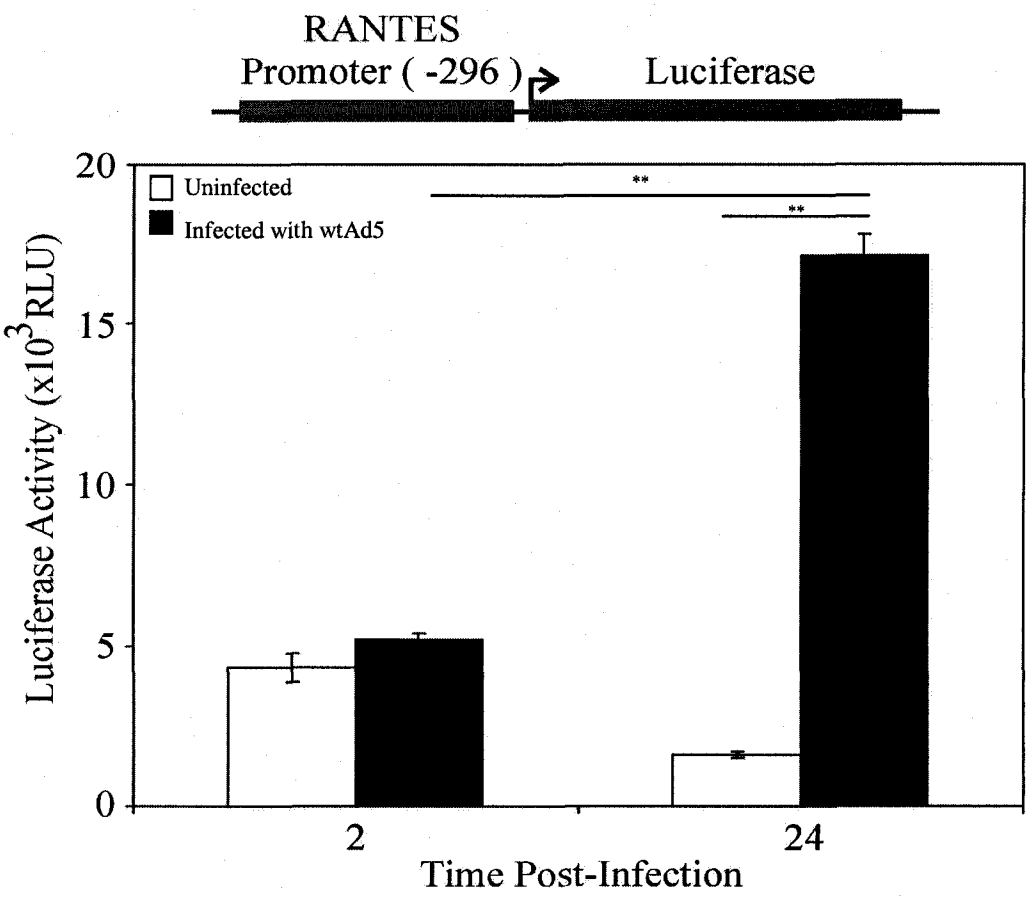

Figure 14. Optimal MOI for wtAd5-induced RANTES expression.
HeLa cells were transfected with pGL2-RANTES(-296) and either mock-infected (-) or infected with wtAd5 (MOI 1, 10, 50, and 100 PFU/cell) 24 hr post-transfection. Cell lysates were harvested with reporter lysis buffer at 24 hr post-infection and analyzed for luciferase activity (expressed in RLU, relative light units). Each value represents the average of duplicate samples, while error bars represent the range between duplicate samples. The data are representative of three different experiments with similar results. Statistical analysis was preformed by a two-tailed Student's t-Test assuming two-sample equal variance.

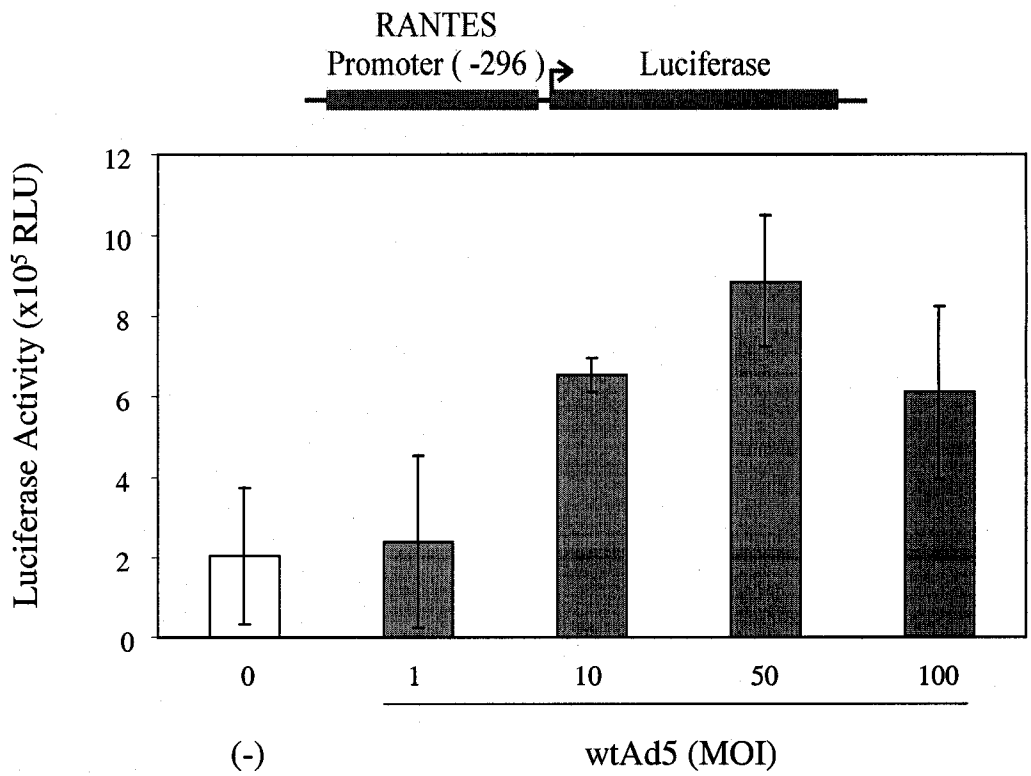

Curiously, like wtAd5-induced IRF-3 phosphorylation, this late wtAd5-induced RANTES expression occurs during the peak of Ad DNA replication. To determine if virus replication is important for RANTES expression in wtAd5-infected cells, HeLa cells were transfected with pGL2-RANTES(-296), and 24 hr later were mock-infected or infected with an ΔE1Ad at increasing MOI (1-100 PFU/cell). Luciferase activity was assayed from cell lysates that were harvested 24 hr post-infection. As previously mentioned, ΔE1Ads are replication deficient vectors, but can circumvent the replication block imposed by the deletion of the E1 gene region at very high MOI (174). In this assay, a notable increase in luciferase activity was not apparent until cells were infected with the ΔE1Ad at an MOI of 100 PFU/cell, an MOI at which ΔE1Ad can replicate in HeLa cells (Fig. 15). This increase in luciferase activity represented a 10-fold increase in the level of RANTES expression when compared to the level measured in the mock-infected cells. Together, these data suggest that like IRF-3 phosphorylation, RANTES expression following wtAd5 infection occurs late and is dependent on viral replication.

Full induction of RANTES expression after wtAd5 infection is dependent on IRF-3

Virus-inducible activation of RANTES gene expression is regulated through binding of both IRF-3 and NF-κB to specific binding domains on the RANTES promoter (100, 148, 149, 163). To determine the relative contribution of each transcription factor to RANTES expression, HeLa cells were transfected with a series of luciferase reporter constructs containing deletional mutants of the fragment of the human RANTES promoter contained within pGL2-RANTES(-296) (75). While constructs pGL2-RANTES(-296) and pGL2-RANTES(-181) contain both NF-κB and IRF-3 binding sites, pGL2-RANTES(-90) contains

Figure 15. ΔE1Ad-induced RANTES expression.
HeLa cells were transfected with pGL2-RANTES(-296) and either mock-infected (-) or infected with ΔE1Ad (AdCA35, MOI 10, 50, 100, and 500 PFU/cell) 24 hr post-transfection. Cells lysates were harvested with reporter lysis buffer at 24 hr post-infection and analyzed for luciferase activity (expressed in RLU, relative light units). Each value represents the average of duplicate samples, while error bars represent the range between duplicate samples. The data are representative of three different experiments with similar results. Statistical analysis was preformed by a two-tailed Student's t-Test assuming two-sample equal variance.

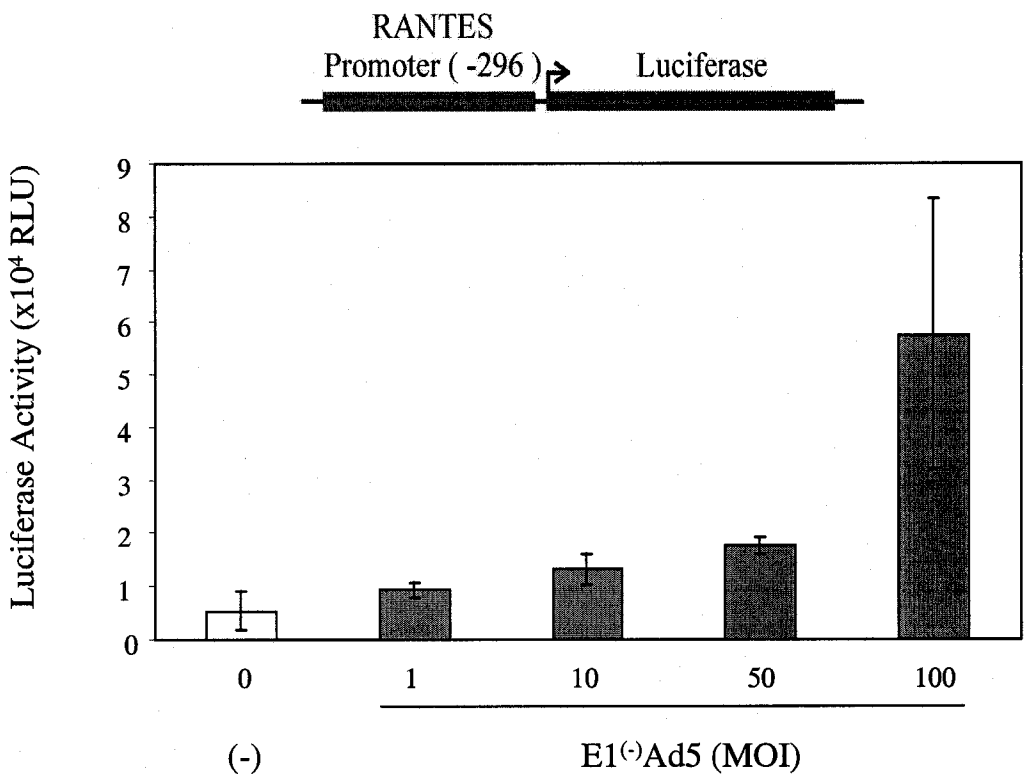

only the NF-κB binding sites, and pGL2-RANTES(-296mutκB) contains point mutations within the NF-κB binding sites thus containing only the IRF-3 binding sites (Fig. 16*A*). At 24 hr post-transfection, the HeLa cells were either mock-infected or infected with wtAd5 (MOI 50 PFU/cell), and luciferase activity was assayed from cell lysates that were harvested 24 hr post-infection. We observed significant increases in luciferase activity levels in each of the transfected wtAd5-infected cells when compared to their mock-infected counterparts (Fig. 16*B*). However, relative to the -296 construct, wtAd5-infected cells that were transfected with -90 and -296mutκB induced almost 2-fold and 8-fold less luciferase activity, respectively. Furthermore, wtAd5-infected cells that were transfected with -90 induced 5-fold more luciferase activity than -296mutκB-transfected cells. These data suggest while IRF-3 is important in wtAd5-induced RANTES expression, a slightly higher level of RANTES expression can be attributed to NF-κB binding activity. Nevertheless, both NF-κB and IRF-3 are required for full RANTES induction.

It is possible that decreased luciferase activity observed in the pGL2-RANTES(-90) wtAd5-infected cells, as compared to the -296 and -181 wtAd5-infected cells, could be influenced by structural and conformational restrictions placed on the -90 construct due to its significantly truncated RANTES promoter region. Therefore, we generated a luciferase reporter construct containing point mutations within the IRF-3 binding site of a longer RANTES promoter (-181mutISRE) (Fig. 17*A*). HeLa cells were transfected with pGL2-RANTES(-296), pGL2-RANTES(-181), pGL2-RANTES(-296mutκB), or pGL2-RANTES(-181mutISRE), and either mock-infected or infected with wtAd5 (MOI 10 PFU/cell) 24 hr post-transfection. Cell lysates were harvested and assayed for luciferase activity 24 hr post-infection. A significant increase in luciferase activity levels was observed in wtAd5-infected

Figure 16. Contribution of IRF-3 and NF-κB in wtAd5-induced RANTES expression as observed using fragments of a deletional mutant of the human RANTES promoter. (*A*) Schematic representation of the human RANTES promoter reporter constructs used in this study. All reporter constructs contain fragments of the RANTES promoter, however, -296 and -181 contain both NF-κB and IRF-3 binding sites, while -90 contains the NF-κB binding sites alone. The -296mutκB construct contains point mutations within the NF-κB binding sites. All constructs are from Bowen *et al.* 2002 (75). (*B*) HeLa cells were transfected with luciferase reporter constructs pGL2-RANTES(-296), pGL2-RANTES(-181), pGL2-RANTES(-296mutκB), or pGL2-RANTES(-90), and either mock-infected or infected with wtAd5 (MOI 50 PFU/cell) 24 hr post-transfection. Cells lysates were harvested with reporter lysis buffer at 24 hr post-infection and analyzed for luciferase activity (expressed in RLU, relative light units). Each value represents the average of duplicate samples, while error bars represent the range between duplicate samples. The data are representative of three different experiments with similar results. Statistical analysis was preformed by a two-tailed Student's t-Test assuming two-sample equal variance. Statistically significant differences ($p \leq 0.025$) are noted (**).

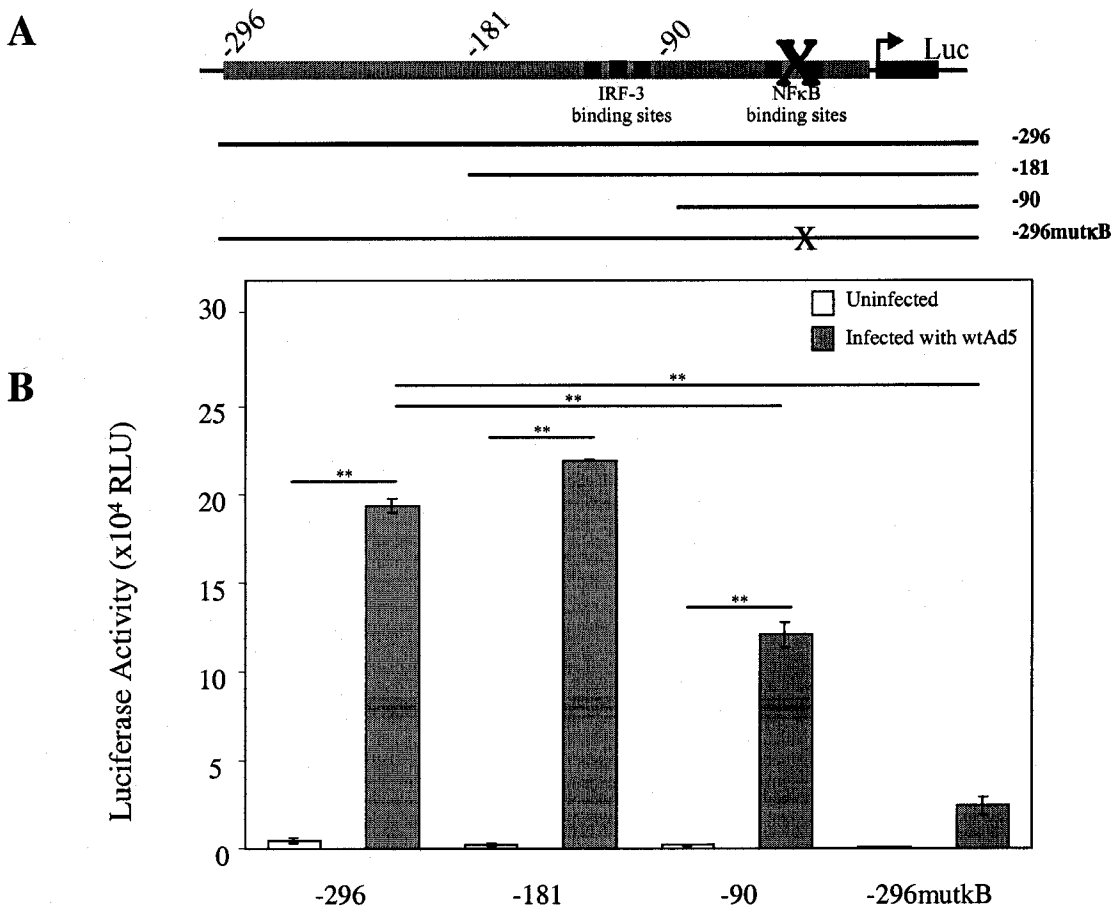

Figure 17. Contribution of IRF-3 and NF-κB in wtAd5-induced RANTES expression as observed using human RANTES promoter constructs containing point mutations within IRF-3 and NF-κB binding sites. (*A*) Schematic representation of the human RANTES promoter reporter constructs containing point mutations. Sequences of wild-type and mutated RANTES promoters are expanded below the schematic and nucleotide substitutions introduced in the ISRE or NF-κB binding motifs are underlined. All constructs with the exception of -181mutISRE, which was constructed for this project, are from Bowen *et al.* 2002 (75). Panel *A* is based on a figure from Génin *et al.* 2000 (149). (*B*) HeLa cells were transfected with luciferase reporter constructs pGL2-RANTES(-296), pGL2-RANTES(-181), pGL2-RANTES(-296mutκB), or pGL2-RANTES(-181mutISRE), and either mock-infected or infected with wtAd5 (MOI 10 PFU/cell) 24 hr post-transfection. Cells lysates were harvested with reporter lysis buffer at 24 hr post-infection and analyzed for luciferase activity (expressed in RLU, relative light units). Each value represents the average of duplicate samples, while error bars represent the range between duplicate samples. The data are representative of two different experiments with similar results. Statistical analysis was preformed by a two-tailed Student's t-Test assuming two-sample equal variance. Statistically significant differences ($p \leq 0.025$) are noted (**).

A

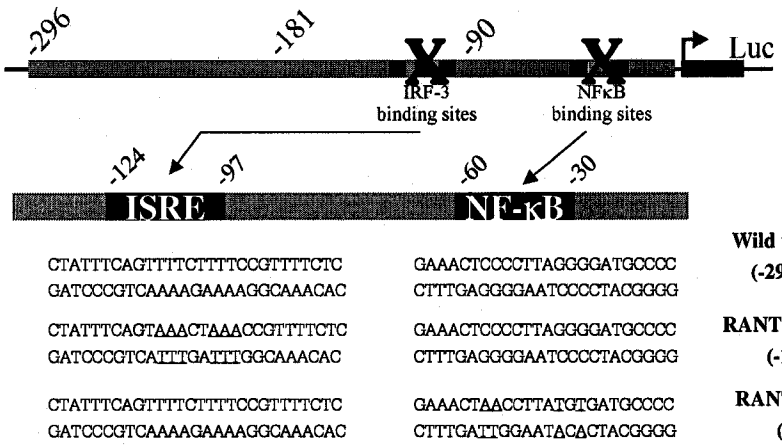

B

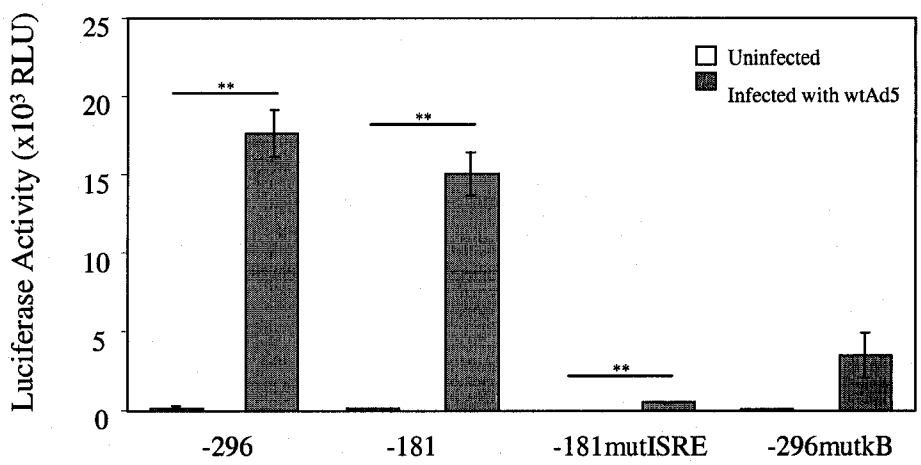

cells that were transfected with -296 and -181 compared to their mock-infected counterparts (105 and 120-fold increases, respectively) (Fig. 17*B*). In comparison, while cells transfected with -181mutISRE and -296mutκB also demonstrated increased luciferase activity levels upon wtAd5-infection when compared to mock infected levels (75 and 56-fold, respectively), these increases were not as high as those observed in cells transfected with the unmutated –296 and –181 constructs. Similar to our previous experiment, these data suggest that binding to both the ISRE and the NF-κB binding site are required for optimal RANTES induction in wtAd5-infected cells. However, in this experiment, a more complete model of RANTES promoter activity, abrogation of NF-κB and IRF-3 binding caused comparable decreases in RANTES expression, suggesting that IRF-3 and NF-κB contribute equally to wtAd5-induced RANTES expression.

Over-expression of phosphorylation-mutant IRF-3 reduces wtAd5-mediated RANTES induction

To further examine whether IRF-3 is important for RANTES induction in wtAd5-infected cells, expression from a RANTES luciferase reporter construct was characterized in the presence of over-expressed wildtype or dominant-negative IRF-3. In the first experiment, HeLa cells were co-transfected with pGL2-RANTES(-296) and either wtIRF-3 or an empty pcDNA3 plasmid. After 24 hr, cells were mock-infected or infected with wtAd5 (MOI 10 PFU/cell), and cell lysates were harvested and assayed for luciferase activity 24 hr post-infection. Luciferase analysis demonstrated that transfection of wtIRF-3 resulted in a significant increase in luciferase expression (Fig.18*C*), suggesting that over-expression of wtIRF-3 in Ad-infected cells leads to increased levels of RANTES expression.

Figure 18. IRF-3 activation in wtAd5-induced RANTES expression.
(*A*) Schematic representation of the human RANTES luciferase reporter construct. (*B*) Schematic representation of an IRF-3 phosphorylation-mutant construct. The region between residues 382-414 is expanded below the schematic to demonstrate the amino acids, *in large letters*, in this construct that were targeted for alanine substitutions. The point mutations are indicated below the sequence: 2A (S385A, S386A) and 5A (S396A, S398A, S402A, T404A, S405A). (*C*) HeLa cells were co-transfected with pGL2-RANTES(-296) and either wtIRF-3 or empty pcDNA3, and mock-infected or infected with wtAd5 (MOI 10 PFU/cell) 24 hr post-transfection. (*D*) HeLa cells were co-transfected with pGL2-RANTES(-296) and either wtIRF-3 or IRF-3(mut2A/5A), and mock-infected or infected with wtAd5 (MOI 10 PFU/cell) 24 hr post-transfection. In panels *C* and *D*, cell lysates were harvested with reporter lysis buffer at 24 hr post-infection and analyzed for luciferase activity (expressed in RLU, relative light units). Each value represents the average of duplicate samples, while error bars represent the range between duplicate samples. Statistical analysis was preformed by a two-tailed Student's t-Test assuming two-sample equal variance. Statistically significant differences ($p \leq 0.025$) are noted (**).

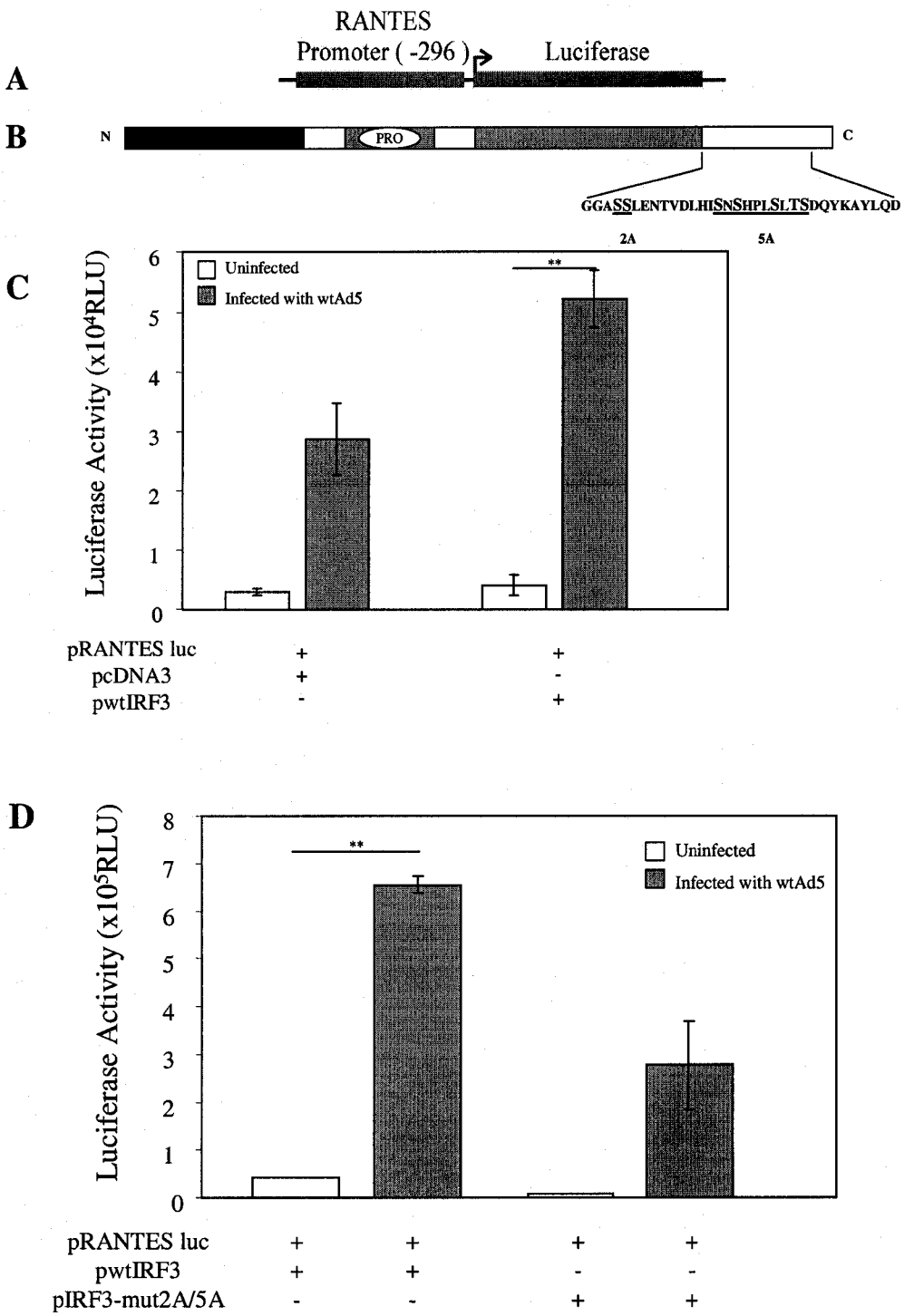

In the second experiment, HeLa cells were co-transfected with pGL2-RANTES(-296) and either wtIRF-3 or IRF-3(mut2A/5A). After 24 hr, cells were either mock-infected or infected with wtAd5 (MOI 10 PFU/cell), and cell lysates were harvested and assayed for luciferase activity 24 hr post-infection. Transfecton of IRF-3(mut2A/5A) resulted in an over 2-fold decrease in luciferase expression, compared to cells transfected with the wtIRF-3 expression construct (Fig.18*D*). These data suggest that full induction of RANTES does not occur when IRF-3 phosphorylation at C-terminal residues Ser^{396}, Ser^{398}, Ser^{402}, Thr^{404} and Ser^{405}, in addition to residues Ser^{385} and Ser^{386}, is not permitted. Taken together, both experiments clearly suggest that IRF-3 phosphorylation at residues located within the 382-414 region of the IRF-3 C-terminus are important in wtAd5-induced activation of IRF-3, and therefore provide additional evidence that IRF-3 activation is important for RANTES expression in wtAd5 infection.

In summary these data suggest that wtAd5 infection results in phosphorylation of IRF-3 on a novel amino acid residue, and this event is dependent on virus replication. Moreover, IRF-3 is an important transcription factor for induction of RANTES expression in wtAd5-infected cells. Taken together, these data suggest that IRF-3 activation in response to Ad DNA replication is important in establishing an anti-viral state within the infected cell.

Chapter 4: DISCUSSION

Adenovirus infection, both naturally and after delivery of an Ad-based gene therapy vector, is accompanied by a strong inflammatory response initiated by the induction of the innate immune response. This response occurs very early, and is stimulated by the binding and/or entry of the Ad capsid to the cell and does not require viral gene expression. Although the signal transduction pathways that direct the innate immune response to Ad are not yet fully elucidated, much evidence has linked transcription factor NF-kB to the activation of pro-inflammatory cytokines and chemokines early in Ad infection. For many RNA viruses, another key transcription factor, IRF-3, is also known to act early in viral infection. Like NF-kB, IRF-3 can initiate pro-inflammatory cytokine and chemokine expression, and is also responsible for the activation of a number of genes involved in the antiviral interferon response. Although many studies have examined the IRF-3 signal transduction pathway in response to RNA viruses, few studies have examined the role of IRF-3 in activating immune responses to DNA viruses.

The goal of this research was to determine if IRF-3 plays a role in the induction of innate immunity against Ad. We hypothesized that following wtAd5 infection, IRF-3 is phosphorylated and activated in order to participate in the establishment of antiviral resistance to wtAd5 infection. Our data indicates that wtAd5 infection results in the phosphorylation of IRF-3 on a novel amino acid residue, and this phosphorylation event is dependent on viral replication. Moreover, in wtAd5-infected cells, IRF-3 is an important transcription factor for the induction of RANTES, our model inflammatory chemokine. Finally, our data also suggests that Ad-infection results in at least two phosphorylation events on IRF-3: one event occurring in the N-terminus (discussed below) resulting in a protein shift

observed by SDS-PAGE and a second event occurring in the C-terminus of a small portion of IRF-3 within the cell leading to activation. Taken together, these data indicate that IRF-3 activation in response to Ad DNA replication is important in establishing an antiviral state within the infected cell.

WtAd5-induced IRF-3 phosphorylation

To establish a positive control capable of serving as a model for the detection of wtAd5-induced IRF-3 phosphorylation, we first studied IRF-3 phosphorylation in response to VSV infection. VSV has been shown previously to activate IRF-3 (99, 101, 102). Through immunoblot analysis of lysates from VSV-infected A549 cells, we detected IRF-3 phosphorylation by the appearance of IRF-3 phosphorylated form III at 6 hr post-infection. We also observed degradation of IRF-3, by 24 hr after VSV infection (Fig. 6*A*). These findings are in agreement with studies conducted by tenOever *et al.* (102), who detected IRF-3 phosphorylated form III early (by 8 hr) with a shift back to isoform II occurring at later time points with VSV infection of A549 cells. A similar experiment with VSV conducted in HeLa cells yielded different results: we identified early phosphorylation of IRF-3 as a shift in band intensity from non-phosphorylated IRF-3 isoform I to isoform II, but isoform III was not detected (data not shown). This effect could be the result of various disruptions in cellular signaling pathways caused by the HPV18 (human papillomavirus 18) genes found within the HeLa genome (176). Indeed, HPV genes E6 and E7 are known to play a role in the suppression of IFN expression and signaling (177), and *in vitro* experiments by Ronco *et al.* (124) have demonstrated that HPV16 E6 interacts strongly with IRF-3 thereby inhibiting its ability to transactivate. However, only a moderate interaction was observed between HPV18 E6 and IRF-3, thus the effect of HPV18 E6 on the IRF-3 activation pathway was not

studied (124). Thus, although HPV genes expressed in HeLa cells may impact visible formation of IRF-3 form III (as assessed by SDS-PAGE), they do not appear to affect IRF-3's ability to transactivate target genes (as assessed by our RANTES-luc reporter constructs).

Once a positive model of IRF-3 phosphorylation in VSV infection was established, we proceeded to examine wtAd5-induced IRF-3 phosphorylation. As previously mentioned, HeLa cells are most often used for Ad studies since Ads grow in them rapidly and to high yield, and as such, the time course of Ad replication in this cell line has been well characterized (14, 15). Ad replication studies conducted by the Parks lab have demonstrated a similar time course of Ad replication in A549 cells (data not shown). Since the IFN signaling pathway is not disrupted in the A549 cell line, we used wtAd5-infected A549 cells to examine IRF-3 activity wherever possible.

In both wtAd5-infected HeLa (data not shown) and A549 cells, we determined that IRF-3 phosphorylation occurs late in the Ad life-cycle (24 hr post-infection), yet can occur early (6 hr post-infection) during infections at very high MOI (500 PFU/cell) (Fig. 6*B*). We detected wtAd5-induced IRF-3 phosphorylation as a shift in band intensity from predominantly non-phosphorylated IRF-3 isoform I to isoform II by SDS-PAGE. Importantly, we established that the shifting pattern we observed upon wtAd5 infection was indeed due to phosphorylation by demonstrating that the majority of the upper IRF-3 band was sensitive to phosphatase treatment (Fig. 7). Thus, Ad infection of a cell does result in a change in the phosphorylation status of IRF-3. It is conceivable that additional post-translational modifications to the IRF-3 protein such as SUMOylation or mono-ubiquitination could account for the portion of IRF-3 in the upper-band that was still visible after phosphatase treatment. Simple experiments involving lysate incubation with inhibitors

of the SUMOylation or ubiquitination pathways would provide further insight into this possibility.

Although we identified wtAd5-induced IRF-3 phosphorylation as a shift in band intensity from predominantly non-phosphorylated IRF-3 isoform I to isoform II, we were not able to detect IRF-3 phosphorylated form III or IV. Studies by Collins *et al.* (175) showed a similar phosphorylation pattern upon infection of cells by another DNA virus, HSV. Comparing the IRF-3 phosphorylation patterns they observed in response to infection by a number of different viruses, they determined that hyper-phosphorylation of IRF-3 is virus and cell-type dependent and ISG induction - a common indicator of IRF-3 activation - can occur without visible levels of hyper-phosphorylated IRF-3. As such, it appears as though hyper-phosphorylation is not a perfect marker of IRF-3 activation, but is most likely representative of the cell's response to strong RNA virus replication (175). Since Ad is a DNA virus, it is perhaps not surprising that we were unable to detect phosphorylated form III upon wtAd5 infection.

WtAd5 immunomodulatory genes interfere with IRF-3 phosphorylation

Intriguingly, we observed a greater proportion of phosphorylated IRF-3 at lower MOI (24 hr) in cells infected with an $E1^{+}\Delta E3$Ad (Fig. 8) than in those infected with wtAd5 (Fig. 6*B*). Therefore, it appears as though the proteins encoded by genes within the E3 region may act to reduce IRF-3 phosphorylation in the infected cell. The E3 genes are most often deleted from Ad vectors used for gene therapy, and are not essential for replication in cultured cells (5). As previously mentioned, much of the Ad E3 gene region encodes for viral immunoregulatory genes that work to prevent the infected cell from being targeted and prematurely killed by the immune system during acute and latent infection (5). Various

functions have been attributed to proteins encoded in the E3 regions including inhibition of peptide presentation by class I MHC, and cell death by TNFα-, Fas-, or TRAIL (TNF-related apoptosis-inducing ligand)-induced mechanisms of cytolysis (178) Specifically, AdE3/10.4K and AdE3/14.5K transmembrane proteins form the receptor internalization and degradation (RID) complex which downregulates a specific set of cell surface receptors including the TNF receptor (TNFR) and family members Fas and TRAIL receptor (TRAIL-R) (179). *In vitro*, the RID complex inhibits TNFα-induced chemokine production and NFκB activation by downregulating cell surface levels of TNFR-1 (180-182). It is possible that E3 proteins could function in much the same way to target upstream signaling events in the pathway to IRF-3 phosphorylation in order to inhibit IRF-3 activation. Indeed, many RNA viruses have acquired functions to target different steps of the innate immune response, and a common tactic of RNA viruses involves the production of antagonists of the IFN response (183, 184). Viral proteins that specifically prevent IRF-3 activation pathways have been identified recently in the RSV genome (nonstructural (NS) proteins) as well as in the rabies virus (RV) genome (phosphoprotein (P)) (183, 184). Once the mechanism of IRF-3 activation in Ad infection has been elucidated, it is possible that proteins involved in indirectly targeting IRF-3 activation as well as IRF-3 specific antagonists may be revealed. It would not be surprising to find proteins such as these encoded within the Ad E3 gene region.

WtAd5-induced IRF-3 phosphorylation is dependent on viral replication

Interestingly, wtAd5-induced phosphorylation of IRF-3 occurs late during infection and coincides with the peak of Ad DNA replication (24 hr post-infection). Data from two

separate experiments (Figs. 9, 10) demonstrated that IRF-3 phosphorylation upon wtAd5 infection is dependant on virus replication. Our experiments did not establish if DNA replication *without* viral gene expression is required for IRF-3 phosphorylation upon wtAd5 infection. It would be interesting to determine if IRF-3 phosphorylation is dependent on the expression of viral proteins such as DNA polymerase, which are involved in viral DNA replication and are expressed early in the Ad life cycle.

There are a number of other possible mechanisms the cell may use to detect Ad5 infection/replication that could result in IRF-3 phosphorylation. First, the presence of small sections of replicated Ad DNA triggers DNA repair responses, specifically DNA-PK, a protein involved in sensing DNA damage and inducing proteins involved in DNA repair (185). DNA-PK is also known to directly phosphorylate IRF-3 near the nuclear export sequence on residue Thr^{135}, causing IRF-3 to be retained in the nucleus and triggering a downregulation in IRF-3 proteolysis which is important for maximizing the duration of the response (96, 101). Of course, nuclear retention is also critical for the induction of genes involved in the interferon response. Upon wtAd5 infection, we did not observe phosphorylation at Thr^{135} (Fig. 12). This observation may be explained by the presence of proteins, encoded in the Ad5 E4 gene region, which directly bind to and inhibit DNA-PK (186, 187). Therefore, if a minor portion of DNA-PK escapes inhibition by Ad E4 proteins, IRF-3 phosphorylation is possible.

A second mechanism by which Ad infection may lead to IRF-3 phosphorylation is through the detection of dsRNA within the cell. Most RNA viruses produce dsRNA as part of their natural replicative cycle, and it is this dsRNA that is recognized in the infected cell and ultimately leads to IRF-3 activation. Cellular receptors for dsRNA within the cell include PAMP receptors such as TLR-3, and cytoplasmic pattern recognition receptors such

as RIG-I (128, 129). The role of RIG-I and TLR-3 in dsRNA recognition are cell-type dependent, however, both are key activators of the IRF-3 activation pathway (130, 131). During late adenoviral transcription, dsRNA is produced as a consequence of transcription occurring on both strands of the viral DNA (14). Therefore, it is possible that the dsRNA produced late in Ad infection could be detected by the cell, resulting in late IRF-3 activation.

Finally, studies with DNA viruses human CMV and HSV type I have demonstrated that even in the absence of virally produced dsRNA, IRF-3 is still activated, suggesting that IRF-3 activation may occur through recognition of an alternative component of the viral life cycle (104). While virus internalization is required for HSV-mediated activation of IRF-3, in CMV infection, binding to the cell is sufficient (103, 104). Indeed, IRF-3 is activated when cells are incubated with purified CMV attachment protein, gB (188). In addition, recent studies by tenOever *et al.* (189) demonstrated that in Measles virus (RNA virus) infection, IRF-3 activation is dependent on replication at low MOI and occurs through direct binding of IRF-3 with nucleocapsid (N) protein. Therefore, the detection of Ad proteins by the cell could be an alternative mechanism by which IRF-3 is activated within the infected cell.

Primary target for wtAd5-induced IRF-3 phosphorylation is a novel residue(s)

Extensive studies with RNA viruses have determined that phosphorylation of the IRF-3 protein can occur in four different regions. Within the amino terminus, residues Thr^{135} and Ser^{188} are targets for phosphorylation by DNA-PK and a member of the MAPK family, respectively. While it is recognized that phosphorylation of Thr^{135} leads to nuclear retention and phosphorylation of Ser^{188} occurs in response to stress and DNA damage, little else is known about the exact functional implication of N-terminal phosphorylation (96, 101). Conversely, phosphorylation of residues within the C-terminal region of IRF-3 is indicative

of IRF-3 activation, and occurs upon infection by many viruses (96, 101, 105, 109, 110). Multiple experiments conducted by Mori *et al.* and Servant *et al.* using SeV have narrowed the most probable phosphorylation residues to Ser^{386} (108) or Ser^{396} (99), however, the exact phosphorylation site required for virus-induced IRF-3 activation remains unclear.

Our data demonstrates that mutation of the C-terminal amino acids previously associated with IRF-3 activation by RNA viruses (Ser^{386} and Ser^{396}), or other residues in the C-terminus that have been shown to be phosphorylated, does not significantly alter the pattern of IRF-3 phosphorylation upon wtAd5 infection (Fig.12). This observation suggests that the primary target for Ad-induced phosphorylation is not in the C-terminus. However, Collins *et al.* (175) have suggested that only a minor proportion of IRF-3 needs to be activated (*i.e.* phosphorylation in the C-terminus) in order for a full interferon response to occur, and that this may not be detectable as a visible change in IRF-3 phosphorylation status by SDS-PAGE. Nevertheless, our data using reporter constructs containing the RANTES promoter (discussed below) suggest that IRF-3 is indeed activated.

Infection of cells with Ad appears to induce phosphorylation of IRF-3 at a novel residue. Transfection of a plasmid encoding a mutant IRF-3 containing non-phosphorylatable residues at all previously-identified phosphorylation sites did not yield a different pattern or ratio of type I to type II IRF-3 compared with un-mutated IRF-3 (Fig. 12). Recent experiments in our lab have determined that the novel phosphorylation residue is Ser^{173}, which is located within the N-terminus of the protein (R. Parks, personal communication). Although the function of N-terminal phosphorylation is not known, several possibilities have been suggested. Phosphorylation of the N-terminus may cause a conformational change in IRF-3 structure, making the C-terminal Ser-Thr residues accessible for the phosphorylation by VAK (101, 126). As the mechanism of IRF-3 activation and the

identity of the VAK responsible depend on the virus/stimuli, and it is likely that multiple signaling pathways and kinases lead to activation of IRF-3 (96, 99), perhaps phosphorylation of this novel residue is required for C-terminal phosphorylation that leads to IRF-3 activation during Ad infection.

WtAd5-induced RANTES expression occurs late and is replication-dependent

The data presented above clearly demonstrates that IRF-3 is phosphorylated upon wtAd5 infection. However, we did not observe IRF-3 forms III or IV, which are commonly associated with true activation of IRF-3, at least for RNA viruses (101, 108). Since detection of C-terminal phosphorylation or the presence of IRF-3 phosphorylation isoforms III or IV are not perfect methods of examining of IRF-3 activation (175), we investigated wtAd5-induced IRF-3 activation by examining its role in the induction of RANTES. The RANTES gene is a direct target for IRF-3 activation (100, 148, 149, 163). Our experiments suggest that wtAd5-induced RANTES expression, like IRF-3 phosphorylation, occurs late in the Ad life cycle (Fig.13) and is dependent on Ad replication (Fig.15). Furthermore, phosphorylation of residues 382-414 within the C-terminus of IRF-3 is important in wtAd5-induced RANTES expression since expression of a dominant-negative form of IRF-3 (mutated in these residues) reduced RANTES activation (Fig. 18*D*). Finally, in the wtAd5-infected cell, IRF-3 is required for full induction of RANTES expression (Figs. 16, 17), as shown by RANTES promoter/deletion mutation analysis. Taken together, our data suggests that IRF-3 is indeed important in the induction of inflammatory cytokines/chemokines in Ad-infected cells.

Previous *in vivo* studies have demonstrated an induction of RANTES expression in both lung (alveolar macrophages) (66) and liver tissue (34) within hours of Ad vector

transduction in mice. This early induction of RANTES *in vivo*, however, may reflect the activation of immune cells, such as Kupffer cells (resident macrophage of the liver), which are the prime target for Ad infection after systemic delivery in mice (13, 34). Since these are immune cells, they are likely to respond faster than other cell types. Indeed, we have observed IRF-3 phosphorylation by 2 hr following wtAd5 infection of macrophage-like differentiated THP-1 cells (data not shown).

Early induction of RANTES expression has also been observed after Ad vector transduction in HeLa cells, primary kidney epithelial cells, and in mouse insulinoma cell line TGP61 (34, 75). In addition, Hartman *et al.* (80) have shown recently through micro-array analysis, that many of the early genes induced in ΔE1/E3Ad-infected MEFs have IRF-7 binding sites. Although IRF-7 and IRF-3 do not bind the same sequences, IRF-7 function is coupled with late amplification phases of gene activation that follows the immediate-early phase associated with IRF-3 function (141, 145). Thus, IRF-3 activation is absolutely required for IRF-7 function. Furthermore, through measurement of cytokine secretion by Ad-infected MEFs, Hartman *et al.* (80) confirm that the expression of several genes they identified as Ad-responsive also translated into increased protein expression/secretion. Indeed, RANTES showed a high level of up-regulation at the protein level starting 6 hr post-infection (80).

In our study, we used luciferase reporter constructs to examine RANTES expression in wtAd5-infected HeLa cells. We were intrigued to find that RANTES expression occurred late in infection (24 hr post-infection) contrary to the early Ad5 vector-induced RANTES expression previously observed using similar methods (6 hr post-infection) (75). There are limitations to transfection-based assays, as they represent only simulated systems where plasmid DNA exists in an artificial configuration (*i.e.* not properly chromatinized) with

variable copy numbers that influence results (190). However, we repeated our experiments multiple times and obtained similar results.

In order to ensure complete transduction efficiency, all previously published studies were based on experiments using Ad5 vectors at very high MOI (31, 66, 75, 80). Indeed, Muruve *et al.* (34) observed less efficient hepatocyte-mediated cytokine/chemokine induction when mice were injected with ΔE1-E3-defective Ad5 vectors at lower titers. In our experiments, we used a much lower MOI. When we did use higher MOI, we observed RANTES induction earlier (6 hr - Fig.6). Furthermore, unlike the other studies, our experiments were conducted with wtAd5 and thus contained both E1 and E3 regions. As previously discussed, immunoregulatory proteins in the E3 region appear to interfere with IRF-3 phosphorylation (Fig.8), therefore it is possible that in our experiments with wtAd5, early RANTES expression also may have been hampered by actions of the E3 proteins.

Future Directions

Our data suggests IRF-3 is indeed activated upon wtAd5 infection, however in order to directly confirm these results, ChIP (Chromatin Immuno-precipitation) analysis of IRF-3 binding to ISG promoters should be performed. In addition, several other steps along the IRF-3 activation pathway could be studied including IRF-3 homo-dimerization, migration of IRF-3 from the cytoplasm to the nucleus and binding of IRF-3 with CBP. Simple experiments could be devised to study these steps: analysis of IRF-3 migration though non-denaturing PAGE (IRF-3 dimerization), immuno-precipitation experiments (IRF-3/CBP binding) and immuno-cytochemistry (localization of IRF-3). However, as only a minor proportion of IRF-3 needs to be activated in order for a full interferon response to occur,

these steps along the IRF-3 activation pathway may be difficult to observe and not easily detected (175).

Further analysis of Ser^{173}, the IRF-3 amino terminal residue primarily phosphorylated upon wtAd5 infection, is another important priority for future studies. Uncovering the pathways involved in this phosphorylation event will help to determine the identity of the stimulus and perhaps the functional implication of this specific phosphorylation event. It would also be very interesting to determine if this residue is phosphorylated in response to RNA viruses and other DNA viruses such as HSV and CMV.

At this time, the mechanism of wtAd5-induced IRF-3 activation, including the stimulus responsible for starting the activation pathway and the identity of the VAK responsible for C-terminal phosphorylation that leads to IRF-3 activation, remains unknown. As previously mentioned, there are at several mechanisms by which the cell could detect Ad5 infection/replication that could result in IRF-3 phosphorylation and subsequent activation, including the recognition of small sections of replicated Ad DNA, dsRNA produced during late Ad transcription, or Ad protein expression. Once the stimulus has been determined it will point to an activation pathway for IRF-3. It would also be important to determine if the mechanism of IRF-3 activation differs upon infection by other Ad serotypes. For example, the rate and timing of infection by Ad7 is much different than Ad5 and, indeed, preliminary experiments have suggested that IRF-3 phosphorylation occurs early in Ad7-infected cells.

As discussed above, the immunoregulatory proteins encoded in the Ad E3 gene region appear to interfere with IRF-3 phosphorylation, and may inhibit wtAd5-induced early RANTES expression. Further studies focusing on the effects of the E3 proteins are therefore in order. An examination of the timing and occurrence of specific steps in the IRF-3

activation pathway (*i.e.* IRF-3 homo-dimerization, localization, complex formation with CBP, direct binding to ISRE on ISG promoters) in response to infection by ΔE1-E3-defective Ad or $E1^{+}$ΔE3Ad could reveal additional immunoregulatory functions of the E3 gene region that may interfere directly or indirectly with IRF-3 and the pathways which it activates.

Recently, micro-array studies by Hartman *et al.* (70) have demonstrated a potent cellular transcriptome response in murine liver samples following intravenous administration of high-titer Ad vectors. Using the same methods, they have also demonstrated that the early genes induced in ΔE1/E3Ad-infected MEFs have IRF-7 binding sites (80). Additional micro-array analysis focusing on the identification of IRF-3 binding sites following wtAd5 infection could reveal Ad-specific transcription factor functions of IRF-3 that are unknown at this time.

Finally, once further insights have been made in the areas mentioned above, the next step would be to characterize wtAd5 activation of IRF-3 and innate immune responses *in vivo*. There are significant differences observed between the innate immune response to the Ad5 virus *in vitro* compared to those seen *in vivo*, and no study has attempted to characterize the *in vivo* IRF-3 activation pathway in response to wtAd5 infection.

With information from *in vivo* studies, a greater understanding of the innate immune response to Ad would be achieved, allowing for insights into novel methods that could be used to combat severe Ad diseases as well as innovative strategies for the development of nontoxic Ad vectors for gene therapy.

Recent developments

Since this thesis was originally submitted, three papers investigating the innate immune response to Ad have been published. Zhu *et al.* (191) demonstrated that the innate immune response to ΔE1 and ΔE3Ad5 vectors is mediated by both TLR-dependent and independent pathways in different types of dendritic cells (DC). While infection of conventional DCs generates a TLR-independent immune response through cytosolic detection of Ad DNA, infection of plasmacytoid DCs, elicits an immune response via TLR-9 signaling through MyD88 (191). Equally, Cerullo *et al.* (192) provided evidence that TLR-9 triggers an innate immune response to hdAd in primary macrophages. Conversely, Nociari *et al.* (193) have established that upon ΔE1/E3Ad5 infection of murine bone marrow derived macrophage (BMMO) or dendritic cells (BMDC), IRF-3 activation results from a signaling cascade that is triggered by the recognition of viral DNA by an intracellular sensor and not TLR-9. These studies demonstrate the complexity and diversity of the innate immune response to Ad5-based vectors in cells of the immune system. Future experiments in non-immune cells will likely demonstrate equally interesting results.

Conclusions

Our study is the first to underline the importance of IRF-3 for full induction of RANTES expression upon wtAd5 infection, suggesting that IRF-3 plays a significant role in the establishment of the antiviral state in wtAd5-infected cells, and indirectly implying that IRF-3 is indeed activated upon wtAd5 infection. Furthermore, we observed that although mutation of amino acids previously associated with IRF-3 activation by RNA viruses (Ser^{386} and Ser^{396}) does not significantly alter the pattern of IRF-3 phosphorylation upon wtAd5

infection, over-expression of a dominant-negative form of IRF-3 containing these mutations causes a decrease in RANTES expression. This data suggests that phosphorylation of these residues is also important in wtAd5-induced IRF-3 activation. In addition, we demonstrated that the primary target for IRF-3 phosphorylation in wtAd5 infection is a novel amino terminal residue. Finally, we determined that wtAd5-induced IRF-3 phosphorylation and subsequent activation occurs late in Ad infection (24 hr post-infection) and is dependent on the ability of the cell to detect virus replication. As our study is the first to examine the innate immune response to wtAd5 and Ad5-based vectors with respect to IRF-3 activation *in vitro*, our results have begun to map a major signaling pathway used by many viruses to combat infection, thus bringing new insight into the early immune response to wtAd infection and gene therapy vectors.

REFERENCES

1. Rowe, W.P., R.J. Huebner, L.K. Gilmore, R.H. Parrott, and T.G. Ward. 1953. Isolation of a cytopathogenic agent from human adenoids undergoing spontaneous degeneration in tissue culture. *Proceedings of the Society for Experimental Biology and Medicine. Society for Experimental Biology and Medicine (New York, N. Y* 84:570-573.

2. Horwitz, M.S. 2001. Adenoviruses. In Fields Virology. D.M. Knipe, Howley, P. M., editor Lippincott, Williams and Wilkins, Philadelphia. 2301-2326.

3. Lukashok, S.A., and M.S. Horwitz. 1998. New perspectives in adenoviruses. *Current clinical topics in infectious diseases* 18:286-305.

4. Horne, R.W., Brenner, S., Waterson, A. P., Wildy, P. 1959. The icosahedral form of an adenovirus. *J. Mol. Biol.* 1:84-86.

5. Horwitz, M.S. 2004. Function of adenovirus E3 proteins and their interactions with immunoregulatory cell proteins. *The journal of gene medicine* 6 Suppl 1:S172-183.

6. Rux, J.J., and R.M. Burnett. 2004. Adenovirus structure. *Human gene therapy* 15:1167-1176.

7. Valentine, R.C., and H.G. Pereira. 1965. Antigens and structure of the adenovirus. *Journal of molecular biology* 13:13-20.

8. Tamanini, A., E. Nicolis, A. Bonizzato, V. Bezzerri, P. Melotti, B.M. Assael, and G. Cabrini. 2006. Interaction of adenovirus type 5 fiber with the coxsackievirus and adenovirus receptor activates inflammatory response in human respiratory cells. *Journal of virology* 80:11241-11254.

9. Bergelson, J.M., J.A. Cunningham, G. Droguett, E.A. Kurt-Jones, A. Krithivas, J.S. Hong, M.S. Horwitz, R.L. Crowell, and R.W. Finberg. 1997. Isolation of a common receptor for Coxsackie B viruses and adenoviruses 2 and 5. *Science* 275:1320-1323.

10. Bergelson, J.M., A. Krithivas, L. Celi, G. Droguett, M.S. Horwitz, T. Wickham, R.L. Crowell, and R.W. Finberg. 1998. The murine CAR homolog is a receptor for coxsackie B viruses and adenoviruses. *Journal of virology* 72:415-419.

11. Roelvink, P.W., A. Lizonova, J.G. Lee, Y. Li, J.M. Bergelson, R.W. Finberg, D.E. Brough, I. Kovesdi, and T.J. Wickham. 1998. The coxsackievirus-adenovirus receptor protein can function as a cellular attachment protein for adenovirus serotypes from subgroups A, C, D, E, and F. *Journal of virology* 72:7909-7915.

12. Tomko, R.P., R. Xu, and L. Philipson. 1997. HCAR and MCAR: the human and mouse cellular receptors for subgroup C adenoviruses and group B coxsackieviruses.

Proceedings of the National Academy of Sciences of the United States of America 94:3352-3356.

13. Muruve, D.A. 2004. The innate immune response to adenovirus vectors. *Human gene therapy* 15:1157-1166.

14. Shenk, T. 1996. Adenoviridae: the viruses and their replication. In Fields Virology. B.N. Fields, Knipe, D. M., Howley, P.M., editor Lippincott-Raven Publishers, Philadelphia. 2111-2148.

15. Green, M., and G.E. Daesch. 1961. Biochemical studies on adenovirus multiplication. II. Kinetics of nucleic acid and protein synthesis in suspension cultures. *Virology* 13:169-176.

16. Lozinski, G.M., G.G. Davis, H.F. Krous, G.F. Billman, H. Shimizu, and J.C. Burns. 1994. Adenovirus myocarditis: retrospective diagnosis by gene amplification from formalin-fixed, paraffin-embedded tissues. *Human pathology* 25:831-834.

17. Shirali, G.S., J. Ni, R.E. Chinnock, J.K. Johnston, G.L. Rosenthal, N.E. Bowles, and J.A. Towbin. 2001. Association of viral genome with graft loss in children after cardiac transplantation. *The New England journal of medicine* 344:1498-1503.

18. Bowles, N.E., J. Ni, D.L. Kearney, M. Pauschinger, H.P. Schultheiss, R. McCarthy, J. Hare, J.T. Bricker, K.R. Bowles, and J.A. Towbin. 2003. Detection of viruses in myocardial tissues by polymerase chain reaction. evidence of adenovirus as a common cause of myocarditis in children and adults. *Journal of the American College of Cardiology* 42:466-472.

19. Dettmeyer, R., A. Baasner, M. Schlamann, S.A. Padosch, C. Haag, R. Kandolf, and B. Madea. 2004. Role of virus-induced myocardial affections in sudden infant death syndrome: a prospective postmortem study. *Pediatric research* 55:947-952.

20. Rocholl, C., K. Gerber, J. Daly, A.T. Pavia, and C.L. Byington. 2004. Adenoviral infections in children: the impact of rapid diagnosis. *Pediatrics* 113:e51-56.

21. Montalbano, M.M., and R.F. Lemanske, Jr. 2002. Infections and asthma in children. *Current opinion in pediatrics* 14:334-337.

22. Barraza, E.M., S.L. Ludwig, J.C. Gaydos, and J.F. Brundage. 1999. Reemergence of adenovirus type 4 acute respiratory disease in military trainees: report of an outbreak during a lapse in vaccination. *The Journal of infectious diseases* 179:1531-1533.

23. Gray, G.C., P.R. Goswami, M.D. Malasig, A.W. Hawksworth, D.H. Trump, M.A. Ryan, and D.P. Schnurr. 2000. Adult adenovirus infections: loss of orphaned vaccines precipitates military respiratory disease epidemics. For the Adenovirus Surveillance Group. *Clin Infect Dis* 31:663-670.

24. Hendrix, R.M., J.L. Lindner, F.R. Benton, S.C. Monteith, M.A. Tuchscherer, G.C. Gray, and J.C. Gaydos. 1999. Large, persistent epidemic of adenovirus type 4-associated acute respiratory disease in U.S. army trainees. *Emerging infectious diseases* 5:798-801.

25. Top, F.H., Jr., E.L. Buescher, W.H. Bancroft, and P.K. Russell. 1971. Immunization with live types 7 and 4 adenovirus vaccines. II. Antibody response and protective effect against acute respiratory disease due to adenovirus type 7. *The Journal of infectious diseases* 124:155-160.

26. Hitt, M.M., and F.L. Graham. 2000. Adenovirus vectors for human gene therapy. *Advances in virus research* 55:479-505.

27. Parks, R.J., L. Chen, M. Anton, U. Sankar, M.A. Rudnicki, and F.L. Graham. 1996. A helper-dependent adenovirus vector system: removal of helper virus by Cre-mediated excision of the viral packaging signal. *Proceedings of the National Academy of Sciences of the United States of America* 93:13565-13570.

28. Wilson, J.M. 1996. Adenoviruses as gene-delivery vehicles. *The New England journal of medicine* 334:1185-1187.

29. Bett, A.J., L. Prevec, and F.L. Graham. 1993. Packaging capacity and stability of human adenovirus type 5 vectors. *Journal of virology* 67:5911-5921.

30. Amalfitano, A., and R.J. Parks. 2002. Separating fact from fiction: assessing the potential of modified adenovirus vectors for use in human gene therapy. *Current gene therapy* 2:111-133.

31. Morsy, M.A., Caskey, C. T. 1999. Expanded-capacity adenoviral vectors - the helper dependent vectors. *Molec. Med. Today* 5:18-24.

32. Kafri, T., D. Morgan, T. Krahl, N. Sarvetnick, L. Sherman, and I. Verma. 1998. Cellular immune response to adenoviral vector infected cells does not require de novo viral gene expression: implications for gene therapy. *Proceedings of the National Academy of Sciences of the United States of America* 95:11377-11382.

33. Morral, N., W. O'Neal, H. Zhou, C. Langston, and A. Beaudet. 1997. Immune responses to reporter proteins and high viral dose limit duration of expression with adenoviral vectors: comparison of E2a wild type and E2a deleted vectors. *Human gene therapy* 8:1275-1286.

34. Muruve, D.A., M.J. Barnes, I.E. Stillman, and T.A. Libermann. 1999. Adenoviral gene therapy leads to rapid induction of multiple chemokines and acute neutrophil-dependent hepatic injury in vivo. *Human gene therapy* 10:965-976.

35. Tripathy, S.K., H.B. Black, E. Goldwasser, and J.M. Leiden. 1996. Immune responses to transgene-encoded proteins limit the stability of gene expression after injection of replication-defective adenovirus vectors. *Nature medicine* 2:545-550.

36. Worgall, S., G. Wolff, E. Falck-Pedersen, and R.G. Crystal. 1997. Innate immune mechanisms dominate elimination of adenoviral vectors following in vivo administration. *Human gene therapy* 8:37-44.

37. Yang, Y., F.A. Nunes, K. Berencsi, E.E. Furth, E. Gonczol, and J.M. Wilson. 1994. Cellular immunity to viral antigens limits E1-deleted adenoviruses for gene therapy. *Proceedings of the National Academy of Sciences of the United States of America* 91:4407-4411.

38. Zhang, Y., N. Chirmule, G.P. Gao, R. Qian, M. Croyle, B. Joshi, J. Tazelaar, and J.M. Wilson. 2001. Acute cytokine response to systemic adenoviral vectors in mice is mediated by dendritic cells and macrophages. *Mol Ther* 3:697-707.

39. Raper, S.E., M. Yudkoff, N. Chirmule, G.P. Gao, F. Nunes, Z.J. Haskal, E.E. Furth, K.J. Propert, M.B. Robinson, S. Magosin, H. Simoes, L. Speicher, J. Hughes, J. Tazelaar, N.A. Wivel, J.M. Wilson, and M.L. Batshaw. 2002. A pilot study of in vivo liver-directed gene transfer with an adenoviral vector in partial ornithine transcarbamylase deficiency. *Human gene therapy* 13:163-175.

40. Schnell, M.A., Y. Zhang, J. Tazelaar, G.P. Gao, Q.C. Yu, R. Qian, S.J. Chen, A.N. Varnavski, C. LeClair, S.E. Raper, and J.M. Wilson. 2001. Activation of innate immunity in nonhuman primates following intraportal administration of adenoviral vectors. *Mol Ther* 3:708-722.

41. Raper, S.E., N. Chirmule, F.S. Lee, N.A. Wivel, A. Bagg, G.P. Gao, J.M. Wilson, and M.L. Batshaw. 2003. Fatal systemic inflammatory response syndrome in a ornithine transcarbamylase deficient patient following adenoviral gene transfer. *Molecular genetics and metabolism* 80:148-158.

42. Engelhardt, J.F., X. Ye, B. Doranz, and J.M. Wilson. 1994. Ablation of E2A in recombinant adenoviruses improves transgene persistence and decreases inflammatory response in mouse liver. *Proceedings of the National Academy of Sciences of the United States of America* 91:6196-6200.

43. Goldman, M.J., L.A. Litzky, J.F. Engelhardt, and J.M. Wilson. 1995. Transfer of the CFTR gene to the lung of nonhuman primates with E1-deleted, E2a-defective recombinant adenoviruses: a preclinical toxicology study. *Human gene therapy* 6:839-851.

44. Yang, Y., F.A. Nunes, K. Berencsi, E. Gonczol, J.F. Engelhardt, and J.M. Wilson. 1994. Inactivation of E2a in recombinant adenoviruses improves the prospect for gene therapy in cystic fibrosis. *Nature genetics* 7:362-369.

45. Armentano, D., M.P. Smith, C.C. Sookdeo, J. Zabner, M.A. Perricone, J.A. St George, S.C. Wadsworth, and R.J. Gregory. 1999. E4ORF3 requirement for achieving long-term transgene expression from the cytomegalovirus promoter in adenovirus vectors. *Journal of virology* 73:7031-7034.

46. Brough, D.E., C. Hsu, V.A. Kulesa, G.M. Lee, L.J. Cantolupo, A. Lizonova, and I. Kovesdi. 1997. Activation of transgene expression by early region 4 is responsible for a high level of persistent transgene expression from adenovirus vectors in vivo. *Journal of virology* 71:9206-9213.

47. Dedieu, J.F., E. Vigne, C. Torrent, C. Jullien, I. Mahfouz, J.M. Caillaud, N. Aubailly, C. Orsini, J.M. Guillaume, P. Opolon, P. Delaere, M. Perricaudet, and P. Yeh. 1997. Long-term gene delivery into the livers of immunocompetent mice with E1/E4-defective adenoviruses. *Journal of virology* 71:4626-4637.

48. Kaplan, J.M., D. Armentano, T.E. Sparer, S.G. Wynn, P.A. Peterson, S.C. Wadsworth, K.K. Couture, S.E. Pennington, J.A. St George, L.R. Gooding, and A.E. Smith. 1997. Characterization of factors involved in modulating persistence of transgene expression from recombinant adenovirus in the mouse lung. *Human gene therapy* 8:45-56.

49. Brunetti-Pierri, N., D.J. Palmer, A.L. Beaudet, K.D. Carey, M. Finegold, and P. Ng. 2004. Acute toxicity after high-dose systemic injection of helper-dependent adenoviral vectors into nonhuman primates. *Human gene therapy* 15:35-46.

50. Liu, Q., and D.A. Muruve. 2003. Molecular basis of the inflammatory response to adenovirus vectors. *Gene therapy* 10:935-940.

51. Girardin, S.E., P.J. Sansonetti, and D.J. Philpott. 2002. Intracellular vs extracellular recognition of pathogens--common concepts in mammals and flies. *Trends in microbiology* 10:193-199.

52. Medzhitov, R., and C.A. Janeway, Jr. 2002. Decoding the patterns of self and nonself by the innate immune system. *Science* 296:298-300.

53. Stark, G.R., I.M. Kerr, B.R. Williams, R.H. Silverman, and R.D. Schreiber. 1998. How cells respond to interferons. *Annual review of biochemistry* 67:227-264.

54. Zhang, D., G. Zhang, M.S. Hayden, M.B. Greenblatt, C. Bussey, R.A. Flavell, and S. Ghosh. 2004. A toll-like receptor that prevents infection by uropathogenic bacteria. *Science* 303:1522-1526.

55. Ahmad-Nejad, P., H. Hacker, M. Rutz, S. Bauer, R.M. Vabulas, and H. Wagner. 2002. Bacterial CpG-DNA and lipopolysaccharides activate Toll-like receptors at distinct cellular compartments. *European journal of immunology* 32:1958-1968.

56. Lund, J., A. Sato, S. Akira, R. Medzhitov, and A. Iwasaki. 2003. Toll-like receptor 9-mediated recognition of Herpes simplex virus-2 by plasmacytoid dendritic cells. *The Journal of experimental medicine* 198:513-520.

57. Matsumoto, M., K. Funami, M. Tanabe, H. Oshiumi, M. Shingai, Y. Seto, A. Yamamoto, and T. Seya. 2003. Subcellular localization of Toll-like receptor 3 in human dendritic cells. *J Immunol* 171:3154-3162.

58. Seth, R.B., L. Sun, and Z.J. Chen. 2006. Antiviral innate immunity pathways. *Cell research* 16:141-147.

59. Smith, P.L., G. Lombardi, and G.R. Foster. 2005. Type I interferons and the innate immune response--more than just antiviral cytokines. *Molecular immunology* 42:869-877.

60. Finberg, R.W., and E.A. Kurt-Jones. 2004. Viruses and Toll-like receptors. *Microbes and infection / Institut Pasteur* 6:1356-1360.

61. Inohara, N., and G. Nunez. 2003. NODs: intracellular proteins involved in inflammation and apoptosis. *Nature reviews* 3:371-382.

62. Guidotti, L.G., and F.V. Chisari. 2001. Noncytolytic control of viral infections by the innate and adaptive immune response. *Annual review of immunology* 19:65-91.

63. Vaidya, S.A., and G. Cheng. 2003. Toll-like receptors and innate antiviral responses. *Current opinion in immunology* 15:402-407.

64. Taniguchi, M., K. Seino, and T. Nakayama. 2003. The NKT cell system: bridging innate and acquired immunity. *Nature immunology* 4:1164-1165.

65. Benihoud, K., I. Saggio, P. Opolon, B. Salone, F. Amiot, E. Connault, C. Chianale, F. Dautry, P. Yeh, and M. Perricaudet. 1998. Efficient, repeated adenovirus-mediated gene transfer in mice lacking both tumor necrosis factor alpha and lymphotoxin alpha. *Journal of virology* 72:9514-9525.

66. Otake, K., D.L. Ennist, K. Harrod, and B.C. Trapnell. 1998. Nonspecific inflammation inhibits adenovirus-mediated pulmonary gene transfer and expression independent of specific acquired immune responses. *Human gene therapy* 9:2207-2222.

67. Zhang, S., J. Han, M.A. Sells, J. Chernoff, U.G. Knaus, R.J. Ulevitch, and G.M. Bokoch. 1995. Rho family GTPases regulate p38 mitogen-activated protein kinase through the downstream mediator Pak1. *The Journal of biological chemistry* 270:23934-23936.

68. Bramson, J.L., M. Hitt, J. Gauldie, and F.L. Graham. 1997. Pre-existing immunity to adenovirus does not prevent tumor regression following intratumoral administration of a vector expressing IL-12 but inhibits virus dissemination. *Gene therapy* 4:1069-1076.

69. McCoy, R.D., B.L. Davidson, B.J. Roessler, G.B. Huffnagle, S.L. Janich, T.J. Laing, and R.H. Simon. 1995. Pulmonary inflammation induced by incomplete or inactivated adenoviral particles. *Human gene therapy* 6:1553-1560.

70. Hartman, Z.C., A. Kiang, R.S. Everett, D. Serra, X.Y. Yang, T.M. Clay, and A. Amalfitano. 2006. Adenovirus infection triggers a rapid, MyD88 regulated,

transcriptome response critical to acute phase and adaptive immune responses in vivo. *Journal of virology*

71. Zsengeller, Z., K. Otake, S.A. Hossain, P.Y. Berclaz, and B.C. Trapnell. 2000. Internalization of adenovirus by alveolar macrophages initiates early proinflammatory signaling during acute respiratory tract infection. *Journal of virology* 74:9655-9667.

72. Higginbotham, J.N., P. Seth, R.M. Blaese, and W.J. Ramsey. 2002. The release of inflammatory cytokines from human peripheral blood mononuclear cells in vitro following exposure to adenovirus variants and capsid. *Human gene therapy* 13:129-141.

73. Amin, R., R. Wilmott, Y. Schwarz, B. Trapnell, and J. Stark. 1995. Replication-deficient adenovirus induces expression of interleukin-8 by airway epithelial cells in vitro. *Human gene therapy* 6:145-153.

74. Borgland, S.L., G.P. Bowen, N.C. Wong, T.A. Libermann, and D.A. Muruve. 2000. Adenovirus vector-induced expression of the C-X-C chemokine IP-10 is mediated through capsid-dependent activation of NF-kappaB. *Journal of virology* 74:3941-3947.

75. Bowen, G.P., S.L. Borgland, M. Lam, T.A. Libermann, N.C. Wong, and D.A. Muruve. 2002. Adenovirus vector-induced inflammation: capsid-dependent induction of the C-C chemokine RANTES requires NF-kappa B. *Human gene therapy* 13:367-379.

76. Bruder, J.T., and I. Kovesdi. 1997. Adenovirus infection stimulates the Raf/MAPK signaling pathway and induces interleukin-8 expression. *Journal of virology* 71:398-404.

77. Rafii, S., S. Dias, S. Meeus, K. Hattori, R. Ramachandran, F. Feuerback, S. Worgall, N.R. Hackett, and R.G. Crystal. 2001. Infection of endothelium with E1(-)E4(+), but not E1(-)E4(-), adenovirus gene transfer vectors enhances leukocyte adhesion and migration by modulation of ICAM-1, VCAM-1, CD34, and chemokine expression. *Circulation research* 88:903-910.

78. Stark, J.M., R.S. Amin, and B.C. Trapnell. 1996. Infection of A549 cells with a recombinant adenovirus vector induces ICAM-1 expression and increased CD-18-dependent adhesion of activated neutrophils. *Human gene therapy* 7:1669-1681.

79. Li, Y., D.A. Muruve, R.G. Collins, S.S. Lee, and P. Kubes. 2002. The role of selectins and integrins in adenovirus vector-induced neutrophil recruitment to the liver. *European journal of immunology* 32:3443-3452.

80. Hartman, Z.C., E.P. Black, and A. Amalfitano. 2006. Adenoviral infection induces a multi-faceted innate cellular immune response that is mediated by the toll-like receptor pathway in A549 cells. *Virology*

81. Wickham, T.J., P. Mathias, D.A. Cheresh, and G.R. Nemerow. 1993. Integrins alpha v beta 3 and alpha v beta 5 promote adenovirus internalization but not virus attachment. *Cell* 73:309-319.

82. Li, E., S.L. Brown, D.G. Stupack, X.S. Puente, D.A. Cheresh, and G.R. Nemerow. 2001. Integrin alpha(v)beta1 is an adenovirus coreceptor. *Journal of virology* 75:5405-5409.

83. Greber, U.F., M. Willetts, P. Webster, and A. Helenius. 1993. Stepwise dismantling of adenovirus 2 during entry into cells. *Cell* 75:477-486.

84. Wang, K., T. Guan, D.A. Cheresh, and G.R. Nemerow. 2000. Regulation of adenovirus membrane penetration by the cytoplasmic tail of integrin beta5. *Journal of virology* 74:2731-2739.

85. Wickham, T.J., E.J. Filardo, D.A. Cheresh, and G.R. Nemerow. 1994. Integrin alpha v beta 5 selectively promotes adenovirus mediated cell membrane permeabilization. *The Journal of cell biology* 127:257-264.

86. Wiethoff, C.M., H. Wodrich, L. Gerace, and G.R. Nemerow. 2005. Adenovirus protein VI mediates membrane disruption following capsid disassembly. *Journal of virology* 79:1992-2000.

87. Greber, U.F., M. Suomalainen, R.P. Stidwill, K. Boucke, M.W. Ebersold, and A. Helenius. 1997. The role of the nuclear pore complex in adenovirus DNA entry. *The EMBO journal* 16:5998-6007.

88. Suomalainen, M., M.Y. Nakano, S. Keller, K. Boucke, R.P. Stidwill, and U.F. Greber. 1999. Microtubule-dependent plus- and minus end-directed motilities are competing processes for nuclear targeting of adenovirus. *The Journal of cell biology* 144:657-672.

89. Trotman, L.C., N. Mosberger, M. Fornerod, R.P. Stidwill, and U.F. Greber. 2001. Import of adenovirus DNA involves the nuclear pore complex receptor CAN/Nup214 and histone H1. *Nature cell biology* 3:1092-1100.

90. Dechecchi, M.C., P. Melotti, A. Bonizzato, M. Santacatterina, M. Chilosi, and G. Cabrini. 2001. Heparan sulfate glycosaminoglycans are receptors sufficient to mediate the initial binding of adenovirus types 2 and 5. *Journal of virology* 75:8772-8780.

91. Huang, S., T. Kamata, Y. Takada, Z.M. Ruggeri, and G.R. Nemerow. 1996. Adenovirus interaction with distinct integrins mediates separate events in cell entry and gene delivery to hematopoietic cells. *Journal of virology* 70:4502-4508.

92. Li, E., D. Stupack, R. Klemke, D.A. Cheresh, and G.R. Nemerow. 1998. Adenovirus endocytosis via alpha(v) integrins requires phosphoinositide-3-OH kinase. *Journal of virology* 72:2055-2061.

93. Tibbles, L.A., J.C. Spurrell, G.P. Bowen, Q. Liu, M. Lam, A.K. Zaiss, S.M. Robbins, M.D. Hollenberg, T.J. Wickham, and D.A. Muruve. 2002. Activation of p38 and ERK signaling during adenovirus vector cell entry lead to expression of the C-X-C chemokine IP-10. *Journal of virology* 76:1559-1568.

94. Roelvink, P.W., G. Mi Lee, D.A. Einfeld, I. Kovesdi, and T.J. Wickham. 1999. Identification of a conserved receptor-binding site on the fiber proteins of CAR-recognizing adenoviridae. *Science* 286:1568-1571.

95. Nemerow, G.R., and P.L. Stewart. 1999. Role of alpha(v) integrins in adenovirus cell entry and gene delivery. *Microbiol Mol Biol Rev* 63:725-734.

96. Servant, M.J., N. Grandvaux, and J. Hiscott. 2002. Multiple signaling pathways leading to the activation of interferon regulatory factor 3. *Biochemical pharmacology* 64:985-992.

97. Au, W.C., P.A. Moore, W. Lowther, Y.T. Juang, and P.M. Pitha. 1995. Identification of a member of the interferon regulatory factor family that binds to the interferon-stimulated response element and activates expression of interferon-induced genes. *Proceedings of the National Academy of Sciences of the United States of America* 92:11657-11661.

98. Kim, T., T.Y. Kim, Y.H. Song, I.M. Min, J. Yim, and T.K. Kim. 1999. Activation of interferon regulatory factor 3 in response to DNA-damaging agents. *The Journal of biological chemistry* 274:30686-30689.

99. Servant, M.J., N. Grandvaux, B.R. tenOever, D. Duguay, R. Lin, and J. Hiscott. 2003. Identification of the minimal phosphoacceptor site required for in vivo activation of interferon regulatory factor 3 in response to virus and double-stranded RNA. *The Journal of biological chemistry* 278:9441-9447.

100. Casola, A., R.P. Garofalo, H. Haeberle, T.F. Elliott, R. Lin, M. Jamaluddin, and A.R. Brasier. 2001. Multiple cis regulatory elements control RANTES promoter activity in alveolar epithelial cells infected with respiratory syncytial virus. *Journal of virology* 75:6428-6439.

101. Servant, M.J., B. ten Oever, C. LePage, L. Conti, S. Gessani, I. Julkunen, R. Lin, and J. Hiscott. 2001. Identification of distinct signaling pathways leading to the phosphorylation of interferon regulatory factor 3. *The Journal of biological chemistry* 276:355-363.

102. tenOever, B.R., S. Sharma, W. Zou, Q. Sun, N. Grandvaux, I. Julkunen, H. Hemmi, M. Yamamoto, S. Akira, W.C. Yeh, R. Lin, and J. Hiscott. 2004. Activation of TBK1 and IKKvarepsilon kinases by vesicular stomatitis virus infection and the role of viral ribonucleoprotein in the development of interferon antiviral immunity. *Journal of virology* 78:10636-10649.

103. Navarro, L., K. Mowen, S. Rodems, B. Weaver, N. Reich, D. Spector, and M. David. 1998. Cytomegalovirus activates interferon immediate-early response gene expression and an interferon regulatory factor 3-containing interferon-stimulated response element-binding complex. *Molecular and cellular biology* 18:3796-3802.

104. Preston, C.M., A.N. Harman, and M.J. Nicholl. 2001. Activation of interferon response factor-3 in human cells infected with herpes simplex virus type 1 or human cytomegalovirus. *Journal of virology* 75:8909-8916.

105. Lin, R., C. Heylbroeck, P.M. Pitha, and J. Hiscott. 1998. Virus-dependent phosphorylation of the IRF-3 transcription factor regulates nuclear translocation, transactivation potential, and proteasome-mediated degradation. *Molecular and cellular biology* 18:2986-2996.

106. Karpova, A.Y., L.V. Ronco, and P.M. Howley. 2001. Functional characterization of interferon regulatory factor 3a (IRF-3a), an alternative splice isoform of IRF-3. *Molecular and cellular biology* 21:4169-4176.

107. Karpova, A.Y., P.M. Howley, and L.V. Ronco. 2000. Dual utilization of an acceptor/donor splice site governs the alternative splicing of the IRF-3 gene. *Genes & development* 14:2813-2818.

108. Mori, M., M. Yoneyama, T. Ito, K. Takahashi, F. Inagaki, and T. Fujita. 2004. Identification of Ser-386 of interferon regulatory factor 3 as critical target for inducible phosphorylation that determines activation. *The Journal of biological chemistry* 279:9698-9702.

109. Lin, R., Y. Mamane, and J. Hiscott. 1999. Structural and functional analysis of interferon regulatory factor 3: localization of the transactivation and autoinhibitory domains. *Molecular and cellular biology* 19:2465-2474.

110. Yoneyama, M., W. Suhara, Y. Fukuhara, M. Fukuda, E. Nishida, and T. Fujita. 1998. Direct triggering of the type I interferon system by virus infection: activation of a transcription factor complex containing IRF-3 and CBP/p300. *The EMBO journal* 17:1087-1095.

111. Suhara, W., M. Yoneyama, T. Iwamura, S. Yoshimura, K. Tamura, H. Namiki, S. Aimoto, and T. Fujita. 2000. Analyses of virus-induced homomeric and heteromeric protein associations between IRF-3 and coactivator CBP/p300. *Journal of biochemistry* 128:301-307.

112. Yang, H., C.H. Lin, G. Ma, M. Orr, M.O. Baffi, and M.G. Wathelet. 2002. Transcriptional activity of interferon regulatory factor (IRF)-3 depends on multiple protein-protein interactions. *European journal of biochemistry / FEBS* 269:6142-6151.

113. Fitzgerald, K.A., S.M. McWhirter, K.L. Faia, D.C. Rowe, E. Latz, D.T. Golenbock, A.J. Coyle, S.M. Liao, and T. Maniatis. 2003. IKKepsilon and TBK1 are essential components of the IRF3 signaling pathway. *Nature immunology* 4:491-496.

114. Sharma, S., B.R. tenOever, N. Grandvaux, G.P. Zhou, R. Lin, and J. Hiscott. 2003. Triggering the interferon antiviral response through an IKK-related pathway. *Science* 300:1148-1151.

115. Wathelet, M.G., C.H. Lin, B.S. Parekh, L.V. Ronco, P.M. Howley, and T. Maniatis. 1998. Virus infection induces the assembly of coordinately activated transcription factors on the IFN-beta enhancer in vivo. *Molecular cell* 1:507-518.

116. Kumar, K.P., K.M. McBride, B.K. Weaver, C. Dingwall, and N.C. Reich. 2000. Regulated nuclear-cytoplasmic localization of interferon regulatory factor 3, a subunit of double-stranded RNA-activated factor 1. *Molecular and cellular biology* 20:4159-4168.

117. Agalioti, T., S. Lomvardas, B. Parekh, J. Yie, T. Maniatis, and D. Thanos. 2000. Ordered recruitment of chromatin modifying and general transcription factors to the IFN-beta promoter. *Cell* 103:667-678.

118. Lin, R., P. Genin, Y. Mamane, and J. Hiscott. 2000. Selective DNA binding and association with the CREB binding protein coactivator contribute to differential activation of alpha/beta interferon genes by interferon regulatory factors 3 and 7. *Molecular and cellular biology* 20:6342-6353.

119. Schafer, S.L., R. Lin, P.A. Moore, J. Hiscott, and P.M. Pitha. 1998. Regulation of type I interferon gene expression by interferon regulatory factor-3. *The Journal of biological chemistry* 273:2714-2720.

120. Weaver, B.K., K.P. Kumar, and N.C. Reich. 1998. Interferon regulatory factor 3 and CREB-binding protein/p300 are subunits of double-stranded RNA-activated transcription factor DRAF1. *Molecular and cellular biology* 18:1359-1368.

121. Fan, C.M., and T. Maniatis. 1989. Two different virus-inducible elements are required for human beta-interferon gene regulation. *The EMBO journal* 8:101-110.

122. Fujita, T., H. Shibuya, H. Hotta, K. Yamanishi, and T. Taniguchi. 1987. Interferon-beta gene regulation: tandemly repeated sequences of a synthetic 6 bp oligomer function as a virus-inducible enhancer. *Cell* 49:357-367.

123. Leblanc, J.F., L. Cohen, M. Rodrigues, and J. Hiscott. 1990. Synergism between distinct enhanson domains in viral induction of the human beta interferon gene. *Molecular and cellular biology* 10:3987-3993.

124. Ronco, L.V., A.Y. Karpova, M. Vidal, and P.M. Howley. 1998. Human papillomavirus 16 E6 oncoprotein binds to interferon regulatory factor-3 and inhibits its transcriptional activity. *Genes & development* 12:2061-2072.

125. Karpova, A.Y., M. Trost, J.M. Murray, L.C. Cantley, and P.M. Howley. 2002. Interferon regulatory factor-3 is an in vivo target of DNA-PK. *Proceedings of the National Academy of Sciences of the United States of America* 99:2818-2823.

126. Kim, T., T.Y. Kim, W.G. Lee, J. Yim, and T.K. Kim. 2000. Signaling pathways to the assembly of an interferon-beta enhanceosome. Chemical genetic studies with a small molecule. *The Journal of biological chemistry* 275:16910-16917.

127. Navarro, L., and M. David. 1999. p38-dependent activation of interferon regulatory factor 3 by lipopolysaccharide. *The Journal of biological chemistry* 274:35535-35538.

128. Liu, P., M. Jamaluddin, K. Li, R.P. Garofalo, A. Casola, and A.R. Brasier. 2006. Retinoic Acid Inducible Gene-I Mediates Early Anti-Viral Response and Toll Like Receptor 3 Expression in Respiratory Syncytial Virus -Infected Airway Epithelial Cells. *Journal of virology*

129. Sumpter, R., Jr., Y.M. Loo, E. Foy, K. Li, M. Yoneyama, T. Fujita, S.M. Lemon, and M. Gale, Jr. 2005. Regulating intracellular antiviral defense and permissiveness to hepatitis C virus RNA replication through a cellular RNA helicase, RIG-I. *Journal of virology* 79:2689-2699.

130. Alexopoulou, L., A.C. Holt, R. Medzhitov, and R.A. Flavell. 2001. Recognition of double-stranded RNA and activation of NF-kappaB by Toll-like receptor 3. *Nature* 413:732-738.

131. Kato, H., S. Sato, M. Yoneyama, M. Yamamoto, S. Uematsu, K. Matsui, T. Tsujimura, K. Takeda, T. Fujita, O. Takeuchi, and S. Akira. 2005. Cell type-specific involvement of RIG-I in antiviral response. *Immunity* 23:19-28.

132. Colamonici, O.R., B. Porterfield, P. Domanski, S. Constantinescu, and L.M. Pfeffer. 1994. Complementation of the interferon alpha response in resistant cells by expression of the cloned subunit of the interferon alpha receptor. A central role of this subunit in interferon alpha signaling. *The Journal of biological chemistry* 269:9598-9602.

133. Gupta, S., M. Jiang, and A.B. Pernis. 1999. IFN-alpha activates Stat6 and leads to the formation of Stat2:Stat6 complexes in B cells. *J Immunol* 163:3834-3841.

134. Heim, M.H. 1999. The Jak-STAT pathway: cytokine signalling from the receptor to the nucleus. *Journal of receptor and signal transduction research* 19:75-120.

135. Katze, M.G., Y. He, and M. Gale, Jr. 2002. Viruses and interferon: a fight for supremacy. *Nature reviews* 2:675-687.

136. Leung, S., S.A. Qureshi, I.M. Kerr, J.E. Darnell, Jr., and G.R. Stark. 1995. Role of STAT2 in the alpha interferon signaling pathway. *Molecular and cellular biology* 15:1312-1317.

137. Novick, D., B. Cohen, and M. Rubinstein. 1994. The human interferon alpha/beta receptor: characterization and molecular cloning. *Cell* 77:391-400.

138. Samuel, C.E. 2001. Antiviral actions of interferons. *Clinical microbiology reviews* 14:778-809, table of contents.

139. Velazquez, L., M. Fellous, G.R. Stark, and S. Pellegrini. 1992. A protein tyrosine kinase in the interferon alpha/beta signaling pathway. *Cell* 70:313-322.

140. Martensen, P.M., and J. Justesen. 2004. Small ISGs coming forward. *J Interferon Cytokine Res* 24:1-19.

141. Yoneyama, M., W. Suhara, and T. Fujita. 2002. Control of IRF-3 activation by phosphorylation. *J Interferon Cytokine Res* 22:73-76.

142. Levy, D.E., I. Marie, E. Smith, and A. Prakash. 2002. Enhancement and diversification of IFN induction by IRF-7-mediated positive feedback. *J Interferon Cytokine Res* 22:87-93.

143. Taniguchi, T., and A. Takaoka. 2002. The interferon-alpha/beta system in antiviral responses: a multimodal machinery of gene regulation by the IRF family of transcription factors. *Current opinion in immunology* 14:111-116.

144. Juang, Y.T., W. Lowther, M. Kellum, W.C. Au, R. Lin, J. Hiscott, and P.M. Pitha. 1998. Primary activation of interferon A and interferon B gene transcription by interferon regulatory factor 3. *Proceedings of the National Academy of Sciences of the United States of America* 95:9837-9842.

145. Servant, M.J., B. Tenoever, and R. Lin. 2002. Overlapping and distinct mechanisms regulating IRF-3 and IRF-7 function. *J Interferon Cytokine Res* 22:49-58.

146. Malmgaard, L. 2004. Induction and regulation of IFNs during viral infections. *J Interferon Cytokine Res* 24:439-454.

147. Alam, R., S. Stafford, P. Forsythe, R. Harrison, D. Faubion, M.A. Lett-Brown, and J.A. Grant. 1993. RANTES is a chemotactic and activating factor for human eosinophils. *J Immunol* 150:3442-3448.

148. Casola, A., A. Henderson, T. Liu, R.P. Garofalo, and A.R. Brasier. 2002. Regulation of RANTES promoter activation in alveolar epithelial cells after cytokine stimulation. *American journal of physiology* 283:L1280-1290.

149. Genin, P., M. Algarte, P. Roof, R. Lin, and J. Hiscott. 2000. Regulation of RANTES chemokine gene expression requires cooperativity between NF-kappa B and IFN-regulatory factor transcription factors. *J Immunol* 164:5352-5361.

150. Schall, T.J., K. Bacon, K.J. Toy, and D.V. Goeddel. 1990. Selective attraction of monocytes and T lymphocytes of the memory phenotype by cytokine RANTES. *Nature* 347:669-671.

151. Annunziato, F., L. Cosmi, G. Galli, C. Beltrame, P. Romagnani, R. Manetti, S. Romagnani, and E. Maggi. 1999. Assessment of chemokine receptor expression by human Th1 and Th2 cells in vitro and in vivo. *Journal of leukocyte biology* 65:691-699.

152. Bonecchi, R., G. Bianchi, P.P. Bordignon, D. D'Ambrosio, R. Lang, A. Borsatti, S. Sozzani, P. Allavena, P.A. Gray, A. Mantovani, and F. Sinigaglia. 1998. Differential expression of chemokine receptors and chemotactic responsiveness of type 1 T helper cells (Th1s) and Th2s. *The Journal of experimental medicine* 187:129-134.

153. Nansen, A., O. Marker, C. Bartholdy, and A.R. Thomsen. 2000. CCR2+ and CCR5+ CD8+ T cells increase during viral infection and migrate to sites of infection. *European journal of immunology* 30:1797-1806.

154. Ward, S.G., K. Bacon, and J. Westwick. 1998. Chemokines and T lymphocytes: more than an attraction. *Immunity* 9:1-11.

155. Ortiz, B.D., A.M. Krensky, and P.J. Nelson. 1996. Kinetics of transcription factors regulating the RANTES chemokine gene reveal a developmental switch in nuclear events during T-lymphocyte maturation. *Molecular and cellular biology* 16:202-210.

156. Hiura, T.S., S.J. Kempiak, and A.E. Nel. 1999. Activation of the human RANTES gene promoter in a macrophage cell line by lipopolysaccharide is dependent on stress-activated protein kinases and the IkappaB kinase cascade: implications for exacerbation of allergic inflammation by environmental pollutants. *Clinical immunology (Orlando, Fla* 90:287-301.

157. Miyamoto, N.G., P.S. Medberry, J. Hesselgesser, S. Boehlk, P.J. Nelson, A.M. Krensky, and H.D. Perez. 2000. Interleukin-1beta induction of the chemokine RANTES promoter in the human astrocytoma line CH235 requires both constitutive and inducible transcription factors. *Journal of neuroimmunology* 105:78-90.

158. Moriuchi, H., M. Moriuchi, and A.S. Fauci. 1997. Nuclear factor-kappa B potently up-regulates the promoter activity of RANTES, a chemokine that blocks HIV infection. *J Immunol* 158:3483-3491.

159. Nelson, P.J., B.D. Ortiz, J.M. Pattison, and A.M. Krensky. 1996. Identification of a novel regulatory region critical for expression of the RANTES chemokine in activated T lymphocytes. *J Immunol* 157:1139-1148.

160. Nelson, P.J., H.T. Kim, W.C. Manning, T.J. Goralski, and A.M. Krensky. 1993. Genomic organization and transcriptional regulation of the RANTES chemokine gene. *J Immunol* 151:2601-2612.

161. Ullman, K.S., J.P. Northrop, C.L. Verweij, and G.R. Crabtree. 1990. Transmission of signals from the T lymphocyte antigen receptor to the genes responsible for cell proliferation and immune function: the missing link. *Annual review of immunology* 8:421-452.

162. Song, A., Y.F. Chen, K. Thamatrakoln, T.A. Storm, and A.M. Krensky. 1999. RFLAT-1: a new zinc finger transcription factor that activates RANTES gene expression in T lymphocytes. *Immunity* 10:93-103.

163. Lin, R., C. Heylbroeck, P. Genin, P.M. Pitha, and J. Hiscott. 1999. Essential role of interferon regulatory factor 3 in direct activation of RANTES chemokine transcription. *Molecular and cellular biology* 19:959-966.

164. Marfaing-Koka, A., O. Devergne, G. Gorgone, A. Portier, T.J. Schall, P. Galanaud, and D. Emilie. 1995. Regulation of the production of the RANTES chemokine by endothelial cells. Synergistic induction by IFN-gamma plus TNF-alpha and inhibition by IL-4 and IL-13. *J Immunol* 154:1870-1878.

165. Stellato, C., L.A. Beck, G.A. Gorgone, D. Proud, T.J. Schall, S.J. Ono, L.M. Lichtenstein, and R.P. Schleimer. 1995. Expression of the chemokine RANTES by a human bronchial epithelial cell line. Modulation by cytokines and glucocorticoids. *J Immunol* 155:410-418.

166. Graham, F.L., J. Smiley, W.C. Russell, and R. Nairn. 1977. Characteristics of a human cell line transformed by DNA from human adenovirus type 5. *The Journal of general virology* 36:59-74.

167. Addison, C.L., M. Hitt, D. Kunsken, and F.L. Graham. 1997. Comparison of the human versus murine cytomegalovirus immediate early gene promoters for transgene expression by adenoviral vectors. *The Journal of general virology* 78 (Pt 7):1653-1661.

168. Sargent, K.L., R.A. Meulenbroek, and R.J. Parks. 2004. Activation of adenoviral gene expression by protein IX is not required for efficient virus replication. *Journal of virology* 78:5032-5037.

169. Palmer, D., and P. Ng. 2003. Improved system for helper-dependent adenoviral vector production. *Mol Ther* 8:846-852.

170. Wilkie, N.M., S. Ustacelebi, and J.F. Williams. 1973. Characterization of temperature-sensitive mutants of adenovirus type 5: nucleic acid synthesis. *Virology* 51:499-503.

171. Doyle, K. 1996. Protocols and Applications Guide. Promega Corporation, Madison, Wisconsin. 45-46 pp.

172. Birnboim, H.C., and J. Doly. 1979. A rapid alkaline extraction procedure for screening recombinant plasmid DNA. *Nucleic acids research* 7:1513-1523.

173. Sambrook, J., Fritsch, E.F., Maniatis, T. 1989. Molecular Cloning: A Laboratory Manual. Cold Spring Harbor Laboratory Press, Cold Spring Harbor NY.

174. Nelson, J.E., and M.A. Kay. 1997. Persistence of recombinant adenovirus in vivo is not dependent on vector DNA replication. *Journal of virology* 71:8902-8907.

175. Collins, S.E., R.S. Noyce, and K.L. Mossman. 2004. Innate cellular response to virus particle entry requires IRF3 but not virus replication. *Journal of virology* 78:1706-1717.

176. Matlashewski, G. 1989. The cell biology of human papillomavirus transformed cells. *Anticancer research* 9:1447-1456.

177. Koromilas, A.E., S. Li, and G. Matlashewski. 2001. Control of interferon signaling in human papillomavirus infection. *Cytokine & growth factor reviews* 12:157-170.

178. Wold, W.S., K. Doronin, K. Toth, M. Kuppuswamy, D.L. Lichtenstein, and A.E. Tollefson. 1999. Immune responses to adenoviruses: viral evasion mechanisms and their implications for the clinic. *Current opinion in immunology* 11:380-386.

179. Chin, Y.R., and M.S. Horwitz. 2005. Mechanism for removal of tumor necrosis factor receptor 1 from the cell surface by the adenovirus RIDalpha/beta complex. *Journal of virology* 79:13606-13617.

180. Fessler, S.P., Y.R. Chin, and M.S. Horwitz. 2004. Inhibition of tumor necrosis factor (TNF) signal transduction by the adenovirus group C RID complex involves downregulation of surface levels of TNF receptor 1. *Journal of virology* 78:13113-13121.

181. Friedman, J.M., and M.S. Horwitz. 2002. Inhibition of tumor necrosis factor alpha-induced NF-kappa B activation by the adenovirus E3-10.4/14.5K complex. *Journal of virology* 76:5515-5521.

182. Lesokhin, A.M., F. Delgado-Lopez, and M.S. Horwitz. 2002. Inhibition of chemokine expression by adenovirus early region three (E3) genes. *Journal of virology* 76:8236-8243.

183. Bossert, B., S. Marozin, and K.K. Conzelmann. 2003. Nonstructural proteins NS1 and NS2 of bovine respiratory syncytial virus block activation of interferon regulatory factor 3. *Journal of virology* 77:8661-8668.

184. Brzozka, K., S. Finke, and K.K. Conzelmann. 2005. Identification of the rabies virus alpha/beta interferon antagonist: phosphoprotein P interferes with phosphorylation of interferon regulatory factor 3. *Journal of virology* 79:7673-7681.

185. Dip, R., and H. Naegeli. 2005. More than just strand breaks: the recognition of structural DNA discontinuities by DNA-dependent protein kinase catalytic subunit. *Faseb J* 19:704-715.

186. Boyer, J., K. Rohleder, and G. Ketner. 1999. Adenovirus E4 34k and E4 11k inhibit double strand break repair and are physically associated with the cellular DNA-dependent protein kinase. *Virology* 263:307-312.

187. Stracker, T.H., C.T. Carson, and M.D. Weitzman. 2002. Adenovirus oncoproteins inactivate the Mre11-Rad50-NBS1 DNA repair complex. *Nature* 418:348-352.

188. Boyle, K.A., R.L. Pietropaolo, and T. Compton. 1999. Engagement of the cellular receptor for glycoprotein B of human cytomegalovirus activates the interferon-responsive pathway. *Molecular and cellular biology* 19:3607-3613.

189. tenOever, B.R., M.J. Servant, N. Grandvaux, R. Lin, and J. Hiscott. 2002. Recognition of the measles virus nucleocapsid as a mechanism of IRF-3 activation. *Journal of virology* 76:3659-3669.

190. Smith, C.L., and G.L. Hager. 1997. Transcriptional regulation of mammalian genes in vivo. A tale of two templates. *The Journal of biological chemistry* 272:27493-27496.

191. Zhu, J., X. Huang, and Y. Yang. 2007. Innate immune response to adenoviral vectors is mediated by both Toll-like receptor-dependent and -independent pathways. *Journal of virology* 81:3170-3180.

192. Cerullo, V., M.P. Seiler, V. Mane, N. Brunetti-Pierri, C. Clarke, T.K. Bertin, J.R. Rodgers, and B. Lee. 2007. Toll-like receptor 9 triggers an innate immune response to helper-dependent adenoviral vectors. *Mol Ther* 15:378-385.

193. Nociari, M., O. Ocheretina, J.W. Schoggins, and E. Falck-Pedersen. 2007. Sensing infection by adenovirus: toll-like receptor-independent viral DNA recognition signals activation of the interferon regulatory factor 3 master regulator. *Journal of virology* 81:4145-4157.

APPENDIX A: Reagents

Tissue Culture

- MEM (Modified Eagle Medium) (Sigma)
- DMEM (Dulbecco Modified Eagle Medium) (Sigma)
- DMEM-PBS (Phosphate Buffered Saline) (Sigma)

- MEM/DMEM with 10% FBS (Fetal Bovine Serum):
  500mL MEM/DMEM (Sigma)
  50mL FBS (10%) (Invitrogen)
  5mL antibiotic/antimycotic (1%) (Invitrogen)
  5mL GlutaMax (1%) (Invitrogen)

- 10x Citric Saline:
  100.66g KCl (1.35M)
  44.11g sodium citrate (150mM)
  up to 1L H_2O
  autoclave 45min at 121°C

- 1x Citric Saline:
  50mL 10x Citric Saline
  up to 500mL H_2O

- 5x Trypsin (Invitrogen)

- 1x Trypsin:
  4mL 5x Trypsin (Invitrogen)
  up to 40mL DMEM-PBS (Sigma)

- Lipofectamine 2000 (Invitrogen)

Lysis Buffer

- RIPA (RadioImmunoPrecipitation Assay) Buffer (Phosphatase Treatment Exp.)
  250µL 1M Tris-HCl pH 7.4 (50mM)
  150µL 5M NaCl (150mM)
  50µL Nonidet P-40 (1%)
  500µL Glycerol (10%)
  50µL 0.5M EDTA (5mM)
  5µL aprotinin (5µg/mL)
  5µL leupeptin (5µg/mL)
  50µL 100mM PMSF (phenylmethylsulphonylfluoride) (1mM)
  up to 5mL with H_2O, filter sterilize

Western Blotting

- 2x Denaturing Sample Buffer:
  2.5mL 0.5M Tris-HCl pH 6.8
  25mL Glycerol (25%)
  10mL 20% SDS (2%)
  0.01g bromophenol blue
  up to 100mL H_2O

- 10% APS:
  0.1g ammonium persulfate
  up to 1mL H_2O

- 2x Separating Gel Buffer:
  18.164g Tris (750mM)
  0.4g SDS (0.2%)
  up to 200mL H_2O
  adjust pH to 8.8

- Separating Gel Solution:

Reagents	7.5% SDS-PAGE	10% SDS-PAGE	12% SDS-PAGE
ddH_2O	2.5mL	2.0mL	1.0mL
2x Sep Gel Buffer	5.0mL	5.0mL	5.0mL
30% Acrylamide	2.5mL	3.0mL	4.0mL
10% APS	100µL	100µL	100µL
TEMED	10µL	10µL	10µL

- 2x Stacking Gel Buffer:
  6.056g Tris (250mM)
  0.4g SDS (0.2%)
  up to 200mL H_2O
  adjust to pH to 6.8

- Stacking Gel Solution:
  2mL H_2O
  3mL 2x Stacking Gel Buffer
  1mL 30% Acrylamide
  100 µL 10% APS
  10 µL TEMED.

- 1x Running Buffer:
  6.08g Tris (50mM)
  28.8g glycine (1.44%)
  2.0g SDS (0.1%)
  up to 2L H_2O

- 1x Transfer Buffer:
  5.82g Tris (48mM)
  2.93g glycine (0.293%)
  3.75mL 10%SDS (0.0375%)
  200mL MeOH (20%)
  up to 1L H_2O.

- 0.1% TBST (Tris Buffered Saline with Tween20):
  30mL 5M NaCl (150mM)
  10mL 1M Tris-HCl pH8.0 (10mM)
  1mL TWEEN-20 (0.1%)
  up to 1L H_2O

- 5% Milk Blocking Solution:
  1g skim milk powder
  up to 20mL with 0.1% TBST

Cloning

Bacterial Amplification of Cloned DNA

- LB Broth:
  20g LB Broth up to 1L H_2O
  autoclave 45min at 121°C

- LB Broth with Agar:
  500mL LB Broth
  7.5g Agar

- LB Broth with Agar and AMP:
  500mL LB Broth
  500 µL 50mg/mL Ampicillin (50 µg/mL)

- 30% Glycerol:
  30mL Glycerol,
  up to 100mL H_2O

Plasmid DNA Preparation (as in Bimboim and Dolly (172) and Sambrook *et al.* (173))

- Solution I:
  4.5g dextrose (50mM)
  12.5mL 1M Tris-HCl pH7.5 (250mM)
  10mL 0.5M EDTA pH 8.0 (10mM)
  up to 500mL H_2O
  adjust pH to 8.0, filter sterilize

- Solution II:
  200µL 10M NaOH (200mM)
  500µL 20% SDS (1%)
  up to 10mL H_2O

- Solution III:
  147.21g potassium acetate
  57.5mL glacial acetic acid (11.5%)
  up to 500mL H_2O

- 10x SSC (standard saline citrate):
  87.66g NaCl
  13.23g sodium citrate
  up to 1L H_2O

- 0.1x SSC:
  5mL 10x SSC
  up to 500mL H_2O

RbCl Competent Cells (as in (171))

- 2x YT (Yeast-Tryptone):
  8g Tryptone-peptone
  5g yeast extract
  2.5g NaCl
  up to 500mL H_2O
  adjust to pH 7.0, filter sterilize

- RF1:
  1.2g RbCl (100mM)
  0.99g $MnCl_2.4\ H_2O$ (50mM)
  3mL 1M potassium acetate (30mM)
  0.15g $CaCl_2.2H_2O$ (10mM)
  15mL Glycerol (15% w/v)
  up to 100mL H_2O
  adjust to pH 5.8 with 0.2M acetic acid

- 1M Potassium Acetate:
  9.82g potassium acetate,
  up to 100mL H_2O
  adjust pH to 7.5 with 0.2M acetic acid.

- RF2:
  2mL 0.2M MOPS (10mM)
  0.12g RbCl (10mM)
  1.1g $CaCl_2.2H_2O$ (75mM)
  15mL Glycerol (15% w/v)
  up to 100mL H_2O
  adjust to pH 6.8 with 2N NaOH

- 0.5M MOPS (3-(N-morpholino)propanesulfonic acid:
  10.46g MOPS
  up to 100mL H_2O
  adjust to pH 6.8 with 2N NaOH

Agarose Gel Electrophoresis

- 50x TAE (Tris-AceticAcid-EDTA):
  242g Tris
  57mL acetic acid (5.7%)
  100mL 0.5M EDTA (50mM)
  up to 1L H_2O

- 1x TAE:
  80mL 50x TAE
  up to 4L H_2O

- Agarose gel (1.2%)
  1.2g agarose (1.2%)
  up to 100mL 1x TAE
  1μL ethidium bromide

- 6x Loading Buffer:
  40g sucrose (40%)
  0.125g bromophenol blue (0.125%)
  20mL 0.5M EDTA pH 8.0 (0.1M)
  up to 100mL H_2O

- Loading Buffer + RNAse:
  1.5mL 6x Loading Buffer
  10μL 50mg/mL RNAse

General Chemicals and Reagents

- 1M Tris-HCl pH8.0:
  121.14g Tris
  up to 1L H_2O
  adjust to pH 8.0 with HCl

- 0.5M EDTA:
  146.13g EDTA (ethylenediaminetetraacetic acid)
  up to 1L H_2O
  adjust to pH 8.0 with HCl

- TE: Tris-EDTA
  10mM Tris-HCl pH8.0
  1mM EDTA pH8.0

- 10M NaOH:
  39.978g NaOH
  up to 100mL H_2O

- 5M NaCl:
  146.11g NaCl
  up to 500mL H_2O.

- 20% SDS:
  100g SDS (sodium dodecyl sulfate)
  up to 500mL H_2O

APPENDIX B: Plasmids

List of plasmids created for this project

1. Plasmids containing IRF-3 mutations:

Note: The original commercially purchased IRF-3 cDNA sequence contained an insert that placed the carboxy terminus of the protein out of frame. This error was not discovered until many derivative plasmids had been already generated.

Incorrect Plasmids:

pBS-IRF3

This plasmid contains the incorrect IRF-3 sequence in a pBluescriptKS+ (Stratagene) vector. To construct this plasmid, IRF-3 cDNA was amplified using overlap PCR with the following primers:

5'-CCG TGA TCA GCC ATG GGA ACC CCA AAG CCA CGG ATC CTG -3' (forward)
5'-CCG GAA TTC TCA GCT CTC CCC AGG GCC CTG GAA ATC-3' (reverse)

Amplified IRF-3 cDNA was then ligated into *Eco*RI/*Kpn*I-digested pBluescriptKS+.

pBS-Flag-IRF3

This plasmid contains the incorrect Flag-tagged IRF-3 sequence in a pBluescriptKS+ (Stratagene) vector. To construct this plasmid, a ~36 bp oligonucleotide sequence containing the FLAG tag and flanked by *Nco*I restriction sites was annealed and ligated into *Nco*I-digested pBS-IRF3. The oligonucleotide sequences used are as follows:

5'-CAT GCT TGA TTA CAA GGA TGA CGA CGA TAA GCT TGG -3' (forward)
5'-GAA CTA ATG TTC CTA CTG CTG CTA TTC GAA CCG TAC- 3' (reverse)

pcDNA3-Flag-IRF3

This plasmid contains the incorrect Flag-tagged IRF-3 sequence in a pcDNA3 (Invitrogen) vector. To construct this plasmid, a ~1.3 kb *Eco*RI/*Kpn*I fragment containing the entire IRF-3 open reading frame, was excised from pBS-Flag-IRF3 and cloned into *Eco*RI/*Kpn*I-digested pcDNA3.

pBS-Flag-IRF3-T135A
(see pKC23 for corrected plasmid)

This plasmid contains the incorrect Flag-tagged IRF-3 sequence with the correct T135A mutation in a pBluescriptKS+ vector. To construct this plasmid, pBS-Flag-IRF3 was amplified using overlap PCR with the following primers containing the T135A mutation:

5'-GCG ACT AGT GAT GCC CAG GAA GAC ATT CTG GAT G-3' (forward)
5'-GCG ACT AGT ACT GCC TCC ACC ATT GGT GTC CGG AG-3' (reverse)

Linear amplified pBS-Flag-IRF3 (containing the T135A mutation) was self-ligated after *Spe*I digestion.

pBS-Flag-IRF3-S188A
(see pKC24 for corrected plasmid)

This plasmid contains the incorrect Flag-tagged IRF-3 sequence with the correct S188A mutation in a pBluescriptKS+ vector. To construct this plasmid, pBS-Flag-IRF3 was amplified using overlap PCR with the following primers containing the S188A mutation:

5'-GCG CCT AGG GCC CGC TGA GAA CCC ACT GAA GCG GCT G-3' (forward)
5'-GCG CCT AGG TTT GGG AAG GGA GTG GGA TTG TC-3' (reverse)

Linear amplified pBS-Flag-IRF3 (containing the S188A mutation) was self-ligated after *Avr*II digestion.

pBS-Flag-IRF3-T135A/S188A
(see pKC16 for corrected plasmid)

This plasmid contains the incorrect Flag-tagged IRF-3 sequence with the correct T135A and S188A mutations in a pBluescriptKS+ vector. To construct this plasmid, a ~180 bp *Xmn*I fragment containing the S188A mutation was excised from pBS-Flag-IRF3-S188A and cloned into *Xmn*I-digested pBS-Flag-IRF3-T135A.

pBS-Flag-IRF3-2A

This plasmid contains the incorrect Flag-tagged IRF-3 sequence with the correct 2A mutation in a pBluescriptKS+ vector. To construct this plasmid, a ~177 bp oligonucleotide sequence containing the 2A mutation and flanked by *Bsu*36I/*Sse*8387I restriction sites was annealed and ligated into *Bsu*36I/*Sse*8387I-digested pBS-Flag-IRF3. The oligonucleotide sequences used are as follows:

5'-TCA GGG CCT TGG TAG AAA TGG CCC GGG TAG GGG GTG CCG CAG CAC TGG AGA ATA CTG TGG ACC TGC ACA TTT CCA ACA GCC ACC CAC TCT CCC TCA CCT CCG ACC AGT ACA AGG CTT ACC TGC A-3' (forward)

5'-GGT AAG CCT TGT ACT GGT CGG AGG TGA GGG AGA GTG GGT GGC TGT TGG AAA TGT GCA GGT CCA CAG TAT TCT CCA GTG CTG CGG CAC CCC CTA CCC GGG CCA TTT CTA CCA AGG CCC-3' (reverse)

pBS-Flag-IRF3-5A

This plasmid contains the incorrect Flag-tagged IRF-3 sequence with the correct 5A mutation in a pBluescriptKS+ vector. To construct this plasmid, a ~117 bp oligonucleotide sequence containing the 5A mutation and flanked by *Bsu*36I/*Sse*8387I restriction sites was annealed and ligated into *Bsu*36I/*Sse*8387I-digested pBS-Flag-IRF3. The oligonucleotide sequences used are as follows:

5'-TCA GGG CCT TGG TAG AAA TGG CCA GGG TAG GGG GTG CCT CCT CCC TGG AGA ATA CTG TCG ACC TGC ACA TTG CCA ACG CCC ACC CAC TCG CCC TCG CCG CCG ACC AGT ACA AGG CCT ACC TGC A-3' (forward)

5'-GGT AGG CCT TGT ACT GGT CGG CGG CGA GGG CGA GTG GGT GGG CGT TGG CAA TGT GCA GGT CGA CAG TAT TCT CCA GGG AGG CAC CCC CTA CCC TGG CCA TTT CTA CCA AGG CCC-3' (reverse)

pBS-Flag-IRF3-2A/5A

This plasmid contains the incorrect Flag-tagged IRF-3 sequence with the correct 2A/5A mutation in a pBluescriptKS+ vector. To construct this plasmid, pBS-Flag-IRF3-5A was amplified using overlap PCR with the following primers containing the 2A mutation:

5'-GGC ACG CGT AGG GGG TGC CGC AGC CCT GGA GAA TAC TGT GGA CCT G-3' (forward)
5'-GCG ACG CGT GCC ATT TCT ACC AAG GCC CTG-3' (reverse)

Linear amplified pBS-Flag-IRF3-5A (containing the 2A mutation) was self-ligated after *Mlu*I digestion.

pcDNA3-Flag-IRF3-T135A
(see pKC25 for corrected plasmid)

This plasmid contains the incorrect Flag-tagged IRF-3 sequence with the incorrect T135A mutation in a pcDNA3 vector. To construct this plasmid, a ~1.3 kb *Eco*RI/*Kpn*I fragment containing the entire IRF-3 open reading frame and thus including the T135A mutation, was excised from pBS-Flag-IRF3-T135A and cloned into *Eco*RI/*Kpn*I-digested pcDNA3.

pcDNA3-Flag-IRF3-S188A
(see pKC26 for corrected plasmid)

This plasmid contains the incorrect Flag-tagged IRF-3 sequence with the correct S188A mutation in a pcDNA3 vector. To construct this plasmid, a ~1.3 kb *Eco*RI/*Kpn*I fragment containing the entire IRF-3 open reading frame and thus including the S188A mutation, was excised from pBS-Flag-IRF3-S188A and cloned into *Eco*RI/*Kpn*I-digested pcDNA3.

pcDNA3-Flag-IRF3-2A
(see pKC18 for corrected plasmid)

This plasmid contains the incorrect Flag-tagged IRF-3 sequence with the correct 2A mutation in a pcDNA3 vector. To construct this plasmid, a ~1.3 kb *Eco*RI/*Kpn*I fragment containing the entire IRF-3 open reading frame and thus including the S188A mutation, was excised from pBS-Flag-IRF3-2A and cloned into *Eco*RI/*Kpn*I-digested pcDNA3.

pcDNA3-Flag-IRF3-5A
(see pKC19 for corrected plasmid)

This plasmid contains the incorrect Flag-tagged IRF-3 sequence with the correct 5A mutation in a pcDNA3 vector. To construct this plasmid, a ~1.3 kb *Eco*RI/*Kpn*I fragment containing the entire IRF-3 open reading frame and thus including the S188A mutation, was excised from pBS-Flag-IRF3-5A and cloned into *Eco*RI/*Kpn*I-digested pcDNA3.

pcDNA3-Flag-IRF3-2A/5A
(see pKC20 for corrected plasmid)

This plasmid contains the incorrect Flag-tagged IRF-3 sequence with the correct 2A and 5A mutations in a pcDNA3 vector. To construct this plasmid, a ~1.3 kb *Eco*RI/*Kpn*I fragment containing the entire IRF-3 open reading frame and thus including both the 2A and 5A mutations, was excised from pBS-Flag-IRF3-2A/5A and cloned into *Eco*RI/*Kpn*I-digested pcDNA3.

pcDNA3-Flag-IRF3-T135A/S188A
(see pKC21 for corrected plasmid)

This plasmid contains the incorrect Flag-tagged IRF-3 sequence with the incorrect T135A and correct S188A mutations in a pcDNA3 vector. To construct this plasmid, a ~1.3 kb *Eco*RI/*Kpn*I fragment containing the entire IRF-3 open reading frame and thus including both the T135A and S188A mutations, was excised from pBS-Flag-IRF3-T135A/S188A and cloned into *Eco*RI/*Kpn*I-digested pcDNA3.

pcDNA3-Flag-IRF3-T135A/S188A/2A/5A
(see pKC22 for corrected plasmid)

This plasmid contains the incorrect Flag-tagged IRF-3 sequence with the incorrect T135A and correct S188A, 2A, and 5A mutations in a pcDNA3 vector. To construct this plasmid, a ~171 bp *Eco*RI/*Bsu*36I fragment containing the 2A and 5A mutations, was excised from pBS-Flag-IRF3-T135A/S188A and cloned into *Eco*RI/*Bsu*36I-digested pcDNA3-Flag-IRF3-T135A/S188A.

Correct Plasmids:

pBS-Flag-IRF3fix

This plasmid contains the correct Flag-tagged IRF-3 sequence in a pBluescriptKS+ (Stratagene) vector. To construct this plasmid, pBS-Flag-IRF3 was amplified using overlap PCR with the following primers:

5'-GCG AGA TCT GAT TAC CTT CAC GGA AGG AAG-3' (forward)
5'-GCG AGA TCT ACA ATG AAG GGC CCC AGG TC-3' (reverse)

These primers were created to prevent the 16 bp insert from being amplified (thus putting IRF-3 back in frame). Linear amplified pBS-Flag-IRF3 (without the 16 bp insert) was self-ligated after *Bgl*II digestion.

pcDNA3-Flag-IRF3fix

This plasmid contains the correct Flag-tagged IRF-3 sequence in a pcDNA3 (Invitrogen) vector. To construct this plasmid, a ~1.3 kb *Eco*RI/*Kpn*I fragment containing the entire IRF-3 open reading frame, was excised from pBS-Flag-IRF3fix and cloned into *Eco*RI/*Kpn*I-digested pcDNA3.

pKC16

This plasmid contains Flag-tagged IRF-3 with the T135A and S188A mutations in a pBluescriptKS+ vector. To construct this plasmid, a ~220 bp *Bbs*I/*Bbs*I fragment containing the S188A mutation was excised from pKC23 and cloned into *Bbs*I-digested pKC24.

pKC18

This plasmid contains Flag-tagged IRF-3 with the 2A mutation in a pcDNA3 vector. To construct this plasmid, a ~200 bp *Xba*I/*Bsu*36I fragment containing the 2A mutation was removed from pcDNA3-Flag-IRF3-2A and cloned into *Xba*I/*Bsu*36I-digested pcDNA3-Flag-IRF-3, which contains the correct IRF-3 sequence.

pKC19

This plasmid contains Flag-tagged IRF-3 with the 5A mutation in a pcDNA3 vector. To construct this plasmid, a ~200 bp *Xba*I/*Bsu*36I fragment containing the 5A mutation was removed from pcDNA3-Flag-IRF3-5A and cloned into *Xba*I/*Bsu*36I-digested pcDNA3-Flag-IRF-3, which contains the correct IRF-3 sequence.

pKC20

This plasmid contains Flag-tagged IRF-3 with the 2A and 5A mutations in a pcDNA3 vector. To construct this plasmid, a ~200 bp *XbaI*/*Bsu*36I fragment containing the 2A and 5A mutations was excised from pcDNA3-Flag-IRF3-2A/5A and cloned into *XbaI*/*Bsu*36I-digested pcDNA3-Flag-IRF-3, which contains the correct IRF-3 sequence.

pKC21

This plasmid contains Flag-tagged IRF-3 with the T135A and S188A mutations in a pcDNA3 vector. To construct this plasmid, a ~1.3 kb *Eco*RI/*Kpn*I fragment containing the entire IRF-3 open reading frame and thus including the T135A and S188A mutations, was excised from pKC16 and cloned into *Eco*RI/*Kpn*I-digested pcDNA3.

pKC21b

This plasmid contains Flag-tagged IRF-3 with the T135A, S188A, 2A, and 5A mutations in a pBluescriptKS+ vector. To construct this plasmid, a ~216 bp *XbaI*/*Bsu*36I fragment containing the 2A and 5A mutations was removed from pKC20, and cloned into *XbaI*/*Bsu*36I-digested pKC16.

pKC22

This plasmid contains Flag-tagged IRF-3 with the T135A, S188A, 2A, and 5A mutations in a pcDNA3 vector. To construct this plasmid, a ~216 bp *XbaI*/*Bsu*36I fragment containing the 2A and 5A mutations was removed from pKC20, and cloned into *XbaI*/*Bsu*36I-digested pKC21.

pKC23

This plasmid contains Flag-tagged IRF-3 with the T135A mutation in a pBluescriptKS+ vector. To construct this plasmid, a ~731 bp *Hind*III/*Msc*I fragment containing the T135A mutation was excised from pBS-Flag-IRF3-T135A, and cloned into *Hind*III/*Kpn*I-digested pBS-Flag-IRF3, which contains the correct IRF-3 sequence.

pKC24

This plasmid contains Flag-tagged IRF-3 with the S188A mutation in a pBluescriptKS+ vector. To construct this plasmid, a ~731 bp *Hind*III/*Msc*I fragment containing the S188A mutation was excised from pBS-Flag-IRF3-S188A, and cloned into *Hind*III/*Kpn*I-digested pBS-Flag-IRF3, which contains the correct IRF-3 sequence.

pKC25

This plasmid contains Flag-tagged IRF-3 with the T135A mutation in a pcDNA3 vector. To construct this plasmid, a ~1.3 kb *Eco*RI/*Kpn*I fragment containing the entire IRF-3 open reading frame and thus including the T135A mutation, was excised from pKC23 and cloned into *Xba*I/*Bsu*36I-digested pcDNA3.

pKC26

This plasmid contains Flag-tagged IRF-3 with the S188A mutation in a pcDNA3 vector. To construct this plasmid, a ~1.3 kb *Eco*RI/*Kpn*I fragment containing the entire IRF-3 open reading frame and thus including the S188A mutation, was excised from pKC24 and cloned into *Xba*I/*Bsu*36I-digested pcDNA3.

2. RANTES Promoter Constructs:

The following plasmids were a generous gift from Dr. D.A. Muruve (University of Calgary, Calgary, Alberta). They were generated from the pGL2-RANTES(-900) plasmid, originally constructed by Nelson *et al.* (160). pGL2-RANTES(-900) consists of a 900 bp sequence upstream of the transcriptional start site of the human RANTES gene (GenBank accession no. S64885) cloned into a pGL2 Basic reporter vector (Promega). See Fig. 18*A* and 19*A* for a detailed representation of the human RANTES promoter and the deletional mutants used in this project.

pGL2-RANTES(-296)

This plasmids contains a deletional mutant of pGL2-RANTES(900) at position –296 (296 nucleotides into the immediate upstream region of the promoter region). This deletional mutant was constructed by PCR (Bowen *et al.* (75)), and contains both IRF-3 and NK-κB binding sites upstream of the RANTES promoter.

pGL2-RANTES(-181)

This plasmid contains a deletional mutant of pGL2-RANTES(900) at position –181 (181 nucleotides into the immediate upstream region of the promoter region). This deletional mutant was constructed in a 5' to 3' restriction enzyme digest using *Sac*I (Bowen *et al.* (75)), and contains both IRF-3 and NK-κB binding sites upstream of the RANTES promoter.

pGL2-RANTES(-90)

This plasmid is a deletional mutant of pGL2-RANTES(900) at position –90 (90 nucleotides into the immediate upstream region of the promoter region), thereby removing the IRF-3 binding site upstream from the RANTES promoter. This deletional mutant was constructed by PCR (Bowen *et al.* (75)).

pGL2-RANTES(-296mutκB)

This plasmid is a deletional mutant of pGL2-RANTES(900) at position –296, which also contains site-directed mutagenesis of the proximal NK-κB binding sites at positions –54 and –39 bp (upstream of the transcriptional start site), thereby removing the ability for NK-κB to bind at these sites. This plasmid was constructed using a site-directed mutagenesis kit (see Bowen *et al.* (75)).

pKC27

This plasmid contains a fragment of pGL2-RANTES(-181) cloned into a pBluescript KS+ vector. To construct this plasmid, a ~357 bp *Xba*I fragment containing the IRF-3 binding sites upstream of the RANTES promoter, was removed from pGL2-RANTES(-181) and cloned into *Xba*I-digested pBluescript KS+.

pKC28

This plasmid contains a mutated fragment of pGL2-RANTES(-181) cloned into a pBluescript KS+ vector. To construct this plasmid, a ~63 bp oligonucleotide flanked by *Bsp*EI/*Pfl*MI restriction sites and containing 6 point mutations in the ISRE of the RANTES promoter (Invitrogen) was ligated into *Bsp*EI/*Pfl*MI-digested pKC27. The oligonucleotide sequences (containing the mutations) used are as follows:

5'-CCG GAG GCT ATT TCA GTA AAC TAA ACC GTT TTG TGC AAT TTC ACT TAT GAT ACC GCC CAA TGC-3' (forward)

5'-TTG GCC GGT ATC ATA AGT GAA ATT GCA CAA AAC GGT TTA GTT TAC TGA AAT AGC CT-3' (reverse)

pGL2-RANTES(-181mutISRE)

This plasmid is a deletional mutant of pGL2-RANTES(900) at position –181, which also contains site-directed mutagenesis of the proximal ISRE at positions –114/113/112 bp and –109/108/107 bp (upstream of the transcriptional start site), thereby removing the ability for IRF-3 to bind at these sites. To construct this plasmid, a ~357 bp *Xba*I fragment containing the IRF-3 binding sites upstream of the RANTES promoter, was removed from pKC28 and cloned into *Xba*I-digested pGL2-RANTES(-181).

APPENDIX C: Published Manuscript

Michaud, J-L. R., **Chaisson, K.M.**, Parks, R.J., and C.R.J. Kennedy, FSGS-associated α-actinin-4 (K256E) impairs cytoskeletal dynamics in podocytes. *Kidney Int.* (6):1054-61, 2006.

I contributed to the following publication by generating the adenoviral constructs containing the wildtype and mutant murine HA-*ACTN4* sequence (Ad*ACTN4*-wt/mut) used in the study. Generation of these vectors involved several cloning steps: transfection and rescue of the Ad vectors on 293 cells, preparation of large scale virus culture (3L spinner flasks), vector purification by cesium chloride buoyant density centrifugation, and analysis of vector quality and quantity.

FSGS-associated α-actinin-4 (K256E) impairs cytoskeletal dynamics in podocytes

J-LR Michaud[1,2], KM Chaisson[1,3], RJ Parks[1,3] and CRJ Kennedy[1,2]

[1]*Kidney Research Centre and Molecular Medicine Program, Ottawa Health Research Institute, University of Ottawa, Ottawa, Ontario, Canada;* [2]*Department of Cellular and Molecular Medicine, University of Ottawa, Ottawa, Ontario, Canada and* [3]*Department of Biochemistry Microbiology and Immunology, University of Ottawa, Ottawa, Ontario, Canada*

Mutations in the *ACTN4* gene, encoding the actin crosslinking protein α-actinin-4, are associated with a familial form of focal segmental glomerulosclerosis (FSGS). Mice with podocyte-specific expression of K256E α-actinin-4 develop foot process effacement and glomerulosclerosis, highlighting the importance of the cytoskeleton in podocyte structure and function. K256E α-actinin-4 exhibits increased affinity for F-actin. However, the downstream effects of this aberrant binding on podocyte dynamics remain unclear. Wild-type and K256E α-actinin-4 were expressed in cultured podocytes via adenoviral infection to determine the effect of the mutation on α-actinin-4 subcellular localization and on cytoskeletal-dependent processes such as adhesion, spreading, migration, and formation of foot process-like peripheral projections. Wild-type α-actinin-4 was detected primarily in the Triton-soluble fraction of podocyte lysates and localized to membrane-associated cortical actin and focal adhesions, with some expression along stress fibers. Conversely, K256E α-actinin-4 was detected predominantly in the Triton-insoluble fraction, was excluded from cortical actin, and localized almost exclusively along stress fibers. Both wild-type and K256E α-actinin-4-expressing podocytes adhered equally to an extracellular matrix (collagen-I). However, podocytes expressing K256E α-actinin-4 showed a reduced ability to spread and migrate on collagen-I. Lastly, K256E α-actinin-4 expression reduced the mean number of actin-rich peripheral projections. Our data suggest that aberrant sequestering of K256E α-actinin-4 impairs podocyte spreading, motility, and reduces the number of peripheral projections. Such intrinsic cytoskeletal derangements may underlie initial podocyte damage and foot process effacement encountered in *ACTN4*-associated FSGS.

Kidney International advance online publication, 12 July 2006; doi:10.1038/sj.ki.5001665

KEYWORDS: FSGS; podocyte; cytoskeleton; α-actinin-4; foot processes

Correspondence: *CRJ Kennedy, Kidney Research Centre and Molecular Medicine Program, Division of Nephrology, Ottawa Health Research Institute, Ottawa Hospital and University of Ottawa, 451 Smyth Rd., Rm 1317, Ottawa, Ontario, Canada K1H 8M5. E-mail: ckennedy@uottawa.ca*

Received 9 September 2005; revised 20 March 2006; accepted 9 May 2006

Focal segmental glomerulosclerosis (FSGS) is a common glomerular lesion and a significant cause of end-stage renal disease.[1,2] Clinically, FSGS patients present with variable levels of proteinuria and a progressive loss of renal function. Pathologically, FSGS is characterized by segmental sclerosis in a proportion of glomeruli, the filtering units of the kidney.[3] Accumulating evidence suggests that defects in podocytes initiate processes leading to the degeneration of filtration integrity and the development of sclerotic lesions.[4–8]

Podocytes are terminally differentiated cells that line the outer aspects of the glomerular capillaries.[9] The highly ordered podocyte architecture consists of a cell body from which emerge major processes, which branch into foot processes that interdigitate with those of neighboring podocytes to provide the structural platform upon which a molecular sieve is formed. The foot processes are endowed with a microfilament-based contractile apparatus composed of actin, myosin-II, α-actinin, talin, paxillin, and vinculin,[10] and are anchored to the glomerular basement membrane via an $\alpha_3\beta_1$-integrin complex.[11,12] The intricate morphology of the podocyte, coupled to its exposure to distensile forces within the glomerular capillary render these cells susceptible to damage in many nephropathies, including FSGS.

The actin bundling α-actinins are members of the spectrin superfamily. Four isoforms have been described (α-actinin-1 to -4).[13] While α-actinins-2 and -3 are expressed at the Z-line of striated muscle, α-actinins-1 and -4 are more ubiquitously expressed. α-Actinin-4 is expressed in podocytes and is thought to play a key role in the maintenance of this cell's architecture.[14] The putative function of α-actinin-4, which exists as a head-to-tail homodimer, is to crosslink actin filaments through its N-terminal actin-binding domain comprised of two calponin homology domains. Increasing evidence suggests that α-actinin-4 may interact with a number of other proteins such as β_1-integrin,[13,15,16] synaptopodin,[17] vinculin,[18] and phosphatidylinositol 3-kinase.[19] In addition to an actin-binding domain, a number of other functional domains are found in the α-actinin-4 sequence – including two calcium-binding EF hands, a phosphoinositide-binding domain, as well as a focal adhesion kinase (FAK) tyrosine phosphorylation consensus sequence. Accordingly, phosphorylation by FAK,[20] binding of phosphoinositides,[21,22]

and sensitivity to intracellular calcium[23] may modulate the actin-binding properties and localization of α-actinin following various environmental stimuli.

Mutations in the *ACTN4* gene (K228E, T232I, and S235P) are associated with an autosomal-dominant form of FSGS.[24,25] We developed a mouse model of *ACTN4*-associated FSGS by expressing the murine correlate of the K228E mutation (K256E) in a podocyte-specific manner using the *mNPHS1* promoter.[26] These mice exhibit significant proteinuria and develop FSGS-like lesions, confirming that the disease originates in the podocyte. However, the mechanism by which mutations in α-actinin-4 dysregulate podocyte function is not fully understood. Abrogation of α-actinin-4 expression in mice yields severe glomerular disease.[27] Furthermore, recent studies by Yao *et al.*[28] suggest that the familial mutations promote α-actinin-4 aggregation and thereby target the protein for degradation via the proteasome pathway, resulting in a partial loss-of-function. In contrast, mutations in α-actinin-4 increase its affinity for filamentous actin (F-actin), suggesting a gain-of-function mechanism.[24,26] In support of the latter mechanism, the severity of the FSGS-like phenotype correlates directly with K256E α-actinin-4 levels in transgenic mice.[26] Thus, it remains unclear whether and how these two viewpoints can be reconciled.

To address this issue, we assessed the functional consequences of an FSGS-associated mutation (K256E) in α-actinin-4 at the cellular level. We now report the intracellular mislocalization of K256E α-actinin-4 in mouse podocytes, which undermines the processes of cell spreading and migration, and impairs the formation of actin-rich peripheral projections. Our data suggest that such defects in key cytoskeletal-associated processes may compromise the podocyte's ability to cope with the demands of the glomerular environment, maintain foot processes structure, and thereby initiate the progression towards sclerosis.

RESULTS

Mislocalization of K256E α-actinin-4 in cultured podocytes

Mutations in α-actinin-4 increase its affinity for F-actin *in vitro*.[24,26] However, the subcellular localization of mutant α-actinin-4 is not clearly defined. We therefore generated adenoviral constructs with hemagglutinin (HA)-tagged wild-type or K256E α-actinin-4 and transduced a conditionally immortalized mouse podocyte cell line. Podocytes were infected with a range of virus to determine a concentration yielding efficient expression (Figure 1a). For all subsequent experiments, infections were performed with a multiplicity of infection (MOI) of 25 and incubated for 72 h. There was no apparent degradation of heterologously expressed K256E α-actinin-4 during this timeframe as its expression paralleled that of the wild-type protein (Figure 1a). As shown in Figure 1b, wild-type α-actinin-4 localized predominantly with cortical actin. The wild-type protein was also distributed along stress fibers and at focal adhesions, as identified by vinculin co-immunofluorescence (Figure 1c). Conversely, K256E α-actinin-4 was absent from the cell periphery, but was preferentially associated with stress fibers (Figure 1b) and focal adhesions (Figure 1c).

Differential association of K256E α-actinin-4 with intracellular actin pools

We next performed cellular fractionation experiments to determine the association of wild-type and K256E α-actinin-4 with various intracellular actin pools. Podocytes expressing wild-type or K256E α-actinin-4 were lysed in Triton X-100-containing buffer and subject to differential centrifugation. As shown in Figure 2a and b, only $16.0 \pm 2.5\%$ of the wild-type α-actinin-4 associated with large cytoskeletal structures (Triton X-100 insoluble (TI) fraction), whereas $71.4 \pm 5.5\%$ of the protein remained soluble (Triton X-100 soluble (TS):S fraction). Conversely, $81.0 \pm 9.6\%$ of the K256E α-actinin-4 was associated with large cytoskeletal structures (TI fraction), and only $4.9 \pm 3.4\%$ of the mutant protein remained soluble (TS:S fraction). Expression of both wild-type and K256E α-actinin-4 was similar, as evidenced by the input. Furthermore, neither the expression of wild-type nor K256E α-actinin-4 altered total actin levels. These data reveal a differential association of wild-type versus K256E α-actinin-4, with K256E α-actinin-4 sequestered to large cytoskeletal structures such as actin bundles, whereas wild-type α-actinin-4 remains predominantly soluble.

Effect of K256E α-actinin-4 expression on cell adhesion, spreading, and migration

The inappropriate association of K256E α-actinin-4 with the actin cytoskeleton suggested that it may negatively affect cytoskeletal dynamics. We therefore determined its effect on cytoskeletal-dependent processes, such as cell adhesion, spreading, and migration. Since α-actinin-4 is associated with focal adhesions, we hypothesized that the mutant protein may negatively affect the ability of cells to adhere to an extracellular matrix. Adhesion assays were performed using podocytes expressing green fluorescent protein (GFP) alone (control), wild-type α-actinin-4, or K256E α-actinin-4 measuring their ability to bind to collagen-I-coated wells (Figure 3). The number of adherent cells was quantified at measuring various time points (3–24 h). Irrespective of the time allowed for adhesion, there was no difference in adhesion between wild-type and K256E α-actinin-4-expressing podocytes, suggesting that cell–matrix interactions are not adversely affected by K256E α-actinin-4.

We next performed a replating assay to assess the ability of cells expressing either wild-type or K256E α-actinin-4 to efficiently spread on an extracellular matrix (collagen-I). Podocytes expressing GFP alone (control), wild-type, or K256E α-actinin-4 were harvested and replated onto collagen-I-coated glass coverslips. Adherent cells were fixed after 3 or 6 h and visualized by immunofluorescence. Within 3 h of replating, a significant number of podocytes had adhered to the substratum and had begun to spread. For each condition, we observed no differences in the total number of

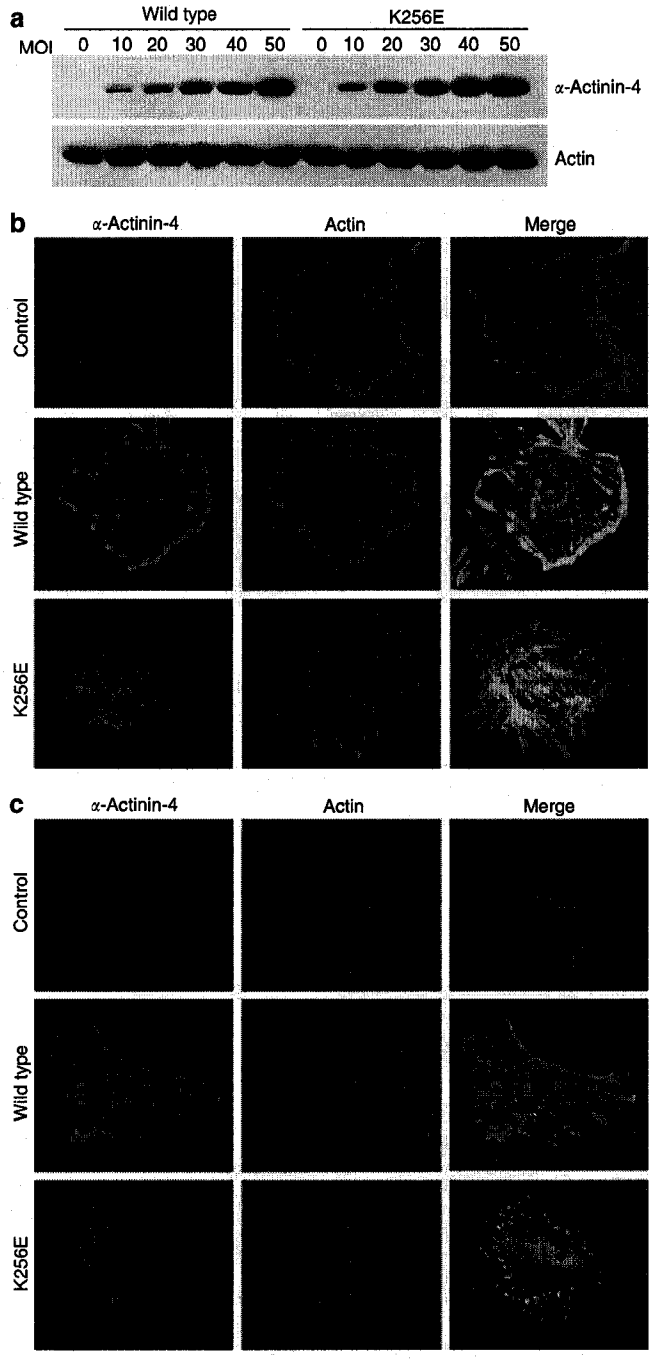

Figure 1 | Subcellular localization of wild-type and K256E α-actinin-4 in mouse podocytes. (**a**) Differentiated podocytes were incubated with a range of adenoviral doses (multiplicity of infection 0–50) for wild-type or K256E α-actinin-4 to determine optimal infection conditions. The expression achieved with both adenoviruses was similar for each condition. (**b**) 3 days following infection with viruses, differentiated podocytes were fixed and stained with an anti-HA tag antibody to detect α-actinin-4 and Alexa Fluor 488-phalloidin to detect F-actin. Uninfected cells were treated in the same manner and serve as control. Wild-type α-actinin-4 is predominantly found with membrane-associated cortical actin and process-like projections with limited expression along stress fibers. Conversely, K256E α-actinin-4 is predominantly associated with stress fibers and is excluded from the cell periphery. (**c**) Wild-type and K256E α-actinin-4 were colocalized with vinculin at focal adhesion complexes.

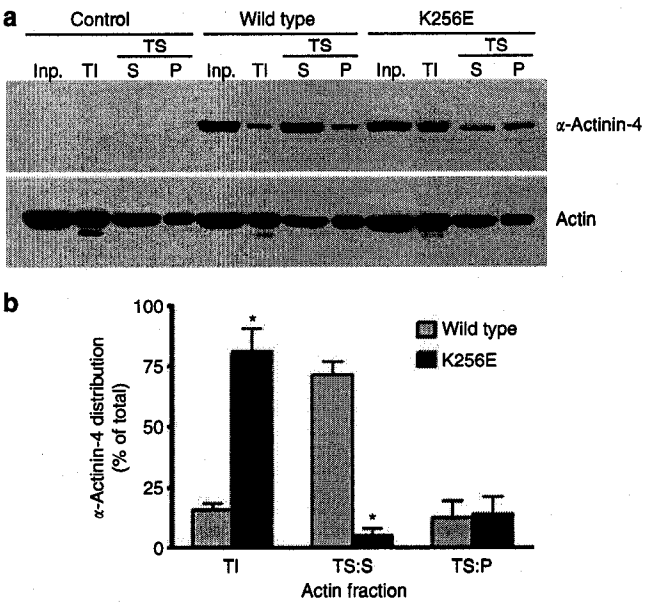

Figure 2 | Distribution of wild-type and K256E α-actinin-4 among intracellular actin pools. At 3 days post-infection, differentiated mouse podocytes were lysed in buffer containing 1% Triton X-100 and centrifuged at 15 000 *g* to pellet the TI fraction containing large cytoskeletal structures such as actin bundles. The TS fraction was further centrifuged at 100 000 *g* to separate G-actin (supernatant, S) from F-actin (pellet, P). Samples were then analyzed by Western blot using an anti-HA tag antibody and an anti-actin antibody. (**a**) A representative blot and (**b**) the graphical representation of three separate experiments illustrate the distribution of α-actinin-4 among the various actin pools. The majority (71.4±5.5%) of wild-type α-actinin-4 remained soluble (S, TS fraction), whereas the majority (81.0±9.6%) of K256E α-actinin-4 was associated with actin bundles (TI fraction). Uninfected cells were treated in the same manner and serve as control. Input lanes (Inp.) show similar expression levels of both wild-type and K256E α-actinin-4. *$P<0.005$ vs wild type ($n=3$).

podocytes adhering to the extracellular matrix. However, at both time points examined, the number of spreading podocytes was significantly lower in K256E α-actinin-4-expressing cells (13.0±0.3% at 3 h; 17.3±1.0% at 6 h) compared to control (29.2±5.8% at 3 h; 37.7±5.2% at 6 h) and wild type (34.7±4.4% at 3 h; 38.4±5.8% at 6 h) (Figure 4a). Within 6 h of replating, wild-type α-actinin-4 was localized with cortical actin at the cell periphery (Figure 4b). Conversely, K256E α-actinin-4 remained associated with F-actin and condensed in the cell body (Figure 4b), consistent with the observed impairment in cell spreading.

Cell migration relies upon a dynamic cytoskeleton. The increased affinity of K256E α-actinin-4 for F-actin could undermine this process. We therefore performed haptotactic transwell migration assays to determine the effect of K256E α-actinin-4 on cell migration. Podocytes expressing GFP alone (control), wild-type, or K256E α-actinin-4 were plated onto the upper surface of transwell inserts. After 24 h, the cells remaining in the upper chamber were removed and the cells that had migrated to the underside of the insert were quantified. Podocytes expressing wild-type α-actinin-4 migrated at a similar rate (90.8±9.2%) to control cells

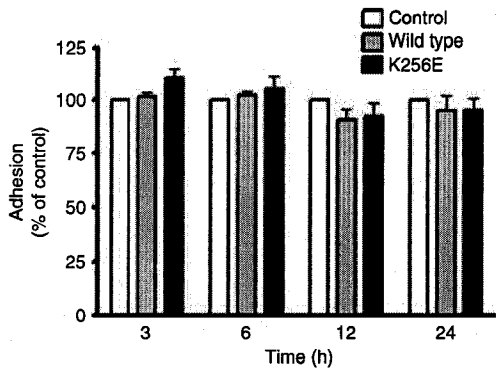

Figure 3 | Effect of α-actinin-4 on podocyte adhesion. Differentiated mouse podocytes expressing either GFP alone (control), wild-type, or K256E α-actinin-4 were trypsinized and replated onto collagen-I-coated 96-well U-bottom plates at a density of 5×10^4 cells/well. Cells were fixed with paraformaldehyde at various time points, stained with crystal violet, and the absorbance of each well measured at 595 nm with a spectrophotometric plate reader. At every time point examined, there was no significant difference in the ability of wild-type or K256E α-actinin-4-expressing cells to adhere to an extracellular matrix. Data are from three separate experiments ($n = 3$) and are expressed as a percent of control for each time point.

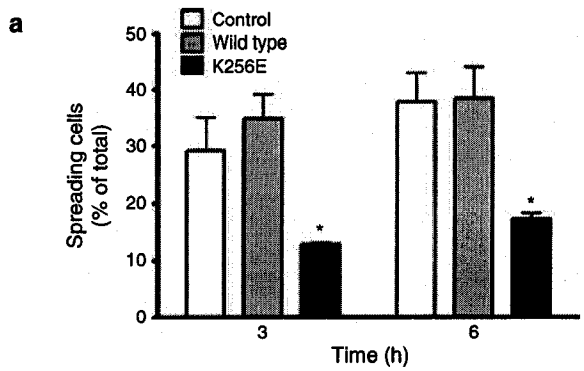

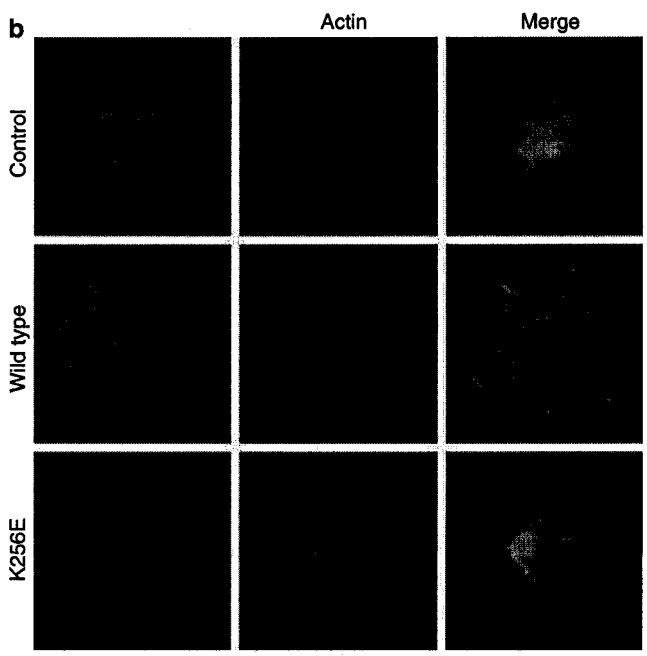

Figure 4 | Effect of α-actinin-4 on podocyte spreading. Differentiated mouse podocytes expressing GFP alone (control), wild-type, or K256E α-actinin-4 were trypsinized, held in suspension for 15 min, and then replated onto collagen-I-coated coverslips and analyzed by immunofluorescence at 3 and 6 h. (**a**) Expression of K256E α-actinin-4 significantly reduced the number of spreading cells at each time point examined. (**b**) After 6 h, wild-type α-actinin-4 was localized to cortical actin, whereas K256E α-actinin-4 remained condensed within the cell. *$P < 0.05$ vs control and wild-type of corresponding time point, ($n = 3$).

(Figure 5). Conversely, the migration of podocytes expressing K256E α-actinin-4 was significantly reduced ($52.1 \pm 10.7\%$; $P < 0.01$ vs control and wild type). These data suggest that K256E α-actinin-4 causes defects in cytoskeletal dynamics and impairs cellular processes such as spreading and migration.

Quantification of peripheral projections in cultured podocytes

Podocyte-specific expression of K256E α-actinin-4 leads to podocyte damage and foot process effacement *in vivo*.[26] The conditionally immortalized podocyte cell line used in the present studies have been shown to form foot process-like peripheral projections when cultured under non-permissive conditions.[29] We therefore assessed the effect of K256E α-actinin-4 on peripheral projections in differentiated podocytes (Figure 6). Podocytes expressing wild-type α-actinin-4 displayed a slight increase in the mean number of projections (3.8 ± 0.8 projections/cell vs 2.9 ± 0.6 for control), whereas podocytes expressing K256E α-actinin-4 exhibited a decrease in the mean number of projections (1.9 ± 0.4) (Figure 6b). Wild-type but not K256E α-actinin-4 was readily detected in the peripheral projections, along with actin (Figure 6a). Furthermore, projections emerging from podocytes expressing wild-type α-actinin-4 appeared longer and thinner than those of control and K256E α-actinin-4-expressing podocytes. These data provide evidence that α-actinin-4 plays a key role in the formation and/or maintenance of peripheral projections in cultured podocytes.

DISCUSSION

We previously developed a mouse model of an inherited form of FSGS by expressing a mutant variant of α-actinin-4 (K256E) under the control of a podocyte-specific promoter (*mNPHS1*).[26] In this model, approximately 50% of mice develop FSGS-like lesions and display podocyte foot process effacement. However, the direct consequences of mutant α-actinin-4 on podocyte structure and function remained unclear. We therefore assessed the effects of K256E α-actinin-4 on the cytoskeletal dynamics of cultured podocytes.

The conditionally immortalized podocyte cell line used in this study has previously been described in detail.[29] These cells are relatively resistant to conventional transfection approaches for achieving heterologous expression of proteins. We therefore developed adenoviruses for both wild-type and K256E α-actinin-4, which yielded significant

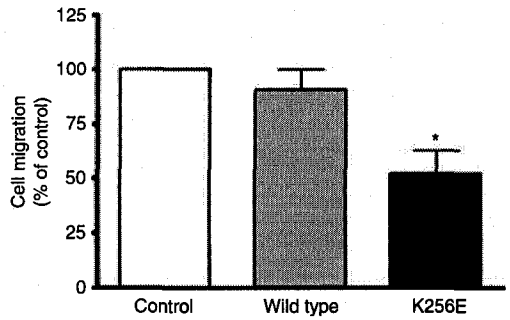

Figure 5 | Effect of α-actinin-4 on podocyte migration. Differentiated mouse podocytes expressing GFP alone (control), wild-type, or K256E α-actinin-4 were trypsinized and replated onto the upper surface of transwell inserts. After 3 h, the cells remaining in the upper chamber were removed and the cells on the lower surface were stained with 4′,6-diamidino-2-phenylindole and counted. K256E α-actinin-4 caused a 48% reduction in the number of migrating cells compared to control and wild type. *$P<0.01$ vs control and wild type ($n=5$).

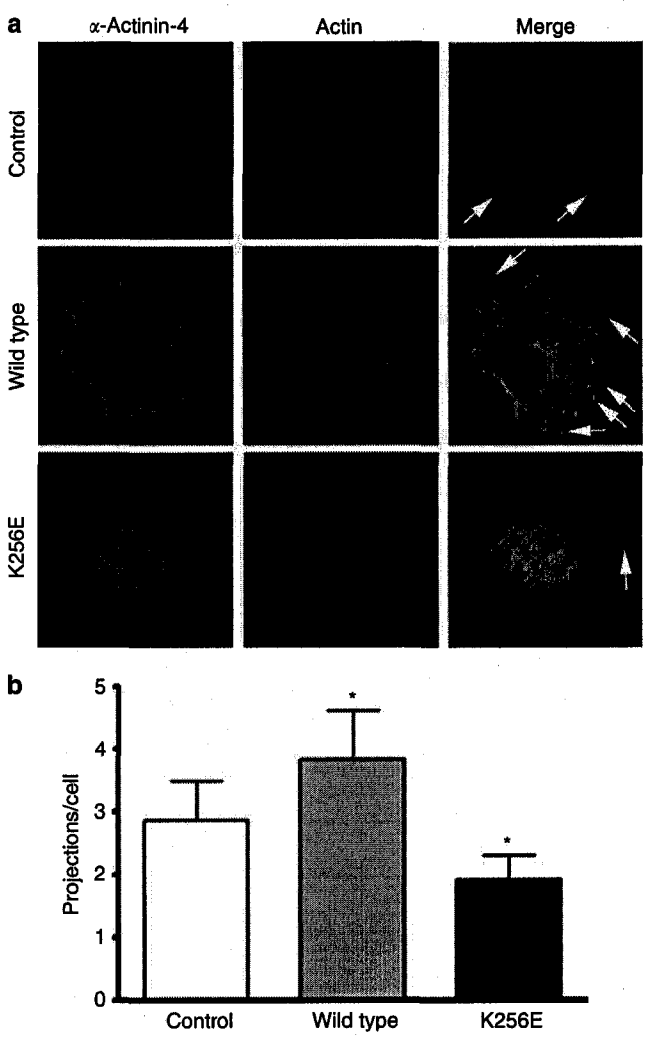

Figure 6 | Effect of α-actinin-4 on peripheral projections of podocytes. At 3 days following infection with viruses for wild-type or K256E α-actinin-4, differentiated podocytes were fixed and stained with an anti-HA tag antibody to detect α-actinin-4 and Alexa Fluor 488-phalloidin to detect F-actin. Images in (**a**) are representative of cells for each condition and demonstrate actin-rich projections (arrows) emanating from the cell body. (**b**) Expression of wild-type α-actinin-4 caused an increase in the mean number of projections (3.8 ± 0.8 projections/cell vs 2.9 ± 0.6 for control), whereas expression of K256E α-actinin-4 caused a decrease in the number of projections (1.9 ± 0.4). *$P<0.05$ vs control ($n=4$).

expression in a high proportion of cells (90%), rendering the cell population much more homogeneous than previously attained. The expression level of both wild-type and mutant K256E α-actinin-4 were similar (Figure 1a), suggesting that the mutant protein is not subject to degradation in these cells.

The most impressive feature upon expression of K256E α-actinin-4 is its distinct intracellular localization. Although the putative function of α-actinin-4 is that of an actin crosslinking protein, we found that the majority of wild-type α-actinin-4 colocalized with membrane-associated cortical actin (Figure 1b) or was detected in the TS pool (Figure 2). In contrast, K256E α-actinin-4 was consistently found along stress fibers and was retained in the TI fraction (Figure 2). This sequestration is likely a direct effect of the increased affinity of K256E α-actinin-4 for F-actin, and is consistent with a gain-of-function effect of such mutations. In support of this, an alternative splice variant of α-actinin-4 has been reported in small-cell lung cancer.[30] The splice variant contains three missense mutations in exon 8, the region containing FSGS-associated mutations. This mutant isoform also displays increased affinity for actin, and was found to colocalize mainly with actin stress fibers, unlike the wild-type protein, which was concentrated along the periphery of the cell.

Several reports have identified an association of actinin isoforms with components of focal adhesion complexes, such as the β_1-integrin subunit and vinculin.[13] Phosphoinositides may also bind to α-actinin and regulate its interaction with actin filaments or integrin receptors.[21,22] Furthermore, α-actinin is phosphorylated by FAK in platelets,[20] reducing its cosedimentation with actin filaments. These findings clearly indicate a role for α-actinin in mediating signals that could modulate the assembly of focal adhesions or the cytoskeleton. It is therefore interesting to speculate that mutations in α-actinin-4, which increase its affinity for actin, may render the protein insensitive to these factors and thereby perturb cytoskeletal dynamics.

The mislocalization of mutant α-actinin-4 led us to investigate its effects on cytoskeletal-dependent processes such as cell adhesion, spreading, and migration. Although we did not observe a significant impact of K256E α-actinin-4 on podocyte adhesion (i.e., adhesion and replating assays), we found that it significantly affected spreading and migration. Indeed, podocytes expressing K256E α-actinin-4 remained rounded and showed severe defects in their ability to spread on collagen-I. This phenotype is reminiscent of that reported in FAK-deficient embryonic mesodermal cells,[31] which can

adhere but fail to spread effectively on ECM, suggesting that FAK signaling may be impaired in cells expressing mutant α-actinin-4. Furthermore, as indicated by the present study, podocytes expressing K256E α-actinin-4 exhibit severe motility defects. These findings are in accordance with a role of actinin-4 in cell motility and cancer invasion,[32–34] where cytoplasmic localization of α-actinin-4 is associated with an infiltrative phenotype in breast cancer cells, whereas cells with nuclear α-actinin-4 are non-invasive. Our results show that α-actinin-4 is significantly involved in cell spreading and migration. The motility deficit seen in cells expressing K256E α-actinin-4 is likely owing to the sequestering of the protein to centrally located actin stress fibers, and away from motility-based structures at the cell's periphery.

Expression of wild-type α-actinin-4 increased the mean number of actin filament-containing peripheral projections emanating from the cell body, reminiscent of podocyte foot processes *in vivo*. In contrast, K256E α-actinin-4 reduced the mean number of such projections (Figure 6). Although the arborized phenotype observed in cultured podocytes is not nearly as extensive as that seen in podocytes *in vivo*,[35] our data suggest that owing to mislocalization, K256E α-actinin-4 does not provide a suitable framework for the maintenance/formation of such projections. We previously showed that podocyte-specific expression of K256E α-actinin-4 leads to foot process effacement and glomerulosclerosis. Such damage may be explained by mislocalization of mutant α-actinin-4, rendering it unresponsive to appropriate signals (e.g., actin remodeling) or unable to provide structural support at the cell membrane, and thereby contribute to foot process effacement.

A recent study by Yao *et al.*[28] attributes podocyte defects encountered in *ACTN4*-associated FSGS to a loss-of-function as mutations render α-actinin-4 more susceptible to forming unstable aggregates, which are rapidly degraded via the proteasome pathway. Conversely, in transgenic mice expressing an FSGS-associated mutant α-actinin-4, podocyte damage and sclerosis correlate directly with mutant transgene expression, consistent with a gain-of-function mechanism.[26] We did not observe any degradation of exogenous K256E α-actinin-4 in cultured podocytes (Figure 1a) within the experimental timeframe. In light of these findings, we favor a synthesis of the two models to explain the dysregulated phenotype of podocytes expressing FSGS-associated mutant α-actinin-4. Gain-of-affinity mutations in α-actinin-4, coupled with some degradation of the mutant protein, could each contribute to a loss-of-function by effectively eliminating this protein from select intracellular locales (e.g., motility-based actin structures and process-like peripheral projections), thereby disturbing cytoskeletal-dependent processes such as cell spreading, migration, and importantly, process maintenance/formation. In support of this hypothesis, dysregulation of the actin cytoskeleton and α-actinin-4 expression/localization has been reported in various glomerular disease models characterized by podocyte foot process effacement,[6,36–38] and is therefore likely to be a key event in the progression of podocyte injury.

In summary, we have further defined the functional consequences of an FSGS-associated form of the actin-crosslinking protein – K256E α-actinin-4. Whereas wild-type α-actinin-4 is predominantly localized to membrane-associated cortical actin in conditionally immortalized podocytes, K256E α-actinin-4 remains tightly associated with stress fibers. Mislocalization of K256E α-actinin-4 causes severe defects in motility, including cell spreading and migration. Furthermore, K256E α-actinin-4 caused a decrease in the number of foot process-like peripheral projections. Our data therefore suggest that dysregulation of the podocyte cytoskeleton may play a key role in the progression of sclerotic lesions resulting from various podocyte injuries.

MATERIALS AND METHODS

Adenoviral constructs

Adenoviral constructs containing wild-type or K256E murine HA-*ACTN4* sequences were generated by subcloning from the previously described pcDNA3-HA-*ACTN4* vectors.[26] In these viruses, the HA-*ACTN4* expression cassette replaced the E1-region and transcription is directed rightward, relative to the conventional human adenovirus serotype 5 map. The E1-deleted, first-generation Adenovirus vectors used in these studies were constructed using a combination of conventional cloning techniques and RecA-mediated recombination,[39,40] and were grown and titered on 293 cells, as described previously.[41]

Cell culture

Conditionally immortalized mouse podocytes were cultured on collagen-I-coated dishes in RPMI-1640 supplemented with 10% fetal bovine serum, 100 U/ml of penicillin, 100 μg/ml of streptomycin, 100 μg/ml of Normocin (InvivoGen, San Diego, CA, USA), and 10 U/ml γ-interferon (Sigma, Oakville, Ontario, Canada) at 33°C (permissive conditions). For differentiation, cells were cultured at 38°C without γ-interferon (non-permissive conditions) for at least 10 days. Cells used for experiments were between passages 5 and 15 only. Differentiated podocytes were infected with a range of viral loads (multiplicity of infection between 0 and 50 plaque-forming units/cell) to determine optimal infection conditions. Lysates (10 μg total protein) were separated by sodium dodecyl sulfate-polyacrylamide gel electrophoresis and transferred to nitrocellulose membranes. Immunoblots were incubated with a monoclonal anti-HA antibody (HA-7, Sigma, 1:1000), followed by a horseradish peroxidase-conjugated secondary antibody and developed using Supersignal West Pico Chemiluminescence (Pierce, Rockford, IL, USA). Immunoblots were stripped and reprobed with an anti-actin antibody (Sigma, 1:1000). For all subsequent experiments, differentiated podocytes were infected at a multiplicity of infection of 25 plaque-forming units/cell and incubated for 72 h to achieve sufficient protein expression.

Fluorescence microscopy

At 3 days post-infection, podocytes grown on collagen-coated coverslips were processed for immunofluorescence. Cells were fixed with 4% paraformaldehyde, washed with phosphate-buffered saline (PBS), permeabilized with 0.2% Triton X-100, blocked with 2% bovine serum albumin, and incubated with an anti-HA tag antibody

(Inter Medico, Markham, Ontario, Canada, 1:200 or HA-7, Sigma, 1:1000). Cells were then double-labeled with appropriate Alexa Fluor-conjugated secondary antibodies and Alexa Fluor-conjugated phalloidin (both form Molecular Probes, Eugene, OR, USA, 1:1000). To visualize focal adhesions, cells were labeled with an anti-vinculin antibody (Vin11.5, Sigma, 1:100) followed by appropriate Alexa Fluor-conjugated secondary antibodies and phalloidin. Images were captured using a Zeiss AxioCam and a Zeiss Axioskop 2 fluorescence microscope (Zeiss Axioskop 2 MOT, Zeiss, Germany).

Fractionation of intracellular actin pools

Infected differentiated mouse podocytes were scraped into ice-cold lysis buffer (10 mM Tris, pH 7.4, 150 mM NaCl, 1 mM ethyleneglycol tetraacetate, 1 mM ethylenediaminetetraacetic acid, 1% Triton X-100, 0.5% Nonidet P-40) supplemented with protease inhibitor cocktail (Sigma, 1:100) and phenylmethylsulfonyl fluoride, and incubated at room temperature for 15 min. Cell lysates were then centrifuged at 15 000 *g* to isolate the TI fraction. The TS fraction was removed and further centrifuged at 100 000 *g* to separate G-actin (supernatant, S) and F-actin (pellet, P). All pellets were resuspended in the original sample volume. A small aliquot of the total lysate was reserved for protein determination using a Bicinchoninic Acid Protein Assay Kit (Pierce). Samples of equal volume (10 μg total protein in lysate) were separated by sodium dodecyl sulfate-polyacrylamide gel electrophoresis and transferred to nitrocellulose membranes. The membranes were probed with a polyclonal anti-HA tag antibody (Clontech, Palo Alto, CA, USA, 1:1000) followed by a horseradish peroxidase-conjugated secondary antibody and developed using Supersignal West Pico Chemiluminescent Substrate (Pierce). The immunoblots were subsequently stripped and reprobed with an anti-actin antibody (Sigma, 1:1000). The membranes were exposed to film, images were scanned with a Hewlett Packard ScanJet 6100C, and densitometry of the bands measured using Kodak 1D 3.5 software.

Cell adhesion assays

Differentiated mouse podocytes, having been infected with adenovirus 72 h earlier, were harvested by trypsin/ethylenediaminetetraacetic acid treatment, centrifuged, and resuspended in RPMI containing 10% fetal bovine serum and counted with a hemacytometer. Cells were seeded onto collagen-I-coated U-bottom 96-well plates (5×10^4 cells/well) and incubated at 38°C. At various times after seeding (3, 6, 12, and 24 h), the wells were washed with PBS and the cells fixed with 4% paraformaldehyde for 30 min at room temperature. Adherent cells were then stained with 1% crystal violet for 30 min, washed five times with PBS, and solubilized in 20% acetic acid. The absorbance (595 nm) of each well was then measured using a FLUOstar Galaxy plate reader. Data are from three separate experiments and are expressed as a function of control cells.

Cell replating assays

Differentiated mouse podocytes, having been infected with adenovirus 72 h earlier, were harvested by trypsin/ethylenediaminetetraacetic acid treatment. Following trypsin inactivation with soybean trypsin inhibitor (Sigma, 0.5 mg/ml), the cells were collected by centrifugation, washed once, and held in suspension for 15 min at 38°C in RPMI containing 10% fetal bovine serum. Suspended cells were counted with a hemacytometer, seeded onto collagen-I-coated glass coverslips (5×10^4 cells/well), and incubated at 38°C. At 3 and 6 h following replating, the wells were washed with PBS, and adherent cells fixed with 4% paraformaldehyde and processed for immunofluorescence as above. The number of spreading cells was counted (three separate experiments) and is expressed as a percentage of infected cells.

Cell migration assays

Differentiated mouse podocytes, having been infected with adenovirus 72 h earlier, were harvested by trypsin/ethylenediaminetetraacetic acid treatment. Following trypsin inactivation with soybean trypsin inhibitor (0.5 mg/ml), cells were collected by centrifugation and resuspended in RPMI + 10% fetal bovine serum. Suspended cells were counted by hemacytometer and seeded onto the upper chamber of transwell inserts (5×10^4 cells/insert) pre-coated on the lower surface with collagen-I. After a 24 h incubation at 38°C, cells on the upper surface were removed with a cotton-tip applicator and the migrating cells on the lower surface of the insert were washed with PBS, fixed with paraformaldehyde, and stained with 4′,6-diamidino-2-phenylindole. Membranes were removed from the inserts, placed on slides, and migrating cells were quantified by counting 4′,6-diamidino-2-phenylindole-stained nuclei. Data are from five experiments expressed as the percentage of control.

Quantification of peripheral projections in cultured podocytes

Differentiated podocytes grown on collagen-I-coated coverslips were infected with adenoviruses for wild-type or K2565E α-actinin-4 and processed for immunofluorescence as described above (Fluorescence microsocopy). Peripheral projections emanating from the cell body of HA-positive cells were quantified in a minimum of 50 cells from four experiments. Data are the mean number of projections per cell. Uninfected cells served as controls.

Statistics

Values reported are the means ± s.e.m. from at least three experiments. Statistical comparisons were made using unpaired *t*-test or one-way analysis of variance followed by the Newman–Keuls multiple comparison test.

ACKNOWLEDGMENTS

We are grateful to Peter Mundel (Albert Einstein, New York) for the conditionally immortalized podocyte cell line. Robin J Parks is supported by the Canadian Institutes of Health Research (CIHR), CIHR/Muscular Dystrophy Association of Canada/Amyotrophic Lateral Sclerosis Society of Canada Partnership Grant, Premier's Research Excellence Award, and the Jesse Davidson Foundation for Gene and Cell Therapy. CRJ Kennedy and RJ Parks are CIHR New Investigator Awardees. Jean-Louis R Michaud is a recipient of a CIHR Doctoral Award. This work is supported by an operating grant from the Kidney Foundation of Canada.

REFERENCES

1. Conlon PJ, Butterly D, Albers F *et al.* Clinical and pathologic features of familial focal segmental glomerulosclerosis. *Am J Kidney Dis* 1995; **26**: 34-40.
2. Conlon PJ, Lynn K, Winn MP *et al.* Spectrum of disease in familial focal and segmental glomerulosclerosis. *Kidney Int* 1999; **56**: 1863–1871.
3. D'Agati V. The many masks of focal segmental glomerulosclerosis. *Kidney Int* 1994; **46**: 1223–1241.
4. Schwartz MM. The role of podocyte injury in the pathogenesis of focal segmental glomerulosclerosis [in process citation]. *Ren Fail* 2000; **22**: 663-684.
5. Barisoni L, Kriz W, Mundel P *et al.* The dysregulated podocyte phenotype: a novel concept in the pathogenesis of collapsing idiopathic focal

segmental glomerulosclerosis and HIV-associated nephropathy. *J Am Soc Nephrol* 1999; **10**: 51–61.
6. Shirato I, Sakai T, Kimura K *et al.* Cytoskeletal changes in podocytes associated with foot process effacement in Masugi nephritis. *Am J Pathol* 1996; **148**: 1283–1296.
7. Gassler N, Elger M, Kranzlin B *et al.* Podocyte injury underlies the progression of focal segmental glomerulosclerosis in the fa/fa Zucker rat. *Kidney Int* 2001; **60**: 106–116.
8. Kerjaschki D. Caught flat-footed: podocyte damage and the molecular bases of focal glomerulosclerosis. *J Clin Invest* 2001; **108**: 1583–1587.
9. Pavenstadt H, Kriz W, Kretzler M. Cell biology of the glomerular podocyte. *Physiol Rev* 2003; **83**: 253–307.
10. Drenckhahn D, Franke RP. Ultrastructural organization of contractile and cytoskeletal proteins in glomerular podocytes of chicken, rat, and man. *Lab Invest* 1988; **59**: 673–682.
11. Kretzler M. Regulation of adhesive interaction between podocytes and glomerular basement membrane. *Microsc Res Techol* 2002; **57**: 247–253.
12. Adler S. Characterization of glomerular epithelial cell matrix receptors. *Am J Pathol* 1992; **141**: 571–578.
13. Otey CA, Carpen O. Alpha-actinin revisited: a fresh look at an old player. *Cell Motil Cytoskeleton* 2004; **58**: 104–111.
14. Lachapelle M, Bendayan M. Contractile proteins in podocytes: immunocytochemical localization of actin and alpha-actinin in normal and nephrotic rat kidneys. *Virchows Arch B* 1991; **60**: 105–111.
15. Otey CA, Pavalko FM, Burridge K. An interaction between alpha-actinin and the beta 1 integrin subunit *in vitro*. *J Cell Biol* 1990; **111**: 721–729.
16. Pavalko FM, Otey CA, Simon KO *et al.* Alpha-actinin: a direct link between actin and integrins. *Biochem Soc Trans* 1991; **19**: 1065–1069.
17. Asanuma K, Kim K, Oh J *et al.* Synaptopodin regulates the actin-bundling activity of alpha-actinin in an isoform-specific manner. *J Clin Invest* 2005; **115**: 1188–1198.
18. Rajfur Z, Roy P, Otey C *et al.* Dissecting the link between stress fibres and focal adhesions by CALI with EGFP fusion proteins. *Nat Cell Biol* 2002; **4**: 286–293.
19. Shibasaki F, Fukami K, Fukui Y *et al.* Phosphatidylinositol 3-kinase binds to alpha-actinin through the p85 subunit. *Biochem J* 1994; **302**(Part 2): 551–557.
20. Izaguirre G, Aguirre L, Hu YP *et al.* The cytoskeletal/non-muscle isoform of alpha-actinin is phosphorylated on its actin-binding domain by the focal adhesion kinase. *J Biol Chem* 2001; **276**: 28676–28685.
21. Corgan AM, Singleton C, Santoso CB *et al.* Phosphoinositides differentially regulate alpha-actinin flexibility and function. *Biochem J* 2004; **378**: 1067–1072.
22. Fraley TS, Tran TC, Corgan AM *et al.* Phosphoinositide binding inhibits alpha-actinin bundling activity. *J Biol Chem* 2003; **278**: 24039–24045.
23. Furukawa R, Maselli A, Thomson SA *et al.* Calcium regulation of actin crosslinking is important for function of the actin cytoskeleton in *Dictyostelium*. *J Cell Sci* 2003; **116**: 187–196.
24. Kaplan JM, Kim SH, North KN *et al.* Mutations in ACTN4, encoding alpha-actinin-4, cause familial focal segmental glomerulosclerosis. *Nat Genet* 2000; **24**: 251–256.
25. Weins A, Kenlan P, Herbert S *et al.* Mutational and biological analysis of alpha-actinin-4 in focal segmental glomerulosclerosis. *J Am Soc Nephrol* 2005; **16**: 3694–3701.
26. Michaud JL, Lemieux LI, Dube M *et al.* Focal and segmental glomerulosclerosis in mice with podocyte-specific expression of mutant alpha-actinin-4. *J Am Soc Nephrol* 2003; **14**: 1200–1211.
27. Kos CH, Le TC, Sinha S *et al.* Mice deficient in alpha-actinin-4 have severe glomerular disease. *J Clin Invest* 2003; **111**: 1683–1690.
28. Yao J, Le TC, Kos CH *et al.* Alpha-actinin-4-mediated FSGS: an inherited kidney disease caused by an aggregated and rapidly degraded cytoskeletal protein. *PLoS Biol* 2004; **2**: e167.
29. Mundel P, Reiser J, Zuniga Mejia Borja A *et al.* Rearrangements of the cytoskeleton and cell contacts induce process formation during differentiation of conditionally immortalized mouse podocyte cell lines. *Exp Cell Res* 1997; **236**: 248–258.
30. Honda K, Yamada T, Seike M *et al.* Alternative splice variant of actinin-4 in small cell lung cancer. *Oncogene* 2004; **23**: 5257–5262.
31. Ilic D, Furuta Y, Kanazawa S *et al.* Reduced cell motility and enhanced focal adhesion contact formation in cells from FAK-deficient mice. *Nature* 1995; **377**: 539–544.
32. Honda K, Yamada T, Endo R *et al.* Actinin-4, a novel actin-bundling protein associated with cell motility and cancer invasion. *J Cell Biol* 1998; **140**: 1383–1393.
33. Menez J, Le Maux Chansac B, Dorothee G *et al.* Mutant alpha-actinin-4 promotes tumorigenicity and regulates cell motility of a human lung carcinoma. *Oncogene* 2004; **23**: 2630–2639.
34. Honda K, Yamada T, Hayashida Y *et al.* Actinin-4 increases cell motility and promotes lymph node metastasis of colorectal cancer. *Gastroenterology* 2005; **128**: 51–62.
35. Kobayashi N, Reiser J, Schwarz K *et al.* Process formation of podocytes: morphogenetic activity of microtubules and regulation by protein serine/threonine phosphatase PP2A. *Histochem Cell Biol* 2001; **115**: 255–266.
36. Smoyer WE, Mundel P, Gupta A *et al.* Podocyte alpha-actinin induction precedes foot process effacement in experimental nephrotic syndrome. *Am J Physiol* 1997; **273**: F150–F157.
37. Smoyer WE, Mundel P. Regulation of podocyte structure during the development of nephrotic syndrome. *J Mol Med* 1998; **76**: 172–183.
38. Barisoni L, Kopp JB. Modulation of podocyte phenotype in collapsing glomerulopathies. *Microsc Res Techol* 2002; **57**: 254–262.
39. Chartier C, Degryse E, Gantzer M *et al.* Efficient generation of recombinant adenovirus vectors by homologous recombination in *Escherichia coli*. *J Virol* 1996; **70**: 4805–4810.
40. He TC, Zhou S, da Costa LT *et al.* A simplified system for generating recombinant adenoviruses. *Proc Natl Acad Sci USA* 1998; **95**: 2509–2514.
41. Ng P, Graham FL. Construction of first-generation adenoviral vectors. *Methods Mol Med* 2002; **69**: 389–414.

Koralee Chaisson

246 First Ave. Apt#2
Ottawa, ON K1S 2G6
613-799-1530
kchai093@uottawa.ca

EDUCATION

2004 - 2007 — *The* University *of* Ottawa, Ottawa, ON
Master of Science
Department of Biochemistry, Microbiology and Immunology

2000 - 2004 — Mount Allison University, Sackville, NB
Bachelor of Science, Honours Biochemistry
Department of Biology and Biochemistry

1997 - 2000 — Colonel Gray Senior High School, Charlottetown, PEI
Formal Education

EMPLOYMENT

2004 - 2006 — *The* University *of* Ottawa, Ottawa, ON

MSc. Thesis Project, Department of Biochemistry, Microbiology and Immunology
Supervisor: Dr. Robin Parks
Title: Interferon Regulatory Factor-3 Activation in Adenovirus Infection

Techniques used: SDS-PAGE, western blotting, immunoprecipitation, cell culture, transient transfection of cell cultures, luciferase assays for protein expression, design and construction of plasmid and viral vectors, bacterial transformation, viral titering, DNA/RNA/protein isolation and quantitation, agarose gel electrophoresis, RT-PCR, PCR, immunofluorescence, microscopy.

05/2004 - 06/2004 — Mount Allison University, Sackville, NB

Research Assistant, Department of Biology and Biochemistry
Supervisor: Dr. Suzanne Currie

Assisted with lab maintenance, chemical inventory, and data entry.

2003- 2004 Mount Allison University, Sackville, NB

BSc. Honours Thesis Project, Department of Biology and Biochemistry
Supervisor: Dr. Suzanne Currie
Title: Does temperature affect susceptibility of juvenile rainbow trout (*Oncorhynchus mykiss*) to endocrine disruption?

Investigated the role of temperature and heat shock proteins in the mechanism of endocrine disruption in juvenile rainbow trout exposed to the estrogen mimic 4-nonylphenol.

Techniques used: isolation of fish tissues, protein extraction and quantitation, SDS-PAGE, western blotting, ELISA, Gas Chromatography Mass Spectroscopy.

2001, 2003 - 2004 Mount Allison University, Sackville, NB

Teaching Assistant, Department of Biology and Biochemistry
Lab demonstrator for first, second, and third year undergraduate biology and biochemistry labs. Responsibilities included: teaching basic laboratory skills and marking lab assignments.

Summer of 2001, 2002 Agriculture and Agri-Food Canada, Charlottetown, PEI

Research Student, Crops and Livestock Research Center
Supervisor: Dr. Rick Peters

2002 - Investigated the effect of seafood waste as an organic amendment on the soil borne pathogen *Rhizoctonia solani* (a potato fungus)

2001- Assisted Dr. Peters in various research projects concerning the control of soil borne diseases in potatoes.

Skills acquired: sterile technique, bacterial and fungal isolation and culturing, bacterial identification using the MIDI system (volatile fatty-acid fingerprinting via Gas Chromatography), DNA extraction, PCR, basic laboratory skills.

AWARDS

- 2005- 2007 Ontario Graduate Scholarship ($15000/yr)
- 2005- 2007 University of Ottawa Excellence Scholarship ($5535, $4386)
- 2005- 2006 University of Ottawa Student Bursary ($1500)
- 2003 NSERC Undergraduate Research Award ($5750)
- 2002- 2004 Dean's List, Mount Allison University
- 2000- 2001 Mount Allison University Entrance Scholarship ($1000)

DISTINCTIONS

- 2005 Third prize poster presentation, University of Ottawa, Dept. of Microbiology and Immunology Annual Poster Day ($50)
- 2004 Third prize poster presentation, Atlantic Undergraduate Universities Biology Conference, University College of Cape Breton ($75)
- 2003 Lady H. E. Banting Prize, Mount Allison University ($100)

PUBLICATION

Michaud, J-L. R., **Chaisson, K.M.**, Parks, R.J., and C.R.J. Kennedy, FSGS-associated α-actinin-4 (K256E) impairs cytoskeletal dynamics in podocytes. *Kidney Int.* (6):1054-61, 2006.

CONFERENCE PRESENTATIONS

Chaisson, K.M., and S. Currie, **Does 4-Nonylphenol Cause Endocrine Disruption in Juvenile Rainbow Trout?** Atlantic Undergraduate Universities Biology Conference, University College of Cape Breton, Sydney, NS, March 2004

Peters, R.D., A.V. Sturtz, J.A. MacLeod, **K.M. Chaisson**, K.A. MacIsaac, R. Henry, B.J. Murray, A.M. Driscoll, B.G. Matheson, I.K. Macdonald, **Use of raw and composted seafood processing waste for nutrition and disease control in potatoes**, Northeast Potato Technology Forum, Bangor, ME, March 2003